UNIVERSITÀ DEGLI STUDI DI NAPOLI FEDERICO II

Dipartimento di Ingegneria Chimica, dei Materiali e della Produzione Industriale

# ELECTRO-DRAWN POLYMER MICRONEEDLES FOR TRANSDERMIC DELIVERY OF LIPOPHILIC AND HYDROPHILIC COMPOUNDS

Philosophical doctorate thesis in materials and structures engineering

**Coordinator:**

Ch.mo Prof. Giuseppe Mensitieri

**Tutor:**

Ch.mo prof. Paolo Antonio Netti

**Supervisor:**

Ing. Raffaele Vecchione, PhD

**Candidate:**

Eliana Esposito

**March, 2014**

to Parish,
to my family,
because they have always
encouraged me to not give up.

# ELECTRO-DRAWN POLYMER MICRONEEDLES FOR TRANSDERMIC DELIVERY OF LIPOPHILIC AND HYDROPHILIC COMPOUNDS

# Index

Summary pag. vi
List of symbols and abbreviation pag. viii

**Introduction** pag. 1

## CHAPTER 1

## State of art on transdermal drug delivery

1.1 Controlled drug delivery pag.3
1.2 Transdermal Drug Delivery pag. 6
1.2.1 Skin: the first barrier pag. 7
1.2.2 Devices and technologies for transdermal delivery pag. 9
1.3 Microneedles pag. 14
1.3.1 Metallic and silicon microneedles pag. 15
1.3.2 Polymeric microneedles pag. 19
1.3.2.1 Replica molding pag. 20
1.3.2.2 Free mold fabrication pag. 27
1.4 Applications pag. 31

# CHAPTER 2

## Experimental method


2.1 New manufacturing technique pag. 32

2.2 Materials pag. 35

2.2.1 PLGA pag. 36

2.3 Fabrication steps pag. 39

2.3.1 PDMS support pag. 39

2.3.2 Electro-drawing of dissolvable microneedles pag. 40

2.3.3 Microneedles by stamp pag. 42

2.4 Morphological analysis pag. 43

2.4.1 Chromophore distribution pag. 43

2.4.2 Porosity pag. 44

2.5 Mechanical characterization pag. 45

2.5.1 Analysis of mechanical properties pag. 45

2.5.2 Indentations in skin pag. 46

2.6 Drug release kinetics pag. 48

2.6.1 Samples preparation pag. 50

2.6.2 Determination of acquisition parameters pag. 52

2.6.3 Drug loaded quantification pag. 54

# CHAPTER 3

## Results and discussion

3.1 Electro-drawn microneedles pag. 56
3.2 Microneedles on pillars pag. 60
3.3 Hydrophobic and hydrophilic drugs loading pag. 64
3.3.1 Porous microneedles pag. 67
3.3.2 Double drop deposition pag. 69
3.3.3 Porous microneedles by stamp pag. 70
3.4 Quantification of model drug loaded pag. 74
3.5 Drug release kinetics pag. 76
3.6 Indentations pag. 80
3.6.1 Preliminary tests pag. 80
3.6.2 Indentation in skin pag. 82
3.6.3 Nanoindentation pag. 84
3.7 Conclusions pag. 87

**Appendix Instruments** pag. 89
A.I.1 Confocal Microscope pag. 89
A.I.2 Multiphoton fluorescence microscopi pag. 92
A.I.3 Immersion sonicator pag. 93
A.I.3 Fluorescence Spectroscopy pag. 95
A.I.4 Nano Indenter pag. 97
A.I.5 Cryo UltraMicrotome pag. 99
A.I.6 Scanning Electron Microscope pag. 100

**References** pag.102
Acknowledgements pag.110

# Summary

Transdermic drug delivery is emerging more and more since it overcomes some disadvantages of classical route of administration. Indeed, kinetics of delivery can be controlled, avoiding bolus release, and environment in which drugs diffuse is safer way than gastro-intestinal tract. The systems currently used for transdermic delivery, like electroporation, iontophoresis and penetration enhancers, are very complex and relatively dangerous for patient. These systems destabilize the structure of stratum corneum to increase skin permeability, or using chemical substances that interact with lipids, or through the passage of electrical currents in the skin.

By using patches with microneedles, it has been proved that it is possible to solve mechanically problems related to the permeability of the stratum corneum, also for molecules with large size; indeed, microneedles create micro holes in skin, without destabilizing chemically its structure. By various research groups both metallic and polymeric microneedles have been manufactured, using different techniques of production. Polymeric biodegradable microneedles allow obtaining a better control of kinetics release and to load an higher drug's amount.

The purpose of this work was to develop a new manufacturing technique which overcomes the constraints of the techniques already used, preserving the effectiveness of the final device obtained. The new method exploits the electric field, generated by a pyroelectric crystal, for the formation, through the drawing of a polymer solution, of micro conical tips able to cross the stratum corneum. The entire production process takes a few minutes at mild temperatures, without creating any contact between the polymeric solution and other things that may be contaminated. The shaping effect of the electric field can be run on both simple polymer solutions (PLGA in dimethyl carbonate) and on water in oil emulsions. In the latter case it was possible to load both hydrophobic compounds in the polymer matrix, and hydrophilic molecules in the aqueous phase emulsified in the polymer solution. To limit the presence of drug only in the cone and minimize wastage of

active compounds, it was used a double drop deposition. It means that a drop of simple solution of PLGA is used like base, and then a smaller drop loaded with drug is deposited on it.

Another important objective of this project was the manipulation microneedles morphology. To produce several degrees of porosity in the polymeric matrix, it was changed the water content in the emulsion. By increasing water phase, it was possible to obtain higher release rates and degradation of PLGA matrix. However, the maximum amount of water is limited by mechanical properties: microneedles have to preserve enough resistance to indent the skin.

# LIST OF SYMBOLS AND ABBREVIATIONS

BSA-TRITC = Albumin, Tetramethylrhodamine isothiocyanate bovine

CLSM = confocal laser scanning microscopy

CMC = carboxymethyl cellulose

d = distance

$D_c$ = critical distance

DCJIs = disposable cartridge jet injectors

DCM = dicholomethane

DDS = Drug Delivery System

DMC = Dimethylcarbonate

DNA = Deoxyribonucleic acid

DP = driving plate

EHD = Electrohydrodynamic

FDA = Food and Drug Administration

h = needle height

LT = Lithium tantalite

MPM = multiphoton microscopy

MUNJIs = multi-use nozzle jet injectors

NIR = near infrared

NR = Nile Red

PBS = phosphate buffered saline

PDMS = Polydimethylsiloxane

PEGDA = poly (ethylene glycol) diacrylate

$p_i$ = the pyroelectric coefficient

PLA = poly-lactic acid

PLGA = Poly(lactide-co-glycolic acid)

PVP = polyvinylpyrrolidone

Rh6G = Rhodamine 6G

RNA = Ribonucleic acid

SC = stratum corneum

UV = ultra violet

V = volume

$\Delta P_i$ = coefficient of the polarization vector

$\Delta T$ = temperature variation

$\theta$ = contact angle

# Introduction

Hypodermal injection and oral assumption are still common routes for drug administration despite their numerous limits and contro-indications, like one-shot release, pain and drug's degradation due to the digestion system that reduces pharmacological action. To overcome these limits and increase drug's effect, new methods for delivery are being studied: one of these is the transdermic administration.

Release of drugs throughout dermis allows avoiding the passage in gastro-intestinal tract, that is a very aggressive environment, and offers a wide surface to choose the area where to apply the patch and reach as easily as possible the target site. The greatest problem is the stratum corneum, a natural barrier for body, that allows diffusion of small and hydrophobic molecules; for all others, release is too slow to have pharmacological effects.

To increase skin permeability they are presently used methods not very pleasant for patient, like penetration enhancers, that risk to provoke high skin irritation, or electro-poration and iontophoresis that require passage of electrical current in the body.

By using patches with microneedles, it has been proved that it is possible to solve efficiently and easily problems related to the permeability of the stratum corneum also for drugs with high molecular weight. This method, proposed some decades ago, has evolved quickly in the last years with the development of several techniques of fabrication leading to microneedles made of silicon, steel and many types of polymers.

In this study it is discussed a system that uses a pyroelectric cartridge in lieu of the syringe piston as a potential solution. Upon stimulation, the cartridge electro-draws, at room temperature, an array of drug-encapsulated, biodegradable polymer micro-pins, able to deliver both hydrophobic and hydrophilic bioactive agents, according to a predefined chrono-programme when inserted in hypodermal tissue. This mould-free and contact-free method permits the fabrication of biodegradable polymer microneedles into a ready-to-use

configuration. The aim is to realize a device efficacy and user-friendly for patient, with fabrication steps that save drug's integrity.

# Chapter 1

# State of art on transdermal drug delivery

## 1.1 Controlled drug delivery

Conventional pharmacotherapy involves the use of drugs whose absorption and therefore bioavailability depends on many factors, such as solubility, molecular weight, and chemical stability. All these parameters can hinder the achievement of a therapeutic response. Especially a low molecular weight confers them the capability to cross different body compartments and reach numerous cell types. However, this indiscriminate distribution leads to the occurrence of side effects and to the need for higher doses of the drug to elicit a satisfactory pharmacological response [1]. Drug delivery system (DDS) is a broad term for technologies that send drugs to the appropriate target site and release them with a time-controlled kinetics, for generating therapeutically desirable effects reducing drug dose required. DDS are usually high molecular weight carriers, such as nano- and micro-particles or capsules, micelles and dendrimers, in which the drug is embedded or covalently bound. Polymeric carriers aim is to transport drugs until target site protecting them from interaction with others molecules which could cause a change in the chemical structure of the active ingredient causing the loss of pharmaceutical action, especially in case of protein drugs or DNA [2]. By changing polymer and design of carriers, stability of drugs in specific body sections and release kinetics can be modulated [3]. Release control technology has many advantages compared to traditional systemic administration. With traditional systems drugs are administered at once, this means that the concentration of drug in the body may exceed the limit of toxicity. As the concentration of drugs decays over time, to maintain it for a clinically significant time in the therapeutic window the administration of drug should be repeated. Therapeutic window is defined as

drug level range in plasma between the minimum effective level, below which there is no therapeutic effect, and the maximum desired level, above which drug becomes toxic for the body. New controlled release devices can provide a release profile valid for a period as long as included in the therapeutic window, therefore reducing number of administrations (figure 1.1) [4].

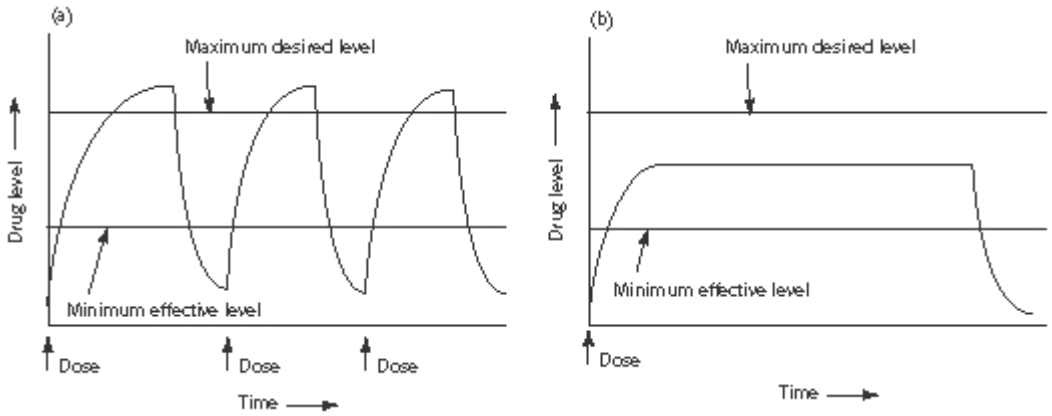


**Fig 1.1:** Comparison between drug concentration in plasma with a conventional delivery system (a) and with a controlled release system (b).

The choice of the polymer used to realize the device, has to be made carefully. An ideal material should be without impurities, biocompatible and easy to be processed. The type of material also depends on the kind of issues that one would accomplish and the type of drug incorporated.

There are several mechanisms by which drugs are delivered from devices. Drugs can be loaded inside polymeric matrix and delivered through diffusion or by degradation of polymer; some systems are formed by capsules with polymeric coating, which permeability dictates release of drugs. These devices realize an extended (or prolonged) release, in which drug release is not necessary constant but extend duration of therapeutic action more than one-shot delivery as represented in figure 1.2.

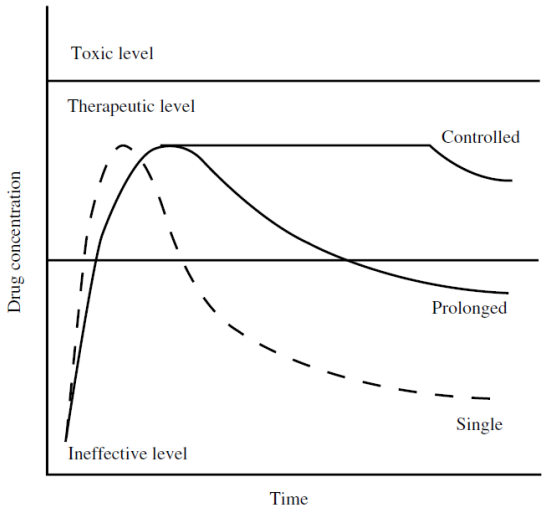


**Fig 1.2:** Plot of drug concentration versus time for different release system.

Other types of devices provide a kinetic profile of zero-order, i.e. drug concentration in plasma remains constant in time for a long period of time, until depletion of drug cargo. In these cases drug outflow is controlled by osmotic potential gradients across semi-permeable polymer barriers. After immersion in water, the system hydrates causing an increase in pressure that pushes out, through orifice in membrane, drug solution [5] (figure 1.3).

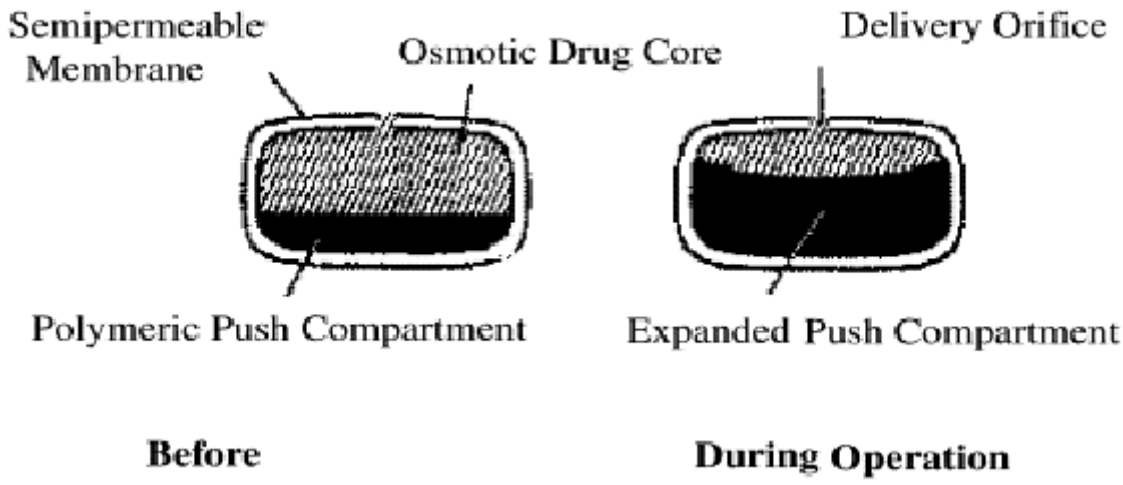


**Fig 1.3:** Operation scheme of an osmotic drug delivery system.

The development of functional delivery systems is strictly correlated to the administration route chosen. In the last years, transdermal delivery is emerging as a high performing and minimally invasive pharmacological treatment.

## 1.2 Transdermal Drug Delivery

Drug can be administered through the most common routes like the oral, parenteral, ophthalmic and transdermal route, each one with specific merit and disadvantages. The parenteral route is the most direct way of getting molecules into the body circulation. Injection of therapeutics through the skin into the blood stream or surrounding tissues produces high delivery efficiency within a very short administration time. This method of delivery is accomplished almost exclusively by needle-syringe system. However, the sharp hypodermic needle generates pain, leading to low patient compliance and needle phobia [6]. Moreover, it entails risk of infection due to the damage induced in the skin. It can be difficult to obtain a sustained drug concentration in plasma, requiring repeated administration carried out by specialized personnel. Especially in case of prolonged care, it becomes even more difficult to make sure that the patient assumes drugs in determined times to ensure continuity in therapeutic effect. Oral drug delivery systems, although very simple, have the great disadvantage of drug degradation in gastro-intestinal tract, which makes it not suitable for release of protein or DNA based compounds, and a variable absorption for each patient, depending on several factors like pH, food, mucus layer[7].

Transdermal drug delivery is an alternative to classical methods of administration. Its key advantages include easy accessibility of skin, which aids in high patient compliance, avoidance of gastrointestinal tract and ability to achieve sustained release. Since skin has a structure that allows passage of only small and hydrophobic molecules, several technique have been developed to temporary increase permeability of stratum corneum. To better understand difficulties involved it is necessary to consider the structure of skin.

### 1.2.1 Skin: the first barrier

Skin is the first barrier for the body against pathogen agent and anything that can be dangerous for the organism. It also provides resistance to shocks for the more sensitive tissues underneath. At the same time, however, skin needs to be supple and able to stretch to accommodate movements.

As showed in figure 1.4, skin can be divided into three layers: (1) the epidermis, which contains the stratum corneum, (2) the middle layer, dermis, and (3) the inner most layer, hypodermis.

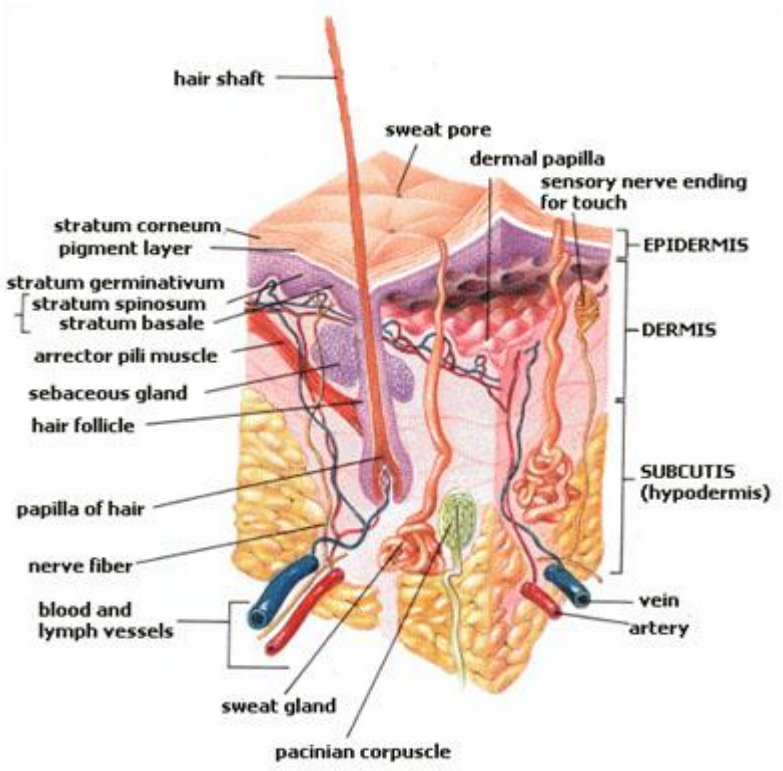


**Fig 1.4:** Structure of skin.

The dermis, an integrated fibro-elastic structure measuring 1-2 mm, gives mechanical strength to the skin. There is a rich capillary bed in the superficial dermis, just below the epidermis, which is the primary site of drug uptake into systemic circulation. Thus, successful transdermal drug delivery typically involves

drug transport across the epidermis to the superficial dermal capillary bed. The pain associated with parenteral drug delivery is due to possible damage to the nerves endings within the dermis [8]. The epidermis layer is 150-200 μm thick and is made up of viable cells with no vascular networks. There is a basement membrane at the base of epidermis and there are tight junctions in the viable epidermis [9], both of which may offer resistance to the transport of molecules across the epidermis. The outermost layer of the epidermis (10-20 μm) consists of dead cells, known as the stratum corneum (SC), which act as a rigorous barrier and protect body from water loss. It is composed of layers of corneocytes which overlap. The major constituent of stratum corneum cells is the keratin and is rather dense in composition. The SC is dynamic in nature and renews itself every 14 days [10], it is constantly maintained by reproduction of inner living epidermal keratinocytes which undergo a process of terminal differentiation and then migrate to the surface as interlocking layers of dead stratum corneum cells.

SC structure is akin to a wall built from bricks and mortar (figure 1.5), the keratinized layer also consists of hard building blocks (the individual corneocytes) stuck together with space-filling mortar (intercorneocyte lipids) [11]. Barrier function of epidermis depends on the good state of its bricks and mortar. There are two main pathways by which drugs can cross the skin and reach the systemic circulation. The more direct route is known as the transcellular pathway. By this route, drugs cross the skin by directly passing through both the phospholipids membranes and the cytoplasm of the dead keratinocytes. The drugs encounter significant resistance to permeation, because they must cross the lipophilic membrane of each cell, then the hydrophilic cell body containing keratin; these steps have to be repeated numerous times to traverse the full thickness of the stratum corneum. The other more common pathway through the skin is via the intercellular route. Drugs must pass through the small spaces between the cells of the skin, making the route more tortuous. Although the thickness of the SC is only about 20 μm, the actual diffusional path of most molecules crossing the skin is on the order of 400 μm [12]. In any case, for almost all drugs, these types of diffusion are too slow to allow enough diffusion and obtain a therapeutic effect.

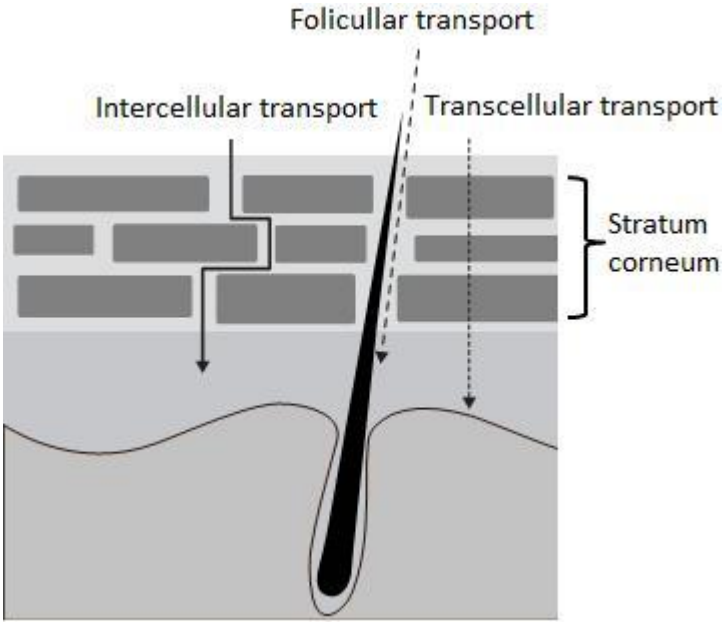


**Fig 1.5:** Possible pathways for delivery of compounds across the stratum corneum.

By destabilizing this structure it is possible to increase skin permeability also for those molecules that would never be able to cross the stratum corneum.

### 1.2.2 Devices and technologies for transdermal delivery

From a global perspective, advances in transdermal delivery systems can be categorized in three different generations. The first generation is mainly based on today's patches produced by judicious selection of drugs that can cross the skin at therapeutic rates with little or no enhancement. In addition to patches, in this class are included liquid spray, gel and other topical formulation. The second generation is characterized by additional advances for the delivery of small-molecules by means of an increase of skin permeability and the use of driving forces for transdermal transport; an example is provided by chemical enhancers conjugated to drug. At the end, the third generation is meant to enable transdermal delivery of small-molecule drugs, macromolecules (including proteins and DNA) and virus-

based and other vaccines through targeted permeabilization of the skin's stratum corneum [13].

The type of technology used by transdermal devices can be divided into passive or active methods based on whether or not an external source of energy is used for skin permeation enhancement. Passive methods include use of chemical enhancers, emulsions and lipid assemblies, that increase stratum corneum permeability through different mechanisms. They may act on the desmosomes, a type of proteic junctional complex localized spot-like on the lateral sides of plasma membranes, forming cohesion between keratinocytes, or modify the intercellular lipid domains to reduce the barrier resistance of the bilayer lipids [14](figure 1.6). but are often associated with higher skin irritation.

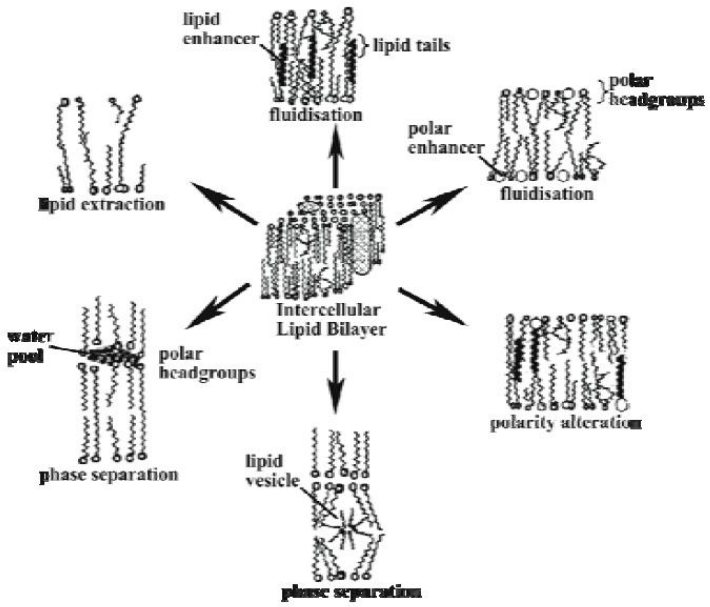


**Fig. 1.6:** Action of penetration enhancers within the intercellular lipid domain.

Chemical approaches have emphasized formulations that selectively disrupt lipid bilayer structures in the stratum corneum to avoid effects in the viable epidermis in order to prevent skin irritation. In this way, the increase of permeability is limited to SC but do not address the barrier of the full epidermis, reducing release efficiency [15].

Active methods, like electroporation and iontophoresis, increase transport across the skin by physically disrupting the barrier or using a driving force for drug transport, through an external energy source.

In particular, electroporation creates a transitory structural perturbation of lipid bilayer membranes due to the application of high voltage impulses. The electrical stimulus causes a reorganization in cellular membrane, whereby phospholipids shift their position opening pores which act as conductive pathway through the bilayer as they are filled with water (figure 1.7). The creation of pores induce a high but reversible increase in transmembrane transport.

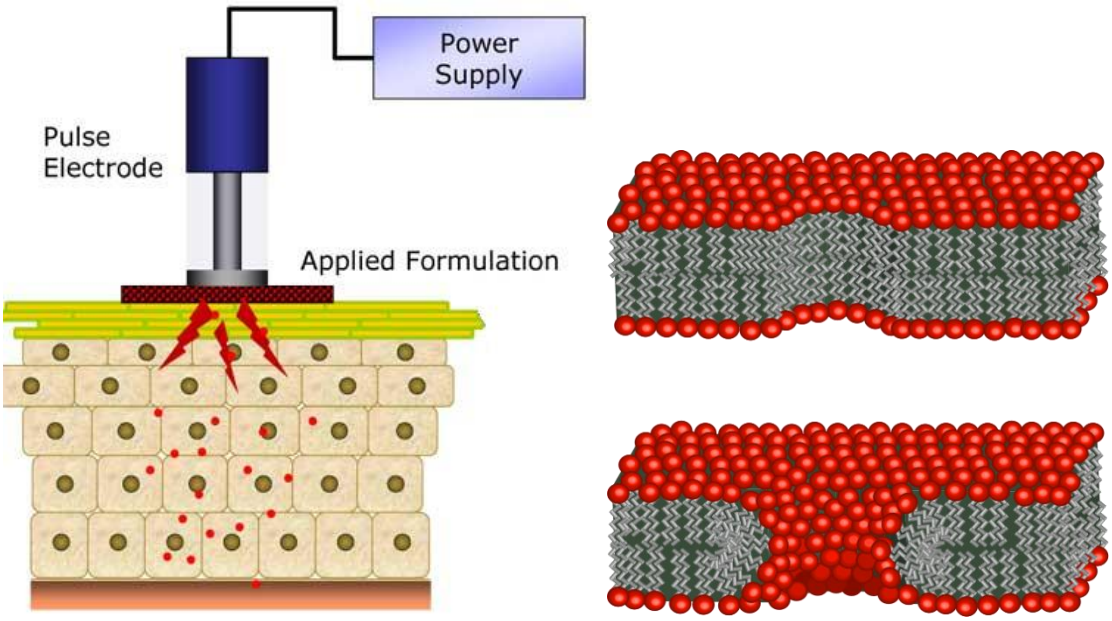


**Fig. 1.7**: (Left) Schematic representation of electroporation system; (Right) Theoretical arrangement of lipids after electrical pulse showing an hydrophobic pre-pore (up) and a hydrophilic pore (down).

Iontophoresis, instead, uses an electric field to move charged substances, usually a medication or a bioactive agent, through the skin by repulsive electromotive force. A small electric current is applied to an iontophoresis chamber placed on the skin, containing a charged active agent and its solvent; another electrode carries the return current (figure 1.8). The positively charged chamber, the cathode, will repel a positively charged chemical species into the skin, whereas negatively charged

substances have to be loaded on the anode. These devices are equipped with a power supply, which adds to the cost and the complexity of the treatment, and requires the passage of current in the body of the patients, resulting annoying or even painful for them [16]. Furthermore, both these methods need the presence of trained sanitary personnel.

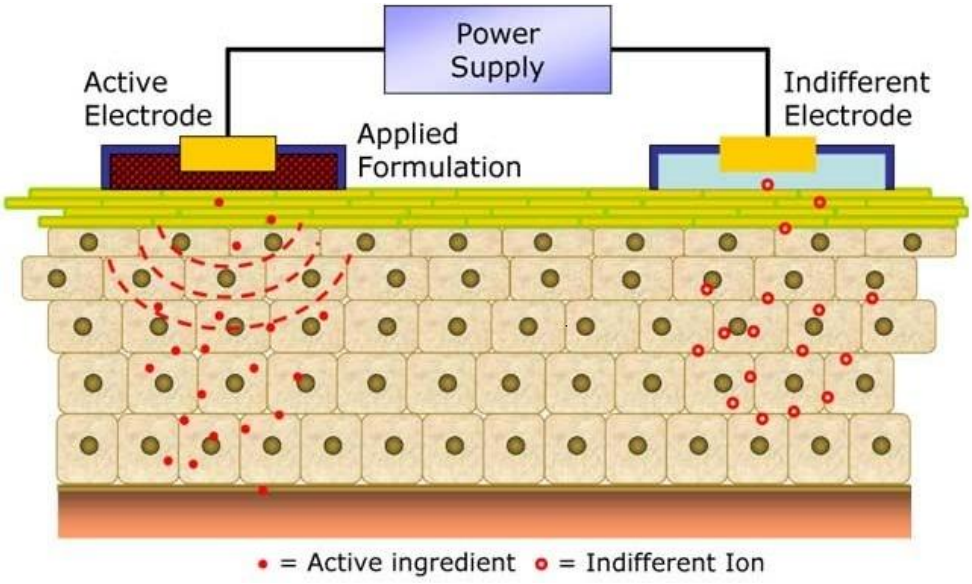


**Fig 1.8:** Scheme of iontophoresis system.

Another active method is liquid jet injection, which use a high-speed jet to puncture the skin and deliver drugs with no use of a needle (figure 1.9). Jet injectors can be broadly classified into multi-use nozzle jet injectors (MUNJIs) and disposable cartridge jet injectors (DCJIs), depending on the number of injections carried out with a single device.

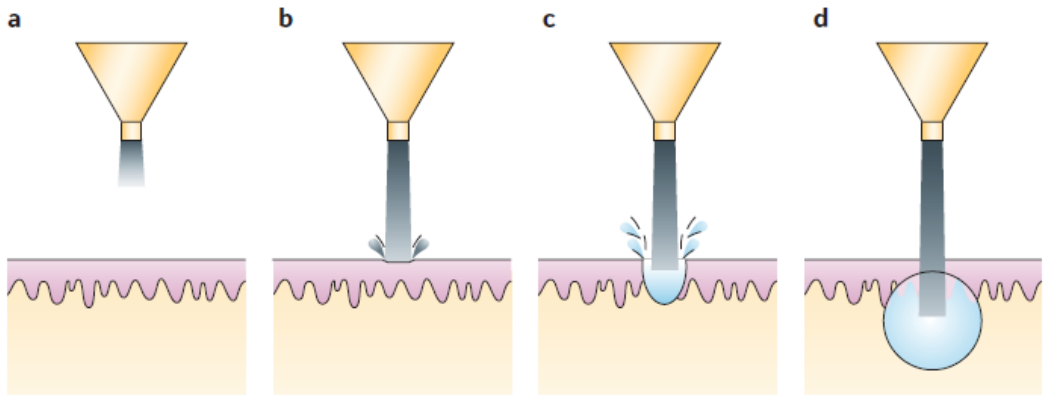


**Fig 1.9:** Schematic depiction of the jet injection process. A) Impact of a piston on a liquid reservoir in the nozzle increases the pressure, which shoots the jet out of the nozzle at high velocity (velocity >100 m s–1). B) Impact of the jet on the skin surface initiates formation of a hole in the skin through erosion, fracture or other skin failure modes. C) Continued impingement of the jet increases the depth of the hole in the skin. If the volumetric rate of hole formation is less than the volumetric rate of jet impinging the skin, then some of the liquid splashes back towards the injector. D)| As the hole in the skin becomes deeper, the liquid that has accumulated in the hole slows down the incoming jet, and the progression of the hole in the skin is stopped.

Liquid jet injections for immunization were first carried out using MUNJIs, which allowed repeated injections of vaccine from the same nozzle and reservoir at a rate of up to 1,000 immunizations per hour. They were successfully adopted for rapid mass immunization using vaccines against a large number of diseases, including measles, smallpox, cholera, HBV, influenza and polio [17]. But after problems of cross-contamination, due to splash back of interstitial liquid from the skin onto the nozzle, it has gone to use DCJIs that have its own sterile orifice and nozzle and is discarded between patients.

All these systems increase skin permeability by disrupting or altering temporary structure of stratum corneum. Unfortunately, after drug delivery has been completed, it takes on the order of several hours or days to recover its integrity and this cause discomfort to the patient and can increase risk of infections specially if treated area is extended[18].

Therefore, it remains a need for an ideal transdermal drug delivery system that a) is safe by maintaining skin permeability only during the desired period of drug delivery, b) can create sustained or bolus delivery profiles, c) can deliver therapeutic volumes/doses of drug quickly with minimal discomfort, d) has

rapidly responsive pharmacokinetics and pharmacodynamics, e) causes minimal pain and irritation, and f) is simple, inexpensive, and self-administrable [19].
All requirements listed above seem to be satisfied by using microneedles. These devices are needles with micron dimension, able to puncture stratum corneum, as to create microchannel that allow also the passage of hydrophilic macromolecules, without stimulation of nerves ending in dermis.

## 1.3 Microneedles

The research on microneedles and their applications began at the end of last century, the aim was to find a safe, viable and pain-free alternative to the over 16 billions of injections per year. By incorporating techniques adapted from microelectronics industry they have been fabricated the first microneedles made of silicon or glass, for drug delivery through cellular membrane or inside tissue [20]. Little by little thanks to advances of the technology, devices have been improved in shape and fabricated in a variety of materials for different applications.
Microneedles have a tipical length above 200 μm, in order to perforate epidermis, and below 1 mm, to not stress too much nerves ending in the dermis. If the target of release is systemic circulation, microneedles that penetrate more deeply in epidermis have a greater success in drug delivery, since drugs reach easier capillary in dermis. Thanks to their small dimensions, microneedles leave only micro damages in stratum corneum therefore limiting permeation of microorganism of several magnitude order respect to the injection with hypodermic needle, reducing risk of infection [21].
Before designing a microneedles array it is important to consider all geometric parameters that allow a good degree of penetration. Width, length and distance between microneedles can be optimized to obtain desired permeability and penetration capability[22], for example if microneedles are too near each other there is a “fakir’s bed” effect which prevents indentation. Moreover, even if

microneedles are spaced, the elastic nature of skin can inhibit microneedles from penetration by folding around the needles during the application, especially in case of blunt and short microneedles. Due to the robustness of the skin, microneedle insertion forces may exceed the ultimate tensile force and thereby determine a breakage of the microneedles, particularly for longer ones, or for those with a large tip's radius, and for microneedles made of relatively weak materials [23,24]. So it is needed to consider both material and geometric parameters in the designing phase, to obtain microneedles with mechanical strength enough to pierce skin.
Another factor conditioning skin penetration is the insertion rate. Indeed, when microneedles are pushed into the skin slowly by hand, it is obtained a partial penetration; instead, applying microneedles with higher velocity, a deeper level is reached. This is explicable by skin's increased mechanical compressive resistance at higher strain rates. Greater resistance to deflection provides for greater penetration of microneedles [25].

### 1.3.1 Metallic and silicon microneedles

Initially microneedles were made from silicon wafers, using techniques of photolithography and ion etching. Although silicon is attractive for its mechanical properties and for the well-established knowledge, coming from the microelectronic field, it is relatively expensive and requires clean room processing. In contrast, metal and glass microneedles have been found to be equally effective in skin penetration and can be produced at relatively much lower cost than silicon ones. Various metals, such stainless-steel, titanium, palladium, palladium-cobalt alloys, and nickel have been used as structural materials for MN fabrication[26]. They have been developed with multiple geometries and can be divided into two major groups: in-plane, formed in parallel with machined surface, and out-of-plane microneedles, perpendicular to the surface [27] as illustrated in figure 1.10.

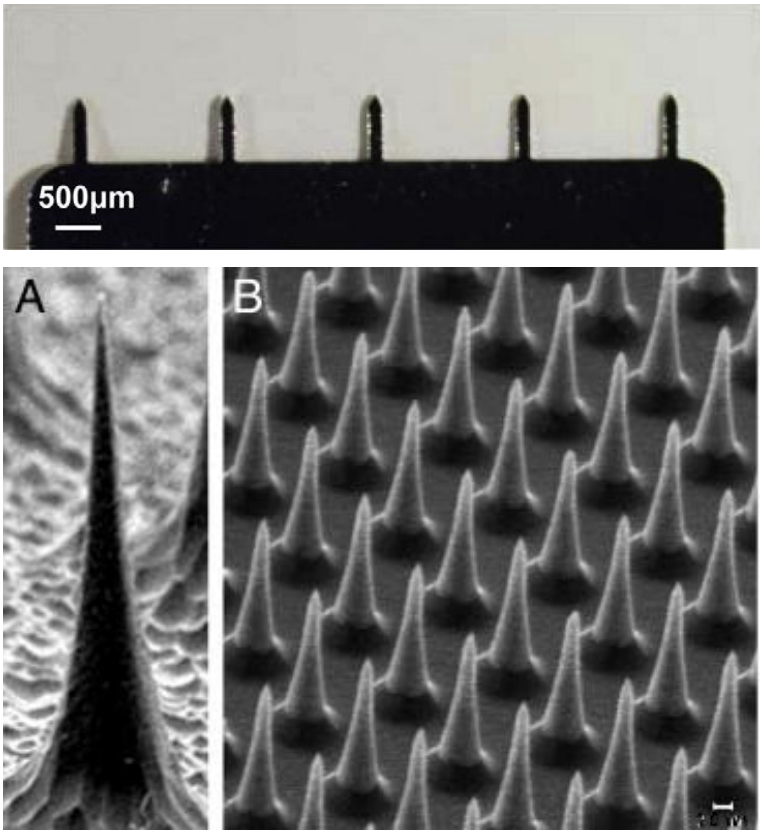


**Fig. 1.10:** Exsamples of fabrication in-plane and out-of-plane: (Up) Array of five stainless microneedles in-plane; (Down-A) Silicon microneedle (150 µm tall) from a 400-needle array etched out of a silicon substrate (B).

Microneedles can be designed to approach delivery following different criteria (figure 1.11). At first, microneedles were designed to make pre-treatment on cute. This approach, called "poke and patch" consists in applying microneedles on skin, so as to increase permeability by creation of micro holes in stratum corneum, and then, after removing array, resting a patch with drug reservoir on the treated area. In this way it is possible to increase penetration capability of macromolecules by up to more than four orders of magnitude [28]; this type of approach is already realized with Dermaroller® [29]. This is a very easy method to realize, but the release from patch lasts until closure of holes, that is not more than 72h after treatment with microneedles preventing any longer release.

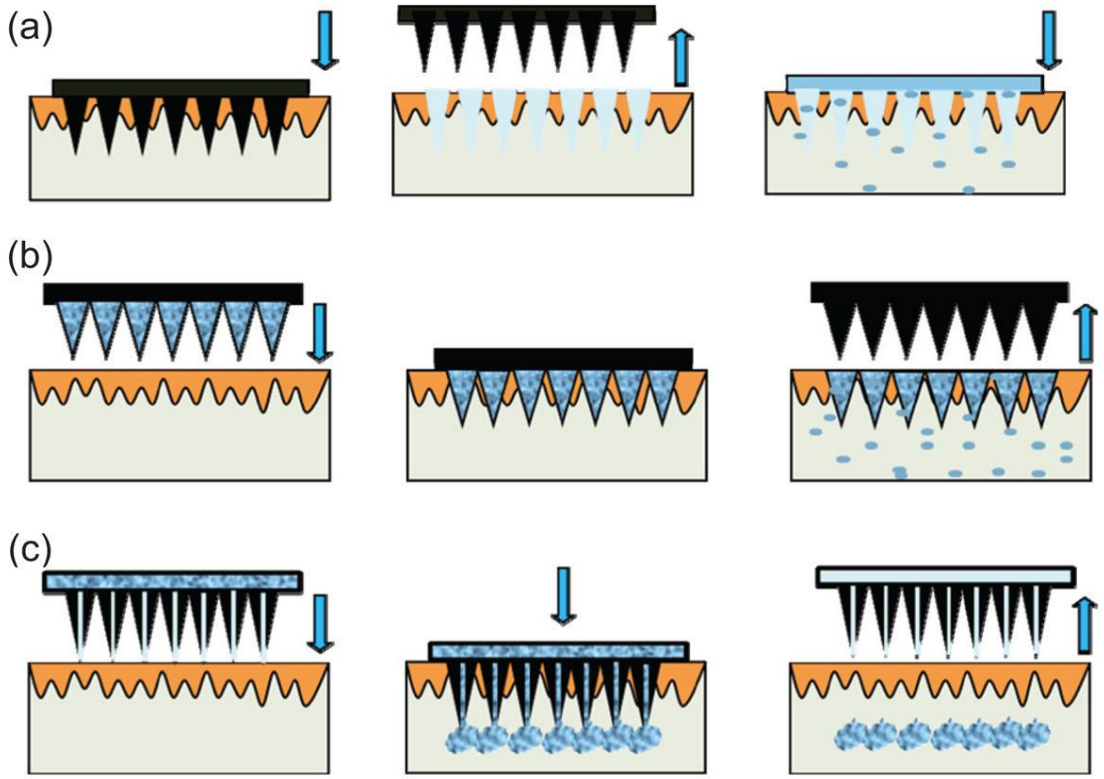


**Fig. 1.11:** Schematic representation of different methods of MN application across the skin. (a) Solid MNs applied and removed to create micropores followed by the application of a traditional transdermal patch. (b) Solid MNs coated with drug molecules applied for instant delivery.(c) Hollow MNs for continuous drug delivery or body fluid sampling.

Solid microneedles are also used for "coat and poke" approach. In this procedure microneedles are dipped in solution with drug and then dried, leading to the conversion of the liquid layer into a solid coating. Microneedles have been coated with a broad range of drugs, such as hydrophilic and hydrophobic low-molecular-weight drugs, DNA, RNA, proteins, peptides, and inactivated pathogens. The compactness of covering layer depends on physico-chemical characteristics of drug solution and on superficial properties of microneedles [30]. However, a drawback of this approach is that solid microneedles can only be coated with small amount of drug to avoid an excessive reduction in aspect ratio, as showed in figure 1.12, so it is just applicable for very powerful drugs, such as vaccines [31,32,33].

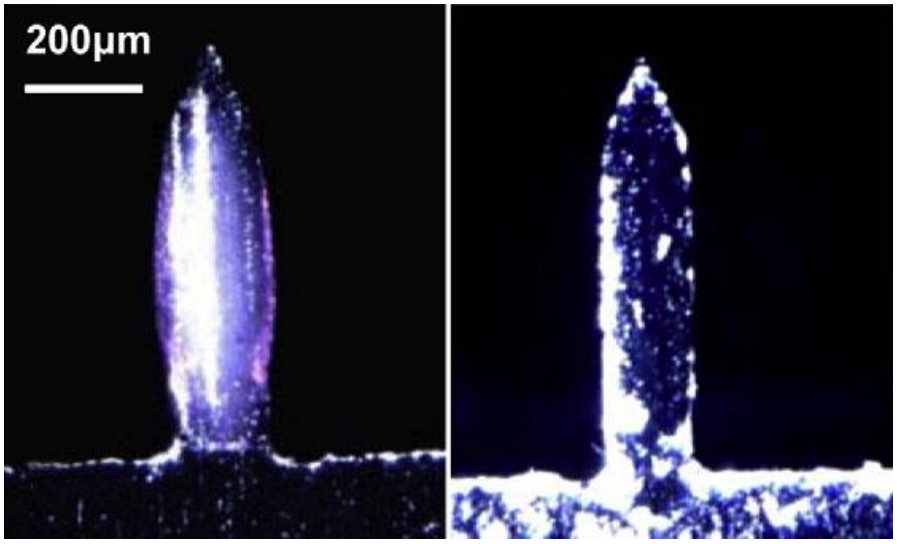


**Fig. 1.12:** Bright-field micrographs of a microneedle coated with red-fluorescent inactivated influenza virus before (left) and 10 min after (right) insertion into human cadaver skin

Gill and Prausnitz have extended this approach fabricating microneedles with "pokets" in metallic structure. In this manner it is possible to localize drug and release it at target depth, or to load different drug, with a multi-step process and obtain a sequential delivery (figure 1.13) [34].

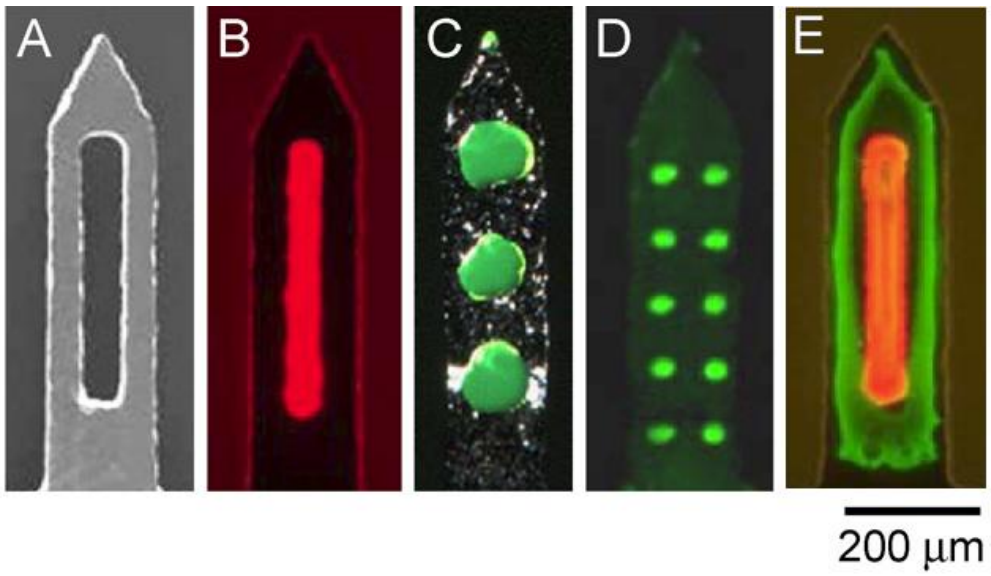


**Fig. 1.13:** Pocketed microneedles. (A) Representative microneedle with a large central pocket. Microneedles with pockets of different sizes and shapes filled with (B) sulforhodamine, (C) fluorescein and (D) plasmid DNA as model drugs. (E) Microneedle with a composite coating that sequestered sulforhodamine within the microneedle pocket and coated fluorescein on the microneedle surface by a multi-step process.

In the case of hollow microneedles (figure 1.14), the release approach is called "poke and flow". Often this microneedles array is combined with a syringe or another external system able to regulate pressure and to drive flow inside dermis. Pumping system can be electrically powered, in this case the presence of trained personnel is required. Other systems, operated by compressed air or osmotic pressure, can be integrated inside the administration device, but in this way structure device is very complex. Furthermore, the dose of the desired drug in solution can be more easily controlled according to the need of the patient. However, to avoid pain is necessary apply flow rate very low (about 100 µl/min) especially when it's necessary dispense large volume (> 1 ml) [35].

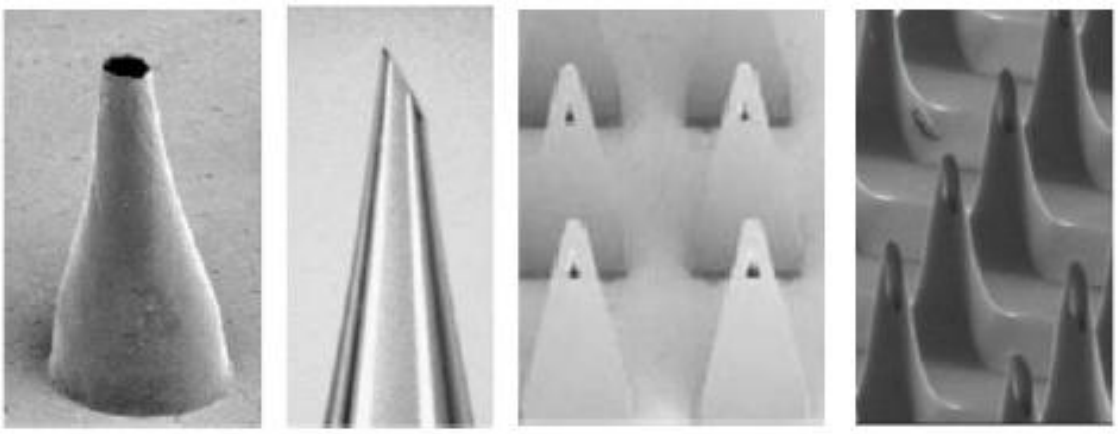

**Fig. 1.14:** Some examples of hollow microneedles with different geometries.

## 1.3.2 Polymeric microneedles

One of the main problems with metallic and silicon microneedles would be if some of them break inside skin, the organism would not be able to remove them. For this reason it is preferred to use biodegradable or dissolvable materials.

Certain types of polymers have optimal properties, as biocompatibility, biodegradability and mechanical strength, to be used for realization of microneedles. Some of these, like poly(lactic-co-glycolic) acid (PLGA), poly-lactic

acid (PLA) [36], carboxymethyl cellulose (CMC) [37], polyvinylpyrrolidone (PVP) [38] are already widely used for these applications. By changing polymer matrix, or using a double inclusion, i.e. drug in nano/microparticles incorporated in microneedles, it is possible to manage drug release kinetics and drive the drug to the target site.

### 1.3.2.1 Replica molding

The classical method to produce polymeric microneedles is a multistep process. There are three phases: 1) manufacturing of a master; 2) mold production; 3) replica molding of the final polymeric device.

Masters have to possess the same shape of final device and they are typically manufactured in photosensitive resins, as SU-8, or in silicon by combining UV lithography and a proper chemical etch.

A common UV lithography process, using SU-8, is illustrated in figure 1.15. The substrate is coated with few hundred microns of photoresist by using a spin coater and then it is soft baked in order to remove the solvent and improve resist-substrate adhesion. UV lithography consists in radiating a photoresist through a chrome mask. In particular, by using a mask with an array of circular or square dots it is possible to obtain microstructures having the shape of needles. After irradiation, a post-exposure bake is performed to increase the cross-linking degree of the irradiated areas and stabilize them against the action of solvents during the development step. Development is performed by immersing the substrate in propylene glycol methyl ether acetate at room temperature, followed by a rinsing step in water or isopropanol [39].

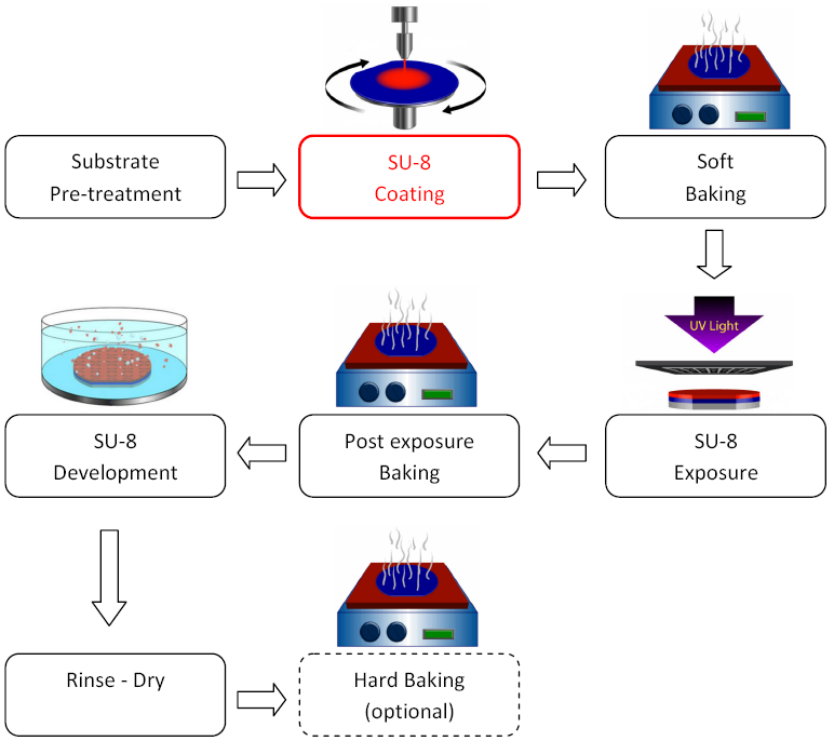


**Fig. 1.15:** Photolitography standard protocol to create SU-8 master molds.

Through elaboration of the lithographic technique J.-H. Park et al. were able to obtain microneedles with different shaped tips. In one case, spaces between cylinders are filled by a sacrificial polymer, then the tip of cylinders are asymmetrically covered with a thin copper layer in order to selectively remove part of the tip by using a reactive ion etching obtaining cylindrical microneedles with beleved tip. In another case, in order to obtain microneedles with pyramidal tips, SU-8 is spun on a wafer on which inverted pyramid-shaped holes have been previously patterned. A second mask with square dots is then aligned on the first structure before irradiating the photoresist. Another special case is based on the exploitation of microlenses for focusing the UV light. Microlenses are fabricated by etching glass substrate masked with metal, on which SU-8 is spun [36] (fig. 1.16).

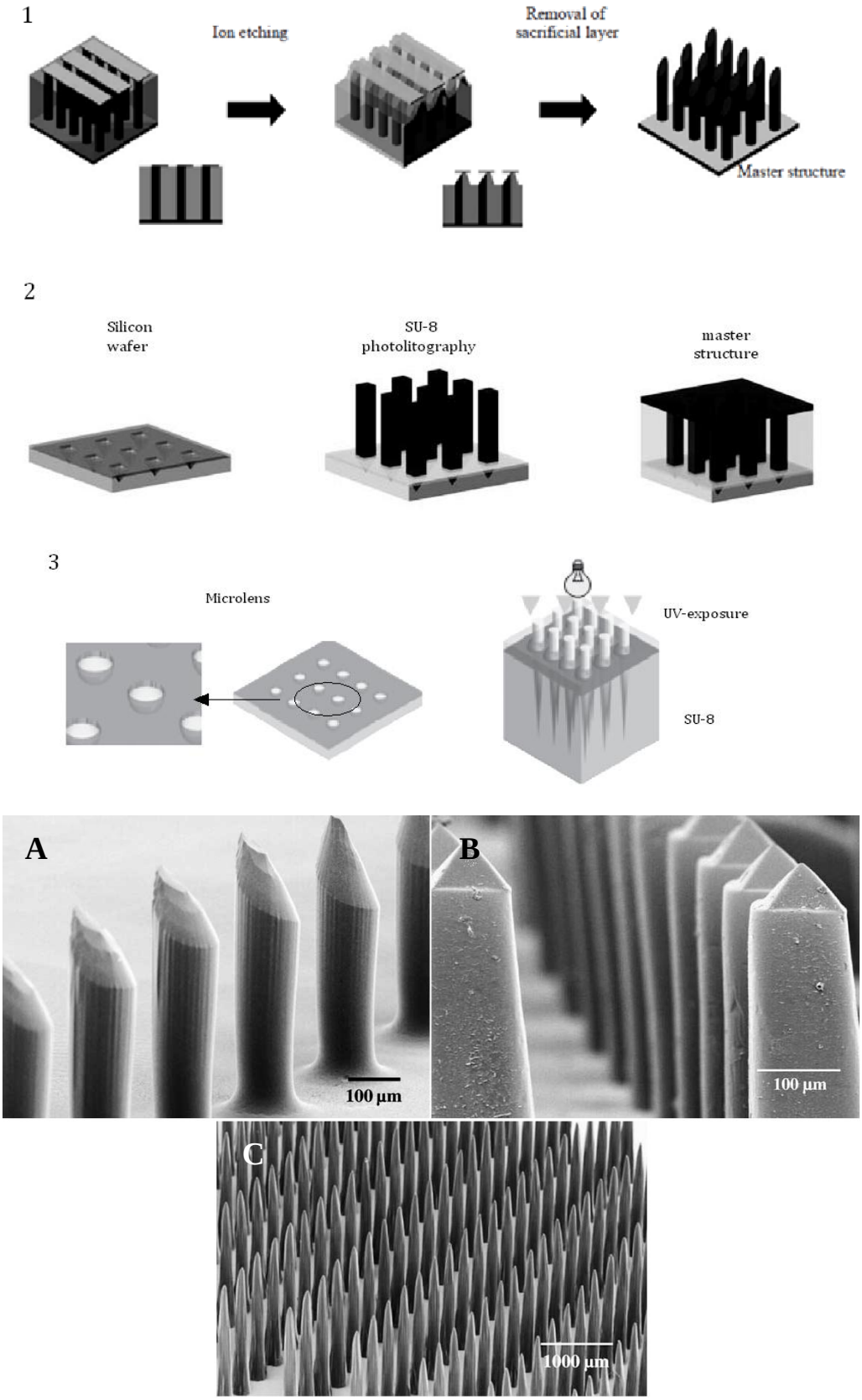


**Fig. 1.16:** Schematic of process to fabricate beveled-tip (1), pyramidal tip (2) and conical (3) microneedles. Scanning electron microscope image of beveled-tip (A), chisel-tip (B) and tapered cone (C) microneedlesi

The second step consists in the fabrication of a mold from which polymeric microneedles will be replicated. Polydimethylsiloxane (PDMS) is the most used silicon-based polymer for the fabrication of stamps; it is considered to be inert and non-toxic. Thanks to its low interfacial free energy, polymers molded in such a stamp do not adhere irreversibly, and its flexibility helps in the detachment phase of the array of microneedles from the stamp. Preparation process, showed in figure 1.17, is very simple and fast. PDMS precursor is mixed with the treating agent, in ratio 10:1, and kept under vacuum to remove air bubbles. To make molds, master structure arrays of needles is coated with liquid PDMS and allowed to cure in oven. After polymerization and cross-linking, solid PDMS presents a hydrophobic surface and this facilitates the separation from hydrophilic materials.

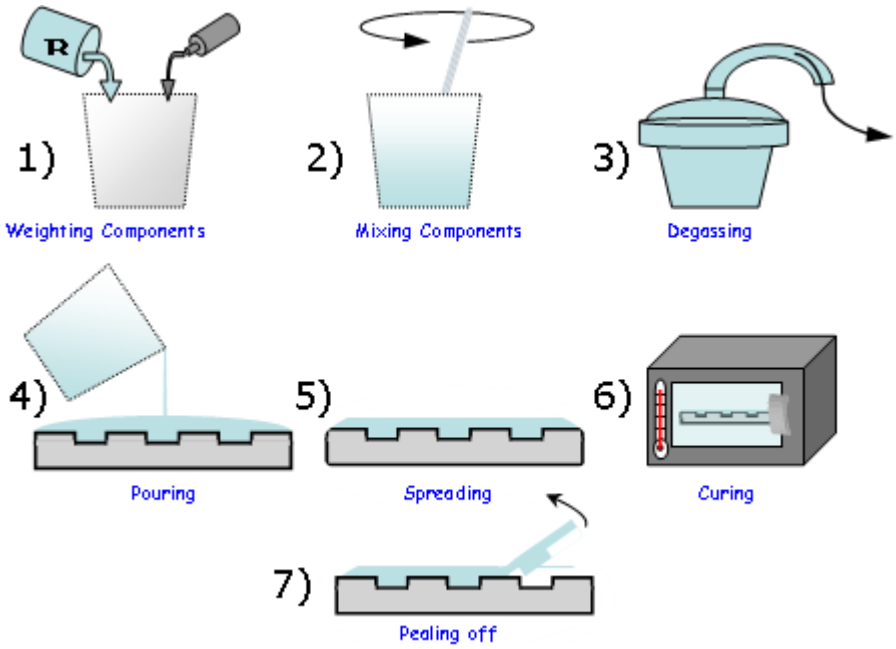


**Fig. 1.17:** Schematic procedure for fabrication of PDMS stamp.

The last phase of production is the replica molding of the final polymeric device. Depending on the polymer chosen, microneedles are created by melting a polymer on the stamp, by drying an aqueous polymer solution or by UV-curing a polymer precursor.

Usually, if a thermo-plastic polymer, like PLGA, is chosen, first PDMS stamp is loaded with a solution containing drug or encapsulated drug. Evaporation of the solvent leaves solid drug particles partially filling the mold; residual particles remaining on the surface of the mold can be removed using adhesive tape, and then, after drying, polymer is melted on the stamp, that is filled with the help of vacuum. Next the mold is recovered with powder of biocompatible polymer and placed in a vacuum oven. Vacuum is necessary to remove entrapped bubble and help pull the polymer melt into the grooves of the mold (figure 1.18).

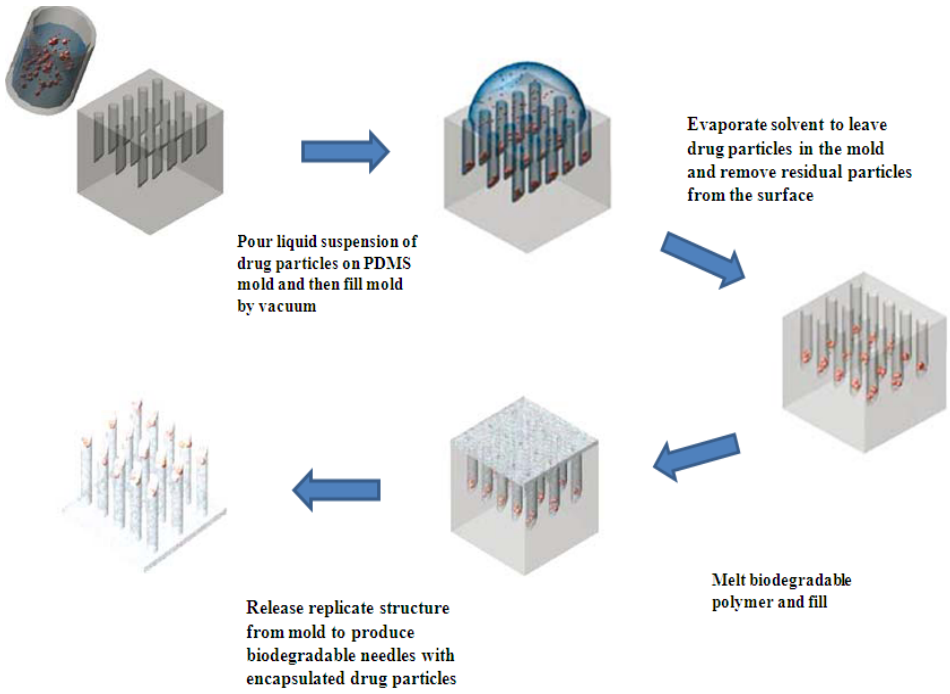


**Fig. 1.18**: Method to fabricate polymer microneedles that encapsulate drug for controlled release.

As showed in figure 1.19, this procedure gives an inhomogeneous distribution of drug inside needle. Indeed the most of it is accumulated towards the tip, and this, even if entail release of entire amount of drug, implies a fast release.

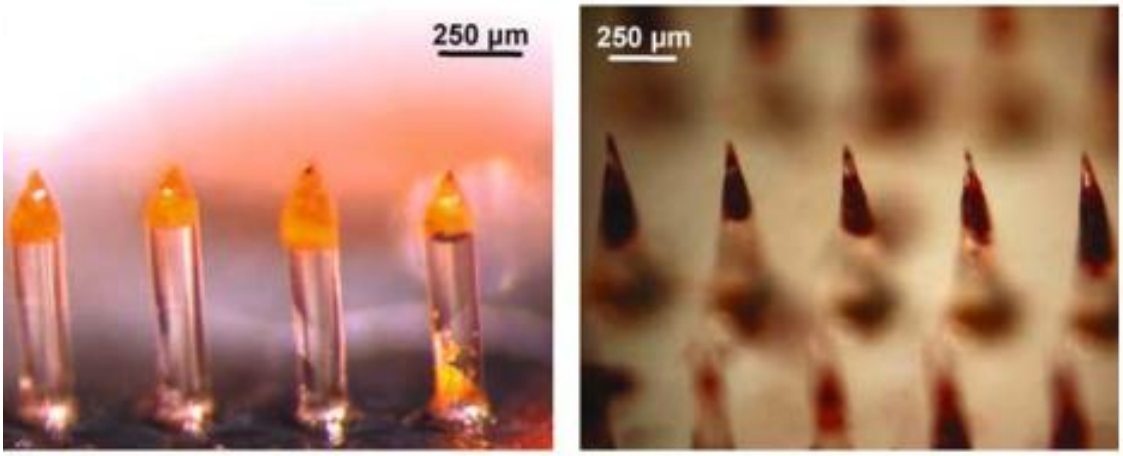


**Fig. 1.19:** Polymer microneedles bevel-tip (left) and tapered-cone (right) made of PLGA and encapsulating calcein within their tips.

Although this fabrication method is very simple and cheap to realize, it is not suitable for all drugs. Indeed, generally, thermoplastic polymers with mechanical strength enough for this application, require an high melting temperature, that is incompatible with a wide drug's variety.

Otherwise photocurable polymers, like PEG and PVP, liquid before reticulation, or hydrogels modeled starting from aqueous solutions can also be used. In this case it is easier to mix the drug directly in the polymer matrix, obtaining an homogeneous distribution. By loading model drug into dissolving microneedles in different ways, one is able to design systems that can achieve rapid or extended release from a microneedle patch. Drug can be selectively incorporated into the microneedles themselves and not into the backing layer. A small volume of solution with drug is cast into the holes of the micromold to form microneedles. After wiping off excess solution from the micromold surface, polymer without drug is added onto the micromold and solidified. To administer larger drug doses as an extended release over at least hours, drug can be incorporated into both the microneedles and backing layer or, alternatively, just the backing layer [37] (figure 1.20).

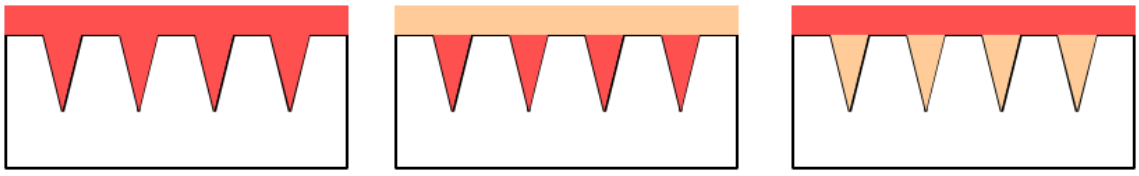

(a) (b) (c)

**Fig. 1.20:** Schematic representation of drug loaded in entire device's volume (a), into microneedles (b) and in back layer but not in microneedles (c).

Also these fabrication have some limits related to the substances utilized and to the process conditions. Indeed, photoinitiators, needed to start UV reticulation, often are toxic for the body, and UV irradiation can degrade drug loaded in matrix. In case of production with aqueous solutions, it is required a long time to dry microneedles before pulling them away from the mold.
All fabrication techniques above illustrated require use of a PDMS mold to form microneedles. The re-use of the same mold to shape several microneedles-array, can create problem of cross-contamination between devices.

The advantage of this approach is to obtain in a very simple way an array with hundreds of microneedles, all with the same shape. This process is also easily scalable to an industrial level further lowering the cost, so several research groups have focused their attention on these methods, trying to improve efficiency. Chu, Choi and Prausnitz have developed a system to insert an air bubble in the base of microneedles to concentrate drug towards needle's tip, as to minimize drug wastage. Moreover they have incorporated a pedestal at the base of microneedles in order to insert tips more fully in the skin. More complete insertion of the microneedles allowed a higher fraction of the encapsulated drug to be delivered [40]. In some cases, because of long degradation time of PLGA, microneedles array are designed in order to leave tips inside skin, so drug release can continue after removal of the supporting patch, to reduce patient nuisance. This is possible coupling PLGA needles with a polymeric base quickly dissolvable [41], pushing arrowhead needles inside skin with metal shaft [42], or creating complex structure that rest stuck in tissue [43]. In other cases they are used hydrogel microparticles

that by means of a swelling mechanism, cause microneedles breackage and acceleration of drug release [44].
Rimarcherei i limiti di temperature in un caso e i tempi lunghi di evaporazione nell'altro caso.

### 1.3.2.2 Free mold fabrication

In recent years K. Lee et al. have developed a different approach that does not use molds for fabrication of microneedles. This method consists in drawing melt maltose through an array of metal micro-pillars. Maltose is chosen since it is very easy to control its state (liquid, glassy, solid), and thus viscosity, manipulating temperature during drawing phases.
The exact needle's shape, as showed in figure 1.21, is obtained by stepwise controlled drawing, changing temperature, in a two steps process [45].

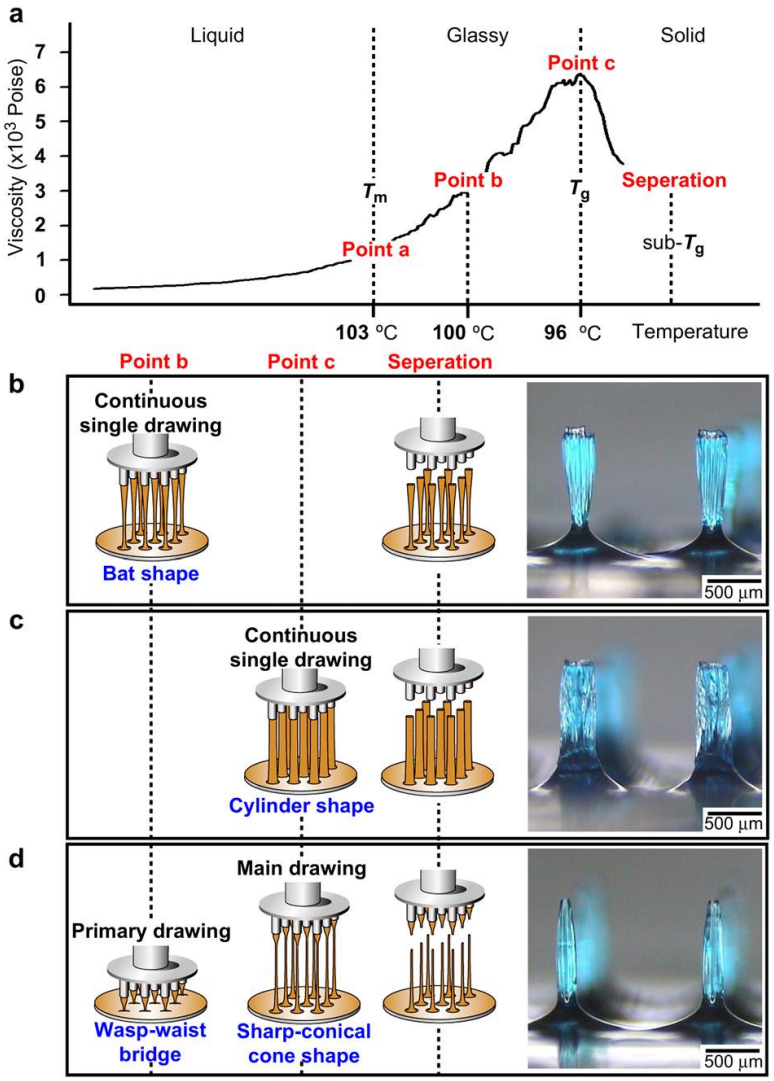


**Fig. 1.21:** The continuous single and stepwise controlled drawing lithography for fabrication of dissolving microneedle. (a) The viscosity change of maltose with temperature. (b) Bat shapes and (c) Cylinder shapes were fabricated by continuous single drawing at point b and c. (d) Sharpe-conical cone shapes were farbricated by stepwise controlled drawing, primary drawing at drawing point b and main drawing of drawing point c.

This fabrication technique is also applied for the realization of hybrid electro microneedles system. Since needles are drawn through metal pillar, this support is used as electrode to apply an electric field and thus accelerate penetration of gene in skin (figure 1.22) [46].

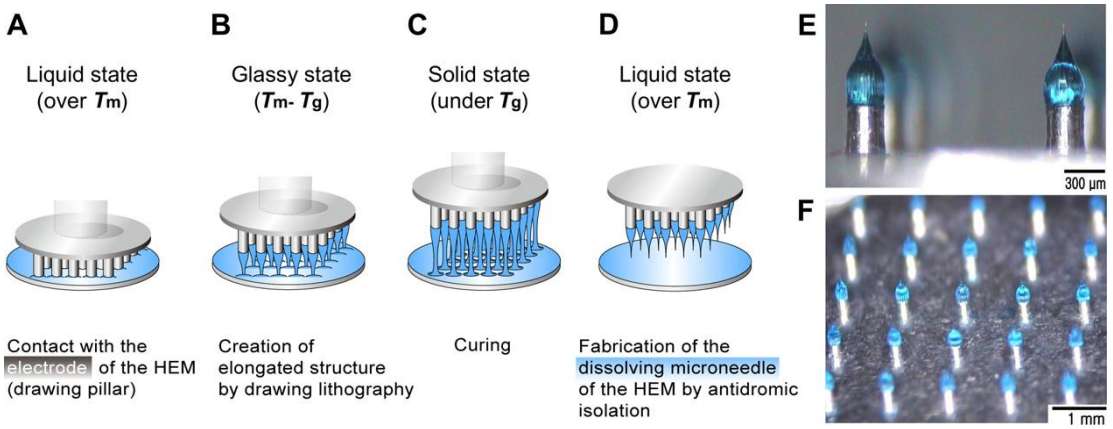


**Fig. 1.22:** Fabrication of a HEM by drawing lithography with antidromic isolation. (A) Liquid maltose, melted at a temperature greater than its Tm, was contacted with electrodes of the HEMs as a drawing pillar. (B) The glassy maltose between Tm and Tg was elongated by drawing of electrodes. (C) After lowering the temperature to sub-Tg, the elongated 3D structures were cured to a solid state. (D) The coating surface was melted at a temperature greater than Tm to isolate elongated 3D structures from 2D coating surface. (E) A bell-shaped dissolving microneedle of the HEM had an ultra-sharp tip diameter of 5 mm and a length of 400 mm. (F) A 5 X 5 array of fabricated HEMs.

Although this fabrication process eliminates the mold and allows a fast delivery, due to the fast dissolution of maltose in water, it requires yet high temperature to melt polymer, making system unusable for thermo-sensitive drugs. Moreover, if prolonged releases are required it is not suitable at all.

Another mold-free fabrication method was contrived by J.S. Kochhar et al., who have developed a simple photo-polymerization method to fabricate microneedles with poly (ethylene glycol) diacrylate (PEGDA) owing to its known biocompatibility and FDA approval for human use. The process consists in two steps: first a thin backing layer and then microneedles are formed. Set-up for fabrication is very simple: the thickness of PEGDA's layer is determined by spacers on which a coverslip is placed. Back layer is produced by irradiating the first polymeric layer through glass, while, to form microneedles is used a photomask, with transparent circle, placed between glass and UV source (figure 1.23) [47].

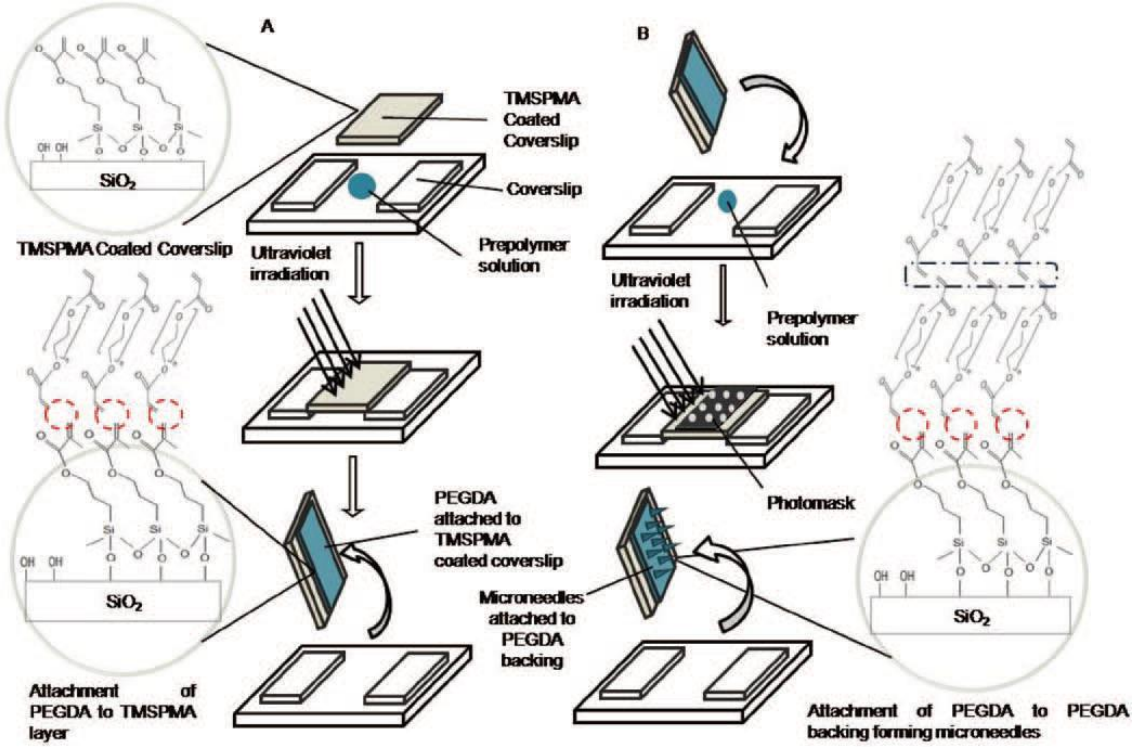


**Fig. 1.23**: (A) Schematic representation of the fabrication process. PEGDA is attached to TMSPMA coated coverslip via free radical polymerisation using UV irradiation, forming the backing for microneedles. (B) Using glass slides as support, the PEGDA backing is mounted onto the set-up with PEDGA filled in the enclosed cavity. Subsequently, the set-up is irradiated with UV light. UV light is only able to pass through the clear regions on the photomask, forming microneedles.

Compared with the other cross-linkable monomers, already mentioned above, the macromer PEGDA can be cross-linked in short time under UV (few seconds). This allows to protect most of the drugs from photo-degradation, but remains the problem of toxicity of photoinitiator.

## 1.4 Applications

The ability of microneedles to release efficiently both small and large molecules has encouraged study of various applications.

Several studies, regarding vaccination through microneedles for influenza [31, 42] and Hepatitis B [49], have demonstrated that with this new method is obtained a clinical response higher than hypodermal injection [50] using a lower drug dosage [51]. Also for other bioactive macromolecules, like insulin, heparine and growth hormone, that cannot be delivered orally because of proteolitic degradation, microneedles represented a valuable alternative. Zosano Pharmahas developed a parathyroid hormone coated microneedle patch system that is now under phase-3 clinical trial. These patches show an ideal plasma profile, indicative of efficient parathyroid hormone therapy in osteoporosis using microneedles [52].

Another, less common, application is drug delivery into eyes through sclera, fibrous membrane containing eyeball, for glaucoma treatment. This administration route has been proved to be more effective than topical administration or systemic delivery [53].

Also in cosmetic and cosmeceutical fields the majority of products can lendthemselves to microneedles technology. So it is possible to apply release through microneedles for treatment against ageing (wrinkles, lax skin), scarring (acne, surgical), photodamage and hyperpigmentation (age/brown spots)[54].

Microneedles can be used, not only to administer drugs, but also to withdraw body fluids for diagnostic purposes. An example is blood withdrawal for glucose estimation: in this way it is possible to reduce blood sample required while making the procedure painless [55].

# Chapter 2

# Experimental method

## 2.1 New manufacturing technique

In this work a new fabrication method that uses an electric field to shape microneedles is discussed. This technique exploits the principle of Taylor's cone formation, for which when an electrically conductive liquid is exposed to an electric field, the shape of the liquid starts to deform. By increasing the voltage, the effect of the electric field becomes greater and a greater and acts on the surface tension of the liquid at the exit of a capillay forming a cone. When it overcomes a certain threshold voltage the tip emits a jet of liquid or breaks in drops (figure 2.1).

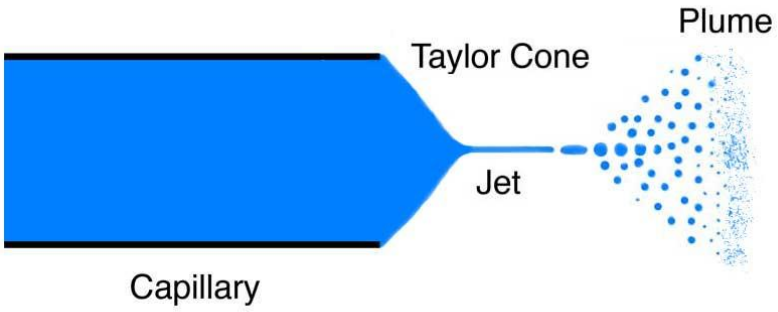


**Fig. 2.1:** Schematic representation of Taylor Cone formation.

This electro-hydro-dynamic (EHD) system for liquid dispensing has been already applied in many fields, like blood plasma separation, drop-on-demand printing of conductive ink and for fabrication of drug delivery systems [56]. Recently the classical configuration, in which the high voltage between the dispensing nozzle and the receiving substrate has applied through an electric generator, has been

changed. As source of the electric field a polar dielectric crystal, which exhibits the pyroelectric effect has been exploited [57]. Pyroelectricity is the ability of certain materials to generate a voltage when they are heated or cooled. The change in temperature modifies the position of the atoms slightly within the crystal structure, such that the polarization of the material changes. This polarization change gives rise to a voltage across the crystal. Polarization in crystal is proportional to temperature variation, according to $\Delta P_i = p_i \Delta T$, where $\Delta P_i$ is the coefficient of the polarization vector and $p_i$ is the pyroelectric coefficient (figure 2.2) [58]. If the temperature stays constant at its new value, the pyroelectric voltage gradually disappears.

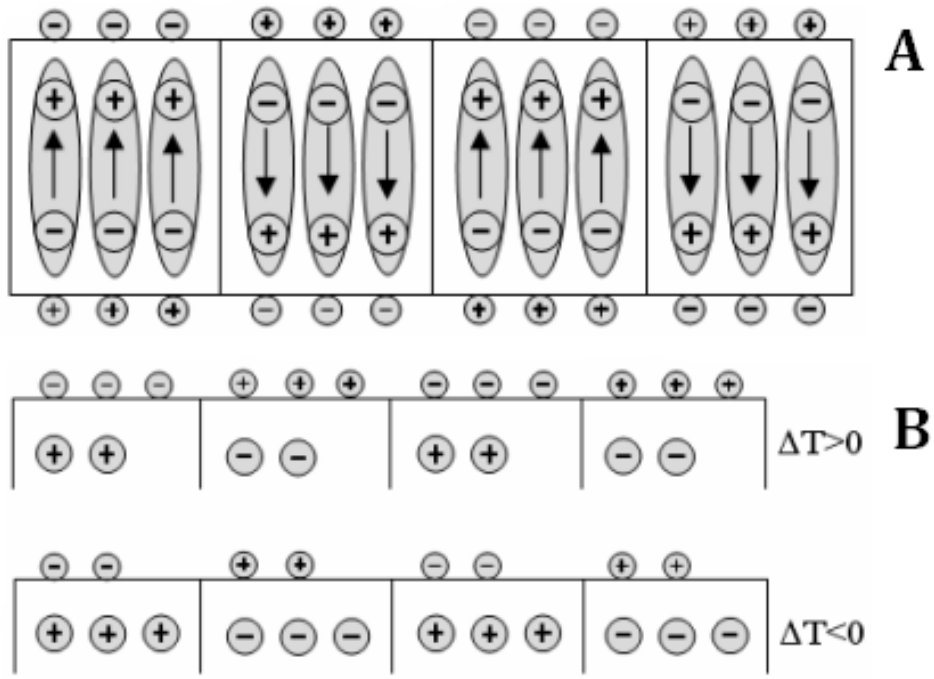


**Fig. 2.2:** Schematic view of the periodically poled pyroelectric crystal sample cross section with the charge distribution exhibited (A) at the equilibrium state; (B) in case of heating (top) and (bottom) cooling process.

In our case electro-drawing is not used to dispense material, in the form of drops or fibers. The process is stopped at the end of Taylor's cone formation, before tip begins to jet liquid. At this point it is essential to be able to lock the structure in the form obtained, in order to preserve a needle shape after removal electric field (figure 2.3).

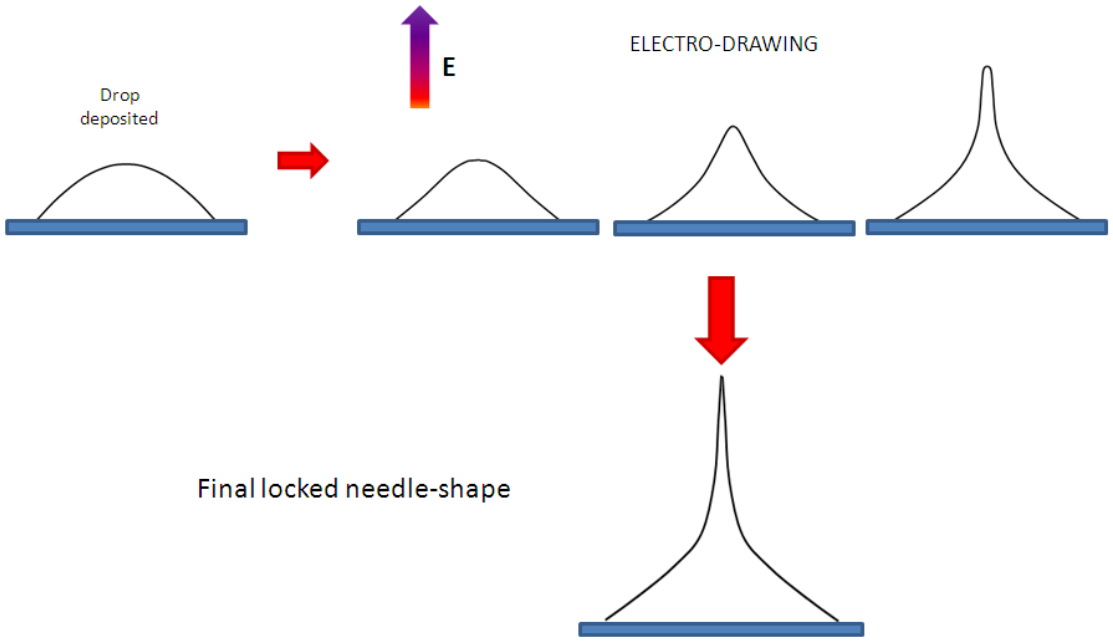


**Fig. 2.3:** Schematic representation of microneedle formation, by using electric field, starting from a polymeric drop deposited on a substrate.

To consolidate the microneedle shape at the end of the electro-drawing step, polymeric material has to become solid enough as much quickly as to prevent its collapse. This is possible by evaporating the solvent if a polymer solution is used, or crosslinking the polymer if using an UV photocurable material.

With this approach main limitations of the classical fabrication methods were avoided. Polymeric solution was deposited directly from the dispensing system to the substrate that will be part of the final device. There is no contact with other elements that can increase risk of cross contamination, like the mold used in the most of fabrication procedures. It is a very fast production that allows obtaining a complete system in few minutes. Moreover the overall procedure is performed at

ambient or bland temperature, thus preserving the integrity of the drug preloaded in the polymeric matrix.

## 2.2 Materials

Poly(lactic-co-glycolic acid) 50 : 50 (PLGA RESOMER® RG 504H), 38000 - 54000 Dalton, was obtained by Boeringer Ingelheim and used as received. Dimethyl Carbonate (DMC, D152927), as solvent of the PLGA, as well as all the chromophores used as model drug like Nile Red (NR, N3013), Rhodamine 6G (Rh6G, R4127) and BSA-TRITC (Albumin, Tetramethylrhodamine isothiocyanate bovine, A2289) and finally 4% Agarose gel (A6689) and Paraffin wax (327204) were obtained by Sigma Aldrich. Poly(dimethyl-siloxane) (PDMS), used as flexible support, was provided by Sylgard® (184 Silicone Elastomer Kit, Dow Corning). Gelatin B, functionalyzed with diacrylates group (substitution degree 64%) was provided by prof. Peter Dubreil from Ghent University. Lithium tantalate crystal was supplied by Roditi International Corporation Ltd (Optical grade LiTaO3 wafer, z- cut, 0.5 mm thickness, both side polished). Pig cadaver skin was kindly provided by dott.ssa Antonelli Carmela of ASL Napoli 2 Nord, taken from the butchery implant ICS (Industria Carni Sud) of Caivano, Naples (IT). Agarose gel (0.4%) was used as model material for the indentation test. The gel was prepared on the day of use by dissolving agarose (Sigma Aldrich Corp, St. Louis, MO) in deionized water.

### 2.2.1 PLGA

The structure of polymeric matrix influences drug release kinetics, so polymer choice depends also on the type of drug that one wants to administer and its optimum release kinetics. In this work the attention was focused on poly(lactic-co-glycolic) acid (PLGA), a polymer widely used for microneedles fabrication [36, 40, 43, 44]. Indeed PLGA is a copolymer used in a host of Food and Drug Administration (FDA) approved therapeutic devices, thanks to its biodegradability and biocompatibility. It is synthesized by means of random ring-opening co-polymerization of two different monomers, the cyclic dimers (1,4-dioxane-2,5-diones) of glycolic acid and lactic acid. Depending on the ratio of lactide to glycolide used for the polymerization, different forms of PLGA can be obtained, each one with different mechanical properties and degradation times. PLGA degrades by hydrolysis of its ester linkages in the presence of water (figure 2.4).

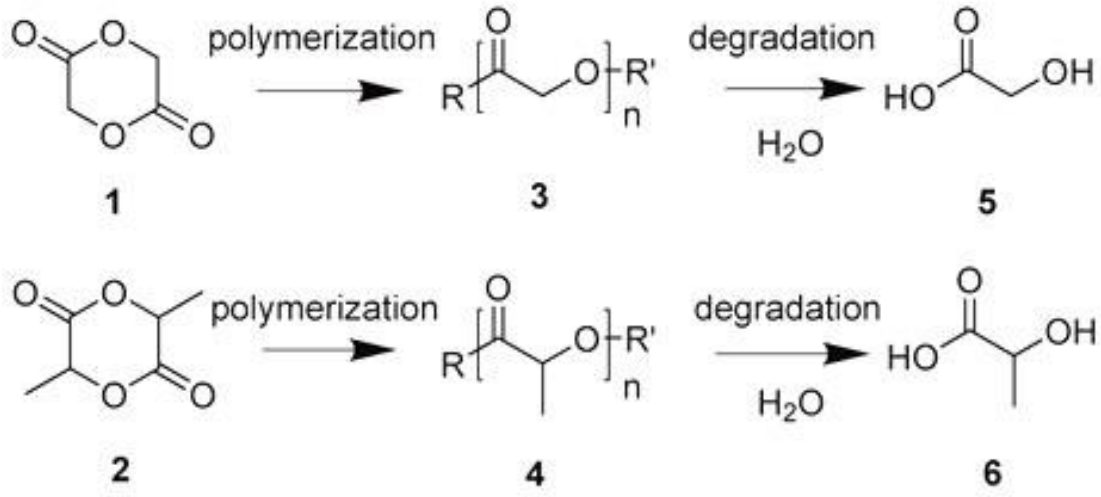


**Fig. 2.4:** Chemical structures of glycolide (1) and lactide (2); the corresponding polymers polyglycolide (PGA) (3) and polylactide (PLA) (4); and glycolic acid (5) and lactic acid (6).

Figure 2.5 illustrates the steps involved in the biodegradation processes. In the first step water wets the surface and diffuses into the polymer. The rate of the diffusion depends on porosity, pore size and surface tension. In the second step, ester linkage hydrolysis cleaves the chain into smaller chain lengths (polymer degradation). As the degradation proceeds, smaller chain segments (<100 g/mole) start to dissolve and polymer erosion takes place (step 3). The solubilized monomers/oligomers are then excreted via the kidney or metabolized into carbon dioxide and water (step 4). PLGA has been successful as a biodegradable polymer because it undergoes hydrolysis in the body to produce the original monomers, lactic acid and glycolic acid. These two monomers under normal physiological conditions, are by-products of various metabolic pathways in the body. Since the body effectively deals with the two monomers, there is minimal systemic toxicity associated with the use of PLGA for drug delivery or biomaterial applications.

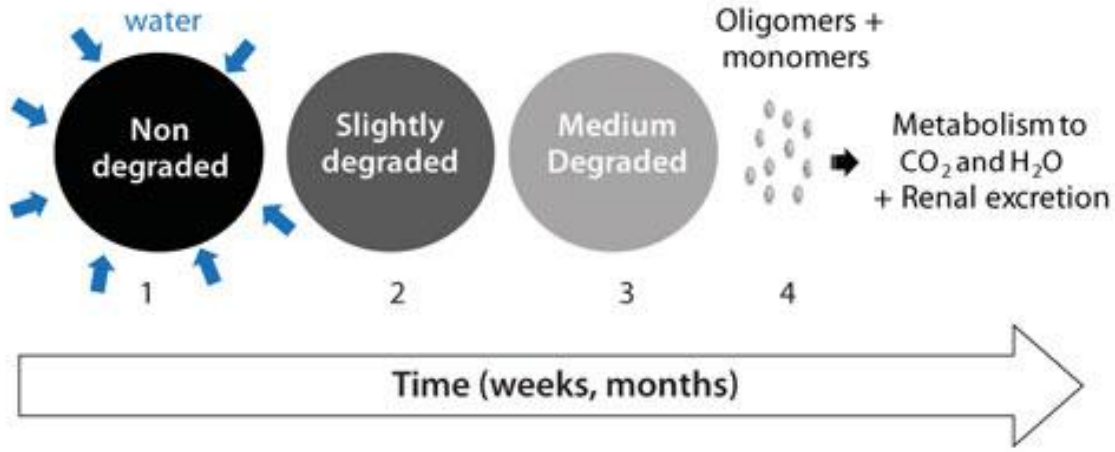


**Fig. 2.5:** PLGA degradation phases: (1) Wetting and water diffusion, (2) Decrease of the molecular weight = Polymer degradation (3) Mass loss = Polymer erosion and (4) Renal excretion or metabolism to carbon dioxide and water.

The complete disappearance of biodegradable polymers after the duration of their lifecycle is a highly desired feature. It has been shown that the time required to degrade PLGA is related to the monomers ratio used in production: the higher the content of glycolide units, the lower the time required for degradation. An exception to this rule is the copolymer with 50:50 monomers ratio which exhibits the faster degradation (complete in about two months). In addition, polymers that are end-capped with esters (as opposed to the free carboxylic acid) demonstrate longer degradation half-lives. The possibility to tailor the polymer degradation time by altering the ratio of the monomers used during synthesis has made PLGA a common choice in the production of a variety of biomedical devices, such as, grafts, sutures, implants, prosthetic devices, surgical sealant films, micro and nanoparticles. Works by the groups of Siepmann, and others show that (i) degradation is often heterogeneous and occurs faster in the central part of the delivery systems, (ii) acidic pH environments are also present in microparticles and (iii) therapeutic agents and/or buffering substances can modify the microclimate and, therefore, the kinetics of polymer degradation and drug release [59, 60].

## 2.3 Fabrication steps

### 2.3.1 PDMS support

A flexible support for microneedles array was fabricated in PDMS. Its superficial hydrophobicity allows drop deposited to assume an emispherical shape that promote electro-drawing. Both flat layer and layers with protruding micropillars were used as base for microneedles. The negative of micropillars array was tooled from a PMMA substrate by using the micro-milling technique [Mini-Mill/GX, Minitech Machinery Corporation], to form cylindrical cavity with a diameter between 500 and 900 μm and 200 μm depth, even though different other sizes are possible. Then, a flexible layer with micropillars was obtained by pouring PDMS, mixed in ratio 10:1 with curing agent, on the above described master and under vacuum until complete disappearance of the air bubbles (figure 2.6). Instead, simple flat layers were obtained by pouring liquid PDMS precursor on a flat glass support for few minutes. Finally PDMS was cured in both cases at 80 °C for 30 min and peeled off from PMMA master or glass.

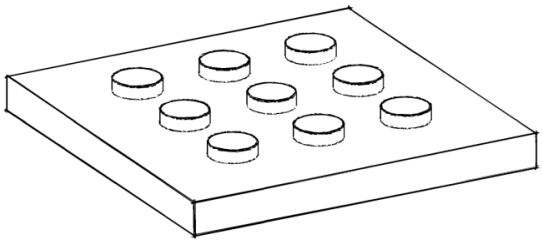

**Fig. 2.6:** Scheme of an array of micropillars made of PDMS as the substrate underneath.

## 2.3.2 Electro-drawing of dissolvable microneedles

Drops of polymer solution at a concentration of 25% w/v were deposited on PDMS or PDMS pillars using a syringe pump (Harvard apparatus – Plus 11), with imposed rate 0.1 µl/min, connected to a capillary of inner diameter 150 µm, and then were positioned on platform of translation stage under a lithium tantalate crystal which was locally heated until 80 °C in correspondence to the drops in order to draw them and create the cone like shape (figure 2.7).

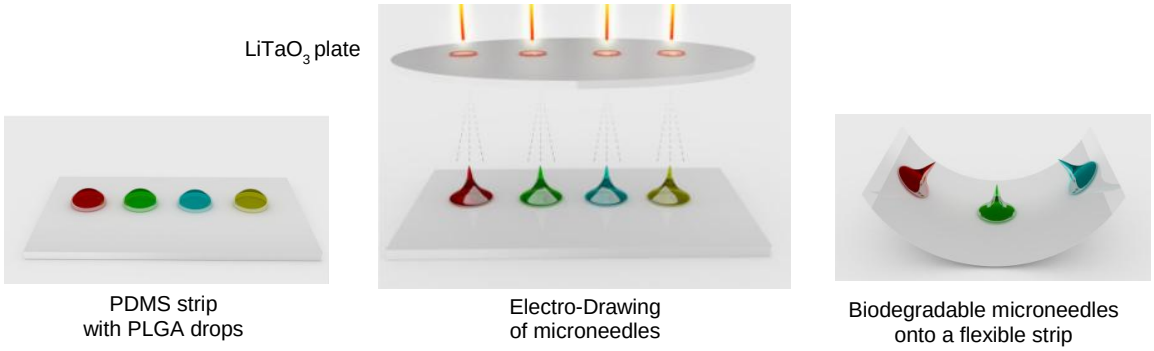


**Fig. 2.7:** Scheme of electro-drawing process: drops are deposited on PDMS strip, $L_iT_aO_3$ plate is heated with metal tip in correspondence of drops, which are deformed under action of electric field. So are obtained microneedles on flexible substrate.

A 5x microscope objective and a high-speed digital CMOS camera (pixel size 12x12 $mm^2$, frame rate of 500 frames/s with 1280(H) x 1024(V) spatial resolution) were used to capture side view pictures and videos during microneedle formation.

Viscosity of PLGA solutions was measured with Ubbelohde viscosimeter to identify concentration range employable to fabrication. It is a fundamental parameter, as a too high viscosity does not allow drops to deform under action of electric field, while a too low viscosity causes loss of needle shape before structure is consolidated.

As DMC has a partial polarity, it was possible to produce microneedles preloaded with hydrophobic, as NR, and hydrophilic, as Rh6G, model drugs, at 0.1%, 0.2% and 0.4% w/w respect to PLGA, to study their distribution inside needle.

To obtain porous microneedles a water solution was prepared with lecithin, a phopholipid used as surfactant, and TRITC-albumin, used as a model drug. This aqueous phase was emulsified in the PLGA solution by using an immersion sonicator (Ultrasonic Processor VCX500 Sonic and Materials) for 20 s at 30% of power, keeping the sample in ice bath. Moreover, to avoid wasting of drug, it was developed a method which allowed to confine it only in the cone which is the part of needle that enters in skin. This was made possible through a double drop deposition: in this way, at first it is deposited a drop of simple solution of PLGA, and then, it is dispensed a second drop of emulsion with drug, with a volume approximately one-tenth of the first one. Successive steps are unchanged (figure 2.8).

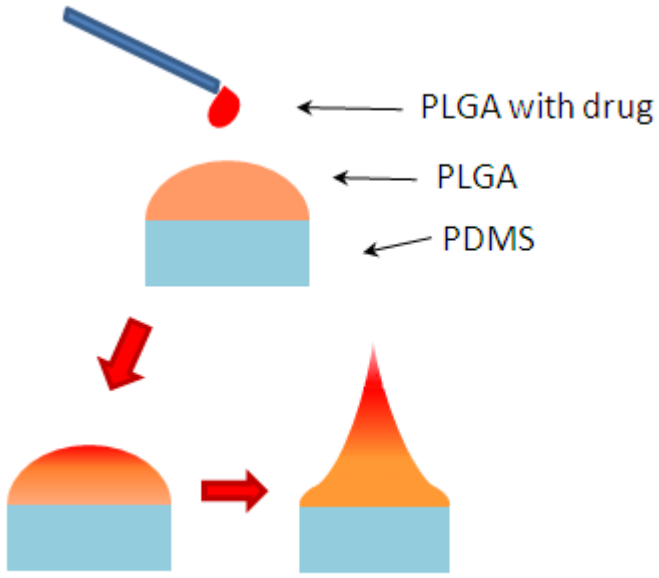


**Fig. 2.8:** Schematic representation of double drop deposition process.

After the electro-drawing process, microneedles can be kept in temperature at about 40 °C for 10 min, to accelerate solvent evaporation and fix needle shape.

### 2.3.3 Microneedles by stamp

As reference, some PLGA microneeedles were produced in a conventional way by replica onto a master. The master utilized was in Cyclic Olefin Polymer (COP) and presented an array of protruding microneedles each one 100 x 100 μm wide and high 250 μm high, with pyramidal tip (figure 2.9).

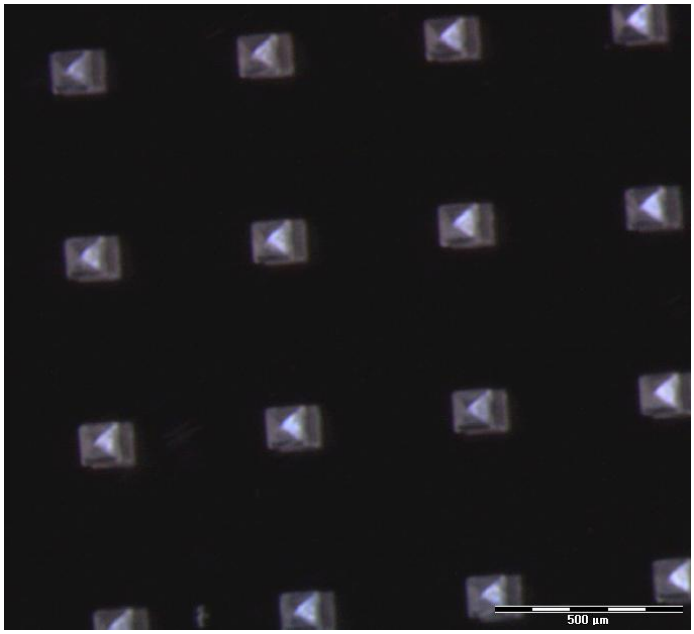


**Fig. 2.9:** Master of microneedles with square base and pyramidal tip.

The final mold was replicated by pouring PDMS, mixed in ratio 10:1 with curing agent, on the master and by curing at 80 °C for 30 min.

Different PLGA solutions were prepared, varying content of water and concentration of lecithin: specifically, water solutions with lecithin concentration of 20, 40 and 60 mg/ml have been used, while the amount of water was about 30 wt%, 60 wt% and 80 wt%, respect to the PLGA mass. These solutions were casted on a PDMS mold, and after few seconds under vacuum to facilitate filling of

cavities, they were rest at 40 °C for 1h and then dried for a day at ambient conditions.

## 2.4 Morphological analysis

Several analyses were performed to study morphological aspects of microneedles, and correlated properties, especially kinetics of drug release and mechanical resistance.

### 2.4.1 Chromophore distribution

To understand how hydrophilic and hydrophobic chromophores were distributed inside the microneedle, in consequence to their interaction with the electric field, electro-drawn microneedles were incorporated in PDMS, cured for 48 h at room temperature, and then frozen at -130 °C in Leica CryoUltra Microtome EM-FC7-UC7. Samples were sectioned at a thickness of 5 μm for confocal analysis in axial direction. Slices of samples were analyzed with a confocal Leica TCS at 543 nm using a 25X water immersion microscope objective. While cutting, slices tend to bend so they are not perfectly outstretched on cover glasses. For this reason, as surface is not included entirely in the same focal plane, to acquire entire slice, stack acquisitions were made on thick layers using 2 μm Z-step. Acquired images were added all together and analyzed using ImageJ (Java-based image processing program developed at the National Institutes of Health) studying fluorescence profile in axial direction and transverse at certain distances from tip, as showed in figure 2.10.

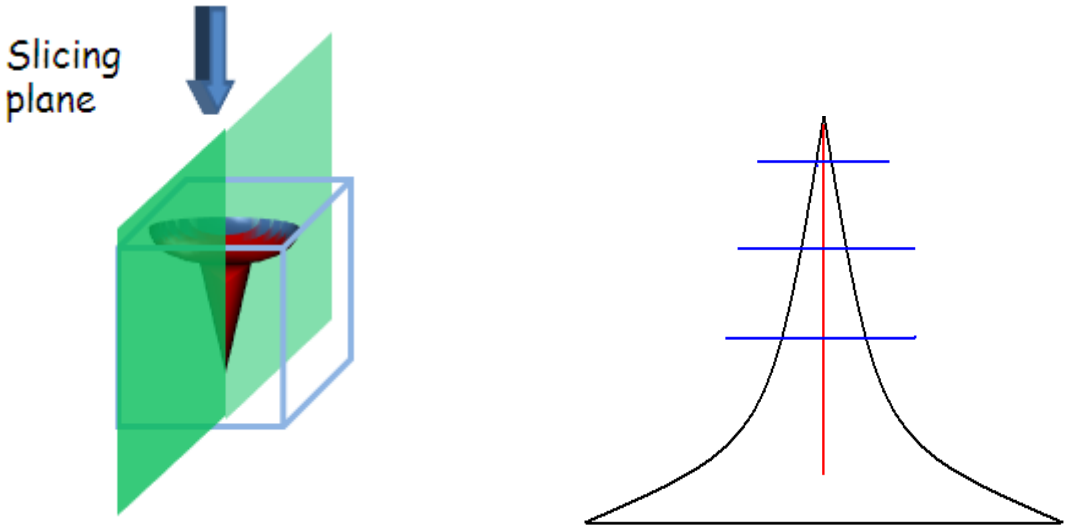


**Fig. 2.10:** Schematic illustration of section plane direction (left) and line direction for acquisition of chromophore intensity.

## 2.4.2 Porosity

Microneedles porosity is of fundamental importance since it affects mechanical proprieties and drug release kinetics. Microneedles were sectioned as described above at a thickness of 10 µm. A morphological analysis was performed using scanning electron microscope (SEM) (field emission Ultra plus Zeiss), on both porous and non-porous microneedle slices, to study how emulsion parameters influences porosity in microneedles matrix. Samples were sputter coated with a 15 nm thick gold layer and to avoid damage inside them, it was imposed a voltage (EHT) of 5 kV. Morphological analysis of porosity was carried out both on electro-drawn microneedles and on microneedles produced by mold, to check if, by using a PLGA solution with same composition, it was possible to obtain in the same morphology even though with different fabrication methods.

## 2.5 Mechanical characterization

The fundamental requirement for microneedles is mechanical resistance adequate, that allows to puncture stratum corneum. For this reason is very important to evaluate mechanical properties of material used to fabricate microneedles and their capability to indent skin.

### 2.5.1 Analysis of mechanical properties

To guarantee a good efficiency in skin indentation the safety factor, defined as the ratio of failure force to insertion force, has to be always above unity. This means that polymer used to fabricate microneedles have to be a Young's modulus greater than 1GPa [36]. PLGA elastic modulus was analyzed through nano-indentation tests, using Nano Indenter G-200, from Agilent Technologies equipped with berkovich tip, a three-sides pyramidal diamond tip, with a semi-angle of 65.03°.

To verify through nanoindentation that matrix, porous and non-porous, of microneedles have enough mechanical resistance, they were prepared small polymeric blocks with same composition used to fabricate microneedles. Several drops were deposited on a microscopy glass and consolidated by keeping glass at 40 °C for 1h and then in vacuum overnight. Last step, to ensure complete solvent evaporation, was lyophilisation.

The test was carried out at 25 °C, by keeping temperature at constant value using a circulating bath (PolyScience). The indentation was performed in dynamic mode, with tip's frequency fixed at 40 Hz and oscillation amplitude of 2 nm. When a value of Harmonic Contact Stiffness higher than 100 N/m was detected during surface approaching phase, the surface of the sample was recognized and the test starts.

### 2.5.2 Indentations in skin

At first, indentation tests were performed in agarose and paraffine wax. Thin layers were prepared using these materials on a microscope slide, which was connected to a computer-controlled x, y axes translation stage, with movement velocity of 0.7mm/s facing down the polymer strip with the microneedle. The indentation experiment was visualized in situ in real time by an optical set-up. A conventional blue collimated led light (wavelength of 470 nm and beam power around 400 mW) illuminated the cross section of the microneedle while a digital CMOS video camera (pixel size 12X12 $\mu m^2$; frame rate of 500 frames/s with 1280(H)X1024(V) spatial resolution) was used for recording the process. A 5X microscope objective was adopted to image the process on the CMOS sensor. By controlling the distance in real time the agarose block was put in contact with the needle tip until reaching the needle base.
Then, a series of three microneedles was inserted in a full thickness cadaver pig skin without subcutaneous fat layer. It was shaved with depilatory cream and washed in a phosphate buffered saline (PBS) solution; finally it was placed on absorbing paper few minutes to eliminate water in excess. The indentation test was carried out with a system emulating the application of the microneedles patch through a bracelet.

Pig skin was positioned onto a cylindrical tube, with diameter of about 5 cm, and gently stretched by hand. Microneedles, previously attached on the plastic plate of the bracelet, were pressed on skin and kept close by means of elastic bands and Velcro for 10 min (figure 2.11).

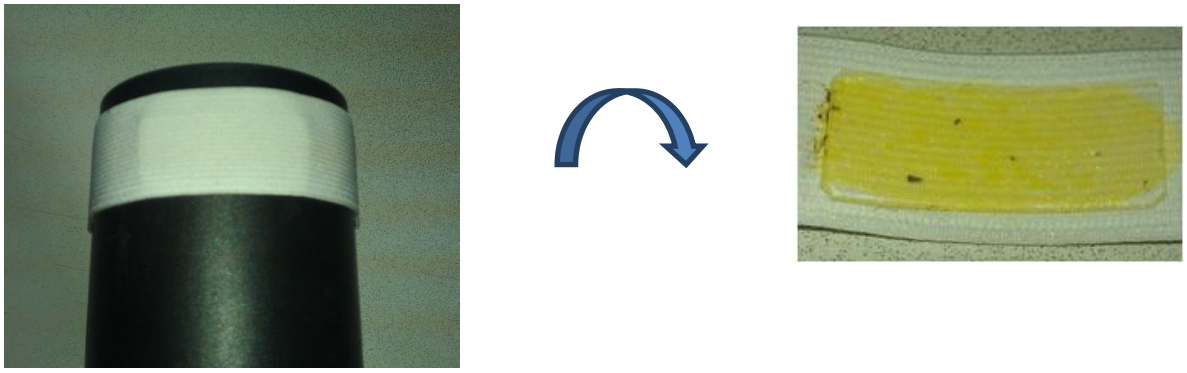

**Fig. 2.11:** System, tube and bracelet, to simulate application of microneedles-patch in a possible final device.

The pressure exerted by tightening the cuff was measured by introducing a pressure sensor (CZN-CP1, TME electronic components) between the cuff and the flexible layer supporting microneedles.

After indentation, microneedles were removed and the skin was fixed in a solution of 10% neutral buffered formaline for 24 h, dehydrated in an incremental series of alcohol (75 %, 85 %, 95 % and 100 %, and 100 % again, each step 20 min at room temperature) treated with xylene and then embedded in paraffin. Successively, samples were sectioned at thickness of 6 μm, and stained with hematoxylin and eosin, and finally the sections were mounted with Histomount Mounting Solution (INVITROGEN) on coverslips and the morphological features of constructs were observed with a light microscope (BX53; Olympus).

## 2.6 Drug release kinetics

The kinetics of drug release was studied in vitro by confocal laser scanning microscopy (CLSM), to follow the release of albumin-TRITC from single microneedles in a gelatin matrix. In this study a new analysis approach was considered, differently from the conventional ones that do not reproduce real release conditions. For example, diffusion tests with Franz Static Diffusion Cell account only for skin permeabilization due to the treatment with microneedles, without considering drug's diffusion time throughout polymeric matrix of needles [36]. From the other side, "*in vitro*" characterization, using PBS solutions, gives a lower degradation rate than *"in vivo"*. The faster degradation under "*in vivo*" conditions is due to the autocatalytic effect of the acidic degradation products which are released from the polymer matrix but accumulated in the medium surrounding the device [62]. On the contrary, characterization in vitro using a "solid" matrix of gelatin, allowed approximating more precisely the delivery conditions in skin. Moreover, this is a non-destructive method that allows acquiring, at scheduled times, images on the same sample. The aim was to understand how porosity influences kinetic release.

CLSM analysis was carried out with a Leica TCS SP5 confocal microscope using a 25x/0.95 water immersion microscope objective. Settings, in terms of laser power, pinhole aperture and detector gain, were optimized at zero time on microneedles. To analyze fluorescence on the entire volume of the microneedle, acquisitions were carried out in z-stack. Fluorescence signal was collected on several slices, spaced by 5 μm, until they covered the whole volume.

Preliminary experiments showed that bleaching, investigated at the highest laser intensity used for the acquisition, was extremely low even after 5 min of continuous irradiation. Therefore, since stack acquisition on microneedle lasts maximum 30 seconds, chromophore degradation due to the laser radiation was considered to be negligible in the following experiments. This means that it is possible to consider fluorescence reduction of microneedles with time, as an effect due only to diffusion of model drug in gelatin. In order to obtain a good signal while diffusion continues, causing concentration reduction of model drug in

microneedles, for the whole period under examination, AOTF (Acousto Optical Tunable Filter) value was changed. Indeed, by increasing laser intensity, it increases the number of chromophore's molecules excited, so it is possible to collect a signal with greater intensity.

In figure 2.12 it is showed the ratio between AOTF value and fluorescence collected from a standard reference. Since to an higher laser intensity corresponds an higher signal collected, at the end of delivery experiment, it was necessary to bring back all fluorescence signals, to the same laser intensity, in order to compare them. This was possible by making a proportion between intensity (showed in table below) corresponding to two laser intensities of interest, and scaling microneedle's fluorescence to the first laser intensity.

| % AOTF | Intensity |
|---|---|
| 0 | 34 |
| 1 | 40 |
| 2 | 45 |
| 3 | 53 |
| 4 | 62 |
| 5 | 74 |
| 10 | 164 |
| 20 | 489 |
| 30 | 971 |
| 40 | 1532 |
| 50 | 2096 |

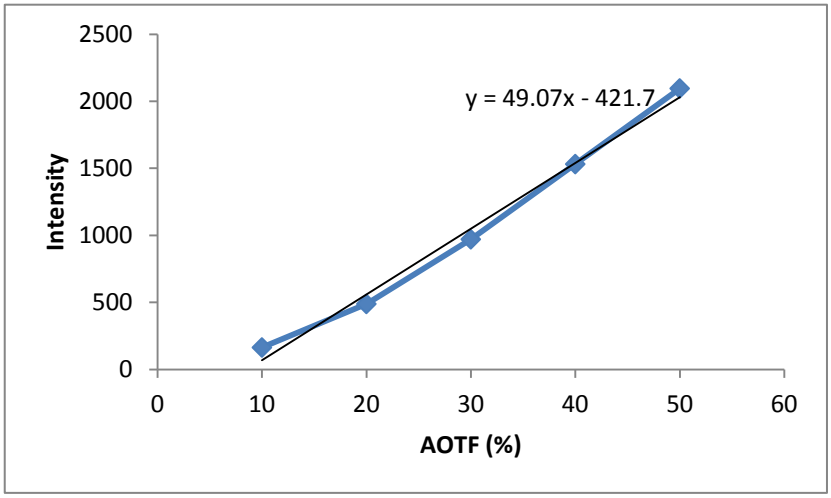


**Fig. 2.12:** Fluorescence signal from standard obtained changing laser intensity (% AOTF). Approximation of experimental points with trend curve (right).

This procedure is justified because a linear relationship exists between laser intensity and fluorescence signal collected; this is true until chromophore saturation is reached. The saturation phenomenon occurs when all chomophore's molecules are excited, so increasing laser intensity, does not provide any increase in the signal collected. Since in these tests low laser intensities were used, saturation has not been reached, thus preserving linearity.

### 2.6.1 Sample preparation

For simplicity, preliminary studies of release kinetics were performed on microneedles obtained by mold. PLGA solutions were prepared with different water content (30 %, 60 % and 80 % respect PLGA mass), in which the concentration of TRITC-albumin was conformed for all of them at 0.625 mg/ml (w/v) respect to final volume of microneedles.

Before starting delivery tests, preliminary experiments were performed, to ensure the preservation of hydratation of gelatine matrix during the release period, to exclude any alteration of diffusion. Gelatin B (DS 64 %), dissolved in a water solution with 5 % DMSO, was prepared at 10 % w/w, and after addition of dare-cure (0.75 % w/w respect to gelatin), about 250 µl was poured in Petri dish's well, closed with cover-glass and cured by UV exposition at 365 nm for 20 min.

The bottom part of the Petri dish and the cover glass above gelatine were sealed. To find the best system to limit water loss they were tested three different sealings: Norland optical adhesive, that was UV cured; picodent twinsil, a bifasic silicon, and hot glue (figure 2.13).

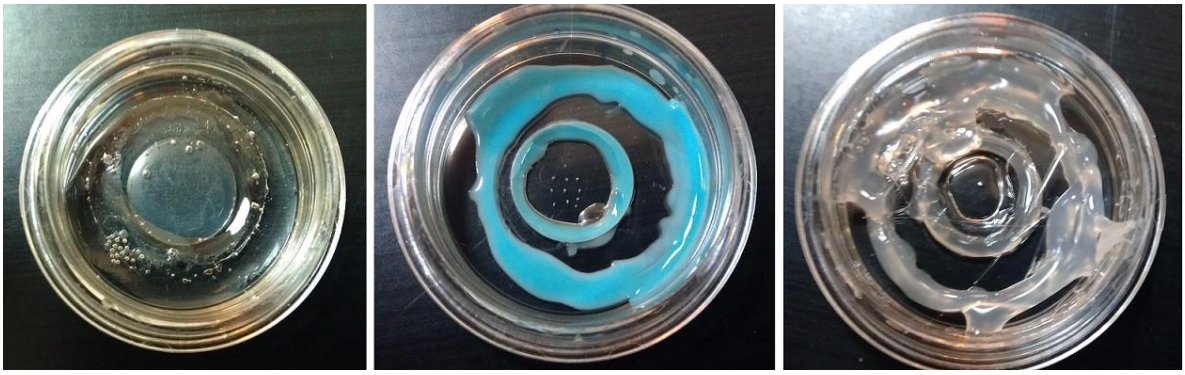

**Fig. 2.13:** Three samples sealed with different methods: Norland optical adhesive (left), Picodent twinsil (centre), hot glue (right).

After three days in incubator at 37 °C, it was evaluated water loss by weighing the samples.

In the preparation of the samples some requirements have to be respected; they depend on the method chosen to analyze drug delivery. In particular, it is necessary to position microneedles at same distance from bottom glass and preserve their position during release period. For this reason it was not possible to use conventional gelatine since at 37 °C, it becomes liquid, causing motion of microneedles. On the contrary, a fixed position for all microneedles included in gelatine is a very important requirement, since intensity of fluorescence signal depends on the distance between needle and bottom of Petri dish. By immobilizing microneedles, a variation in signal can be rightly attributed just to a variation in chromophore's concentration. Therefore, to optimize acquisition and comparison between fluorescence signals all microneedles were positioned at the same level by assembling gelatine matrix through three layers (figure 2.14).

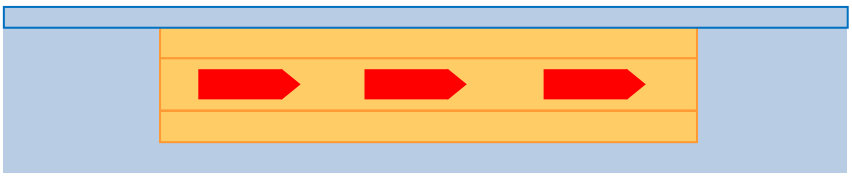

**Fig. 2.14:** Schematic representation of sample prepared for drug release kinetics.

First, 40 µl of gelatine were poured in the central well of a microscopy dish, that has a diameter of 12 mm, and partially photocured for 10 min. On a second layer, that was completely cured, ten microneedles were positioned and finally this layer was turned upside down and kept on the first layer. Liquid gelatine was then added to completely fill the well, closed with a cover glass and again UV cured at 365 nm but this time for 20 min.

## 2.6.2 Determination of acquisition parameters

For quantification analysis it is important to reduce as much as possible the noise and distinguish the signal of interest from everything else. Moreover, especially when there is a low concentration of chromophore, autofluorescence of polymeric matrix can overlap and hide the signal.

Considering excitation band of albumin-TRITC (figure 2.15), used as model drug, to obtain a good signal from chromophore, samples were excited using a laser at 543 nm.

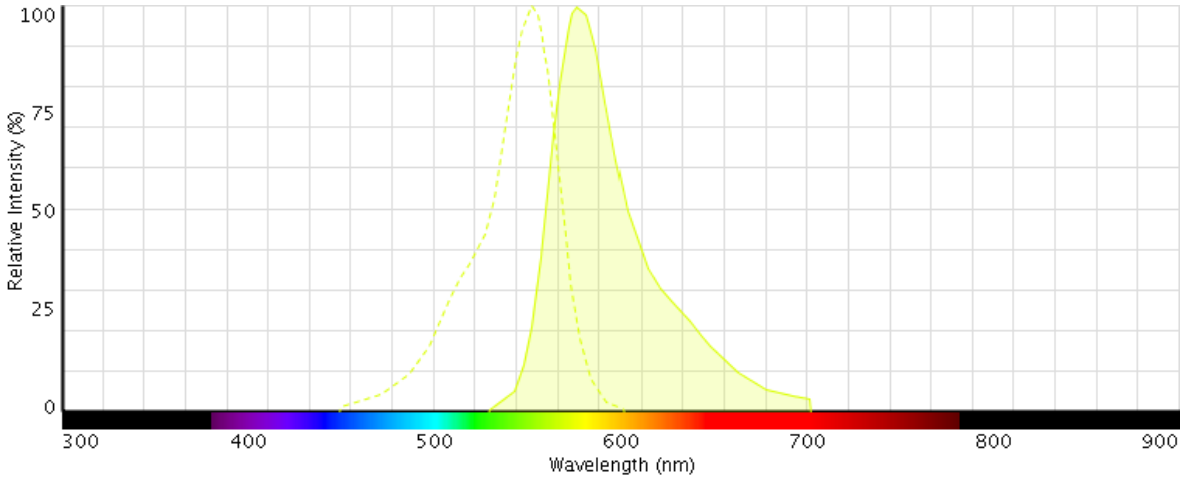


**Fig. 2.15:** Excitation (left) and emission (right) spectra of albumin-TRITC.

Then, in order to maximize signal/noise ratio, auto-fluorescence of PLGA was analyzed between 450 and 700 nm which is the emission frequency band corresponding to BSA-TRITC emission, thus determining the best frequency band to acquire fluorescence. This test was carried out with a Leica TCS MP-SP5 confocal microscope in two-photon mode, at 950 nm. In this mode each photon carries approximately half the energy necessary to excite the molecule, which emits a fluorescence photon if reached by two photons simultaneously. Using laser in infrared range, far from frequency band investigated for autofluorescence, it is possible to acquire it completely. While, using a laser, whose wavelength is included in band analyzed, we should avoid frequencies nearly close to the laser, where the signal would be covered by light emission. Autofluorescence emission spectrum was collected using an acquisition band 10 nm wide. The peak resulted at 660 nm; it means that this wavelength has to be avoided during analysis of release kinetics to minimize noise (figure 2.16). So the detected fluorescence emission bands were set between 560 and 610 nm during measurements.

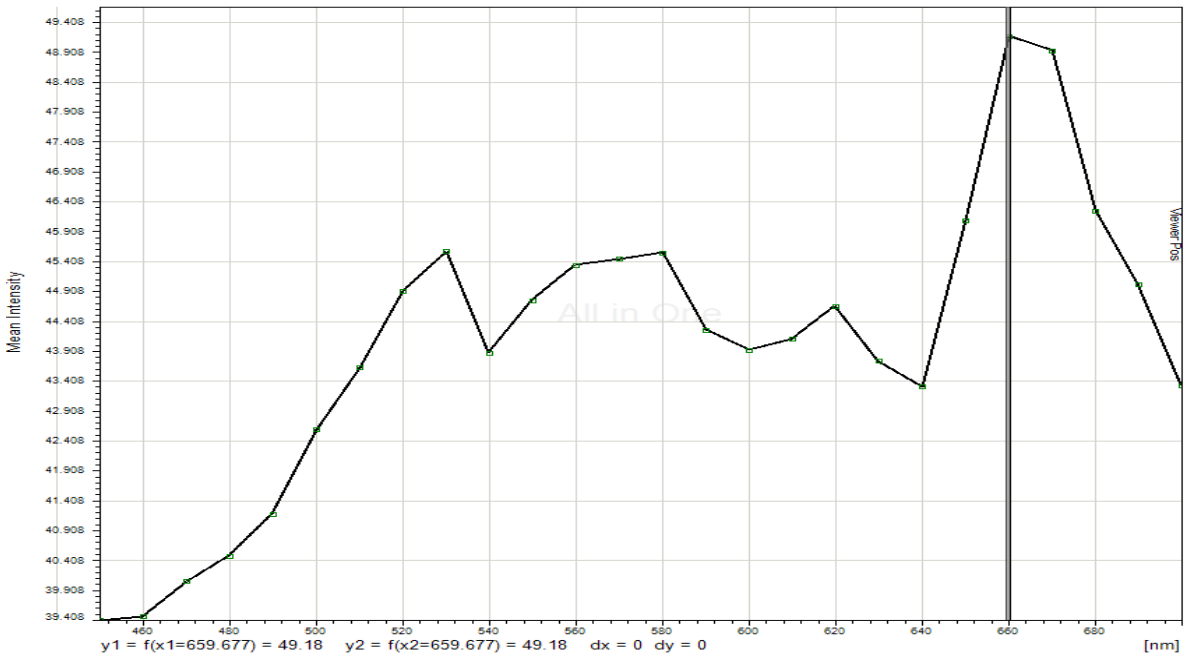


**Fig. 2.16:** Autofluorescence spectrum of PLGA.

### 2.6.3 Drug loaded quantification

To measure the effective amount of drug loaded in microneedles it was used Enspire 2300 Multimode Reader Fluorometer.

A calibration line was calculated by analyzing fluorescence of BSA-TRICT water solution at known concentrations (figure 2.17). Different concentrations were chosen, from 0 to 2.5 µg/ml of model drug. Then, 150 µl of solution were loaded in a 96-well plate, each sample in triplicate to mediate results of analysis. The chromophore was excited at 550 nm and emission signal was collected at 570 nm.

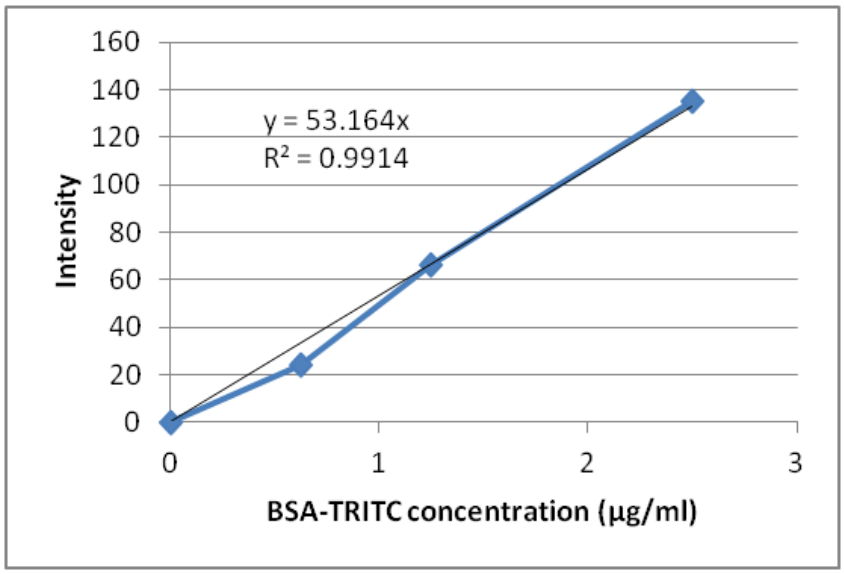


**Fig. 2.17:** Calibration line for BSA-TRITC obtained from spectrofluorometric analysis.

Once obtained the relation between fluorescence signal and BSA-TRITC concentration, it was possible to calculate the amount of drug present in a microneedles array. As microneedles are too small to contain enough cromophore to be detected by the instrument, an entire array, composed by microneedles and back-layer was used to calculate BSA concentration.

Emulsion remains stable during preparation and drying, so it was assumed that water phase compartments have an homogeneous distribution between microneedles and support layer. Consequently also BSA-TRITC was considered

uniformly distributed in entire sample. To quantify model drug loaded, PLGA samples were completely dissolved in 500 µl of dichloromethane (DCM), and then it was added 1ml of water. As BSA-TRITC is water soluble, it diffused from DCM towards water. Finally solutions were centrifuged for 5 min at 5000 rpm; 600 µl of water were collected from each sample and analyzed with spectrofluorometer. At the end, the concentration of BSA-TRITC, detected in solutions, was normalized respect to the mass of entire sample dissolved. To calculate the only mass of the microneedles, 60 of them were cut by hand from a piece of array, weighing sample before and after the cut. In this way it was possible to evaluate the mass of a single microneedle and BSA included in it.

# Chapter 3

# Results and discussion

## 3.1 Electro-drawn microneedles

The electro drawing system is relatively easy to assemble and consists basically of a polar dielectric crystal (lithium tantalate - LT) facing the polymer reservoir deposited onto PDMS strip. The deposition of a multiple base drop allows the formation of microneedles under an array-like configuration. The reservoir drops dispensed, using a syringe pump, directly onto the substrate, are subjected to the electro-drawing process under the action of the pyro-electrohydrodynamic (EHD) force. The local heating induced onto the drop reservoir by the termal stimulus applied to the crystal was measured during the experiment by color change using a termo camera (Flir i7) and it is < 40 °C. During the drawing process, the liquid cone becomes solid thanks to the evaporation of the solvent, that blocks the electro-drawn cone, thus giving to microneedles the desired shape. A post thermal treatment (40 °C for 10 min), performed by holding microneedles with tip downwards, can be applied to the microneedles to accelerate and complete solvent removal. With a fast evaporation, polymeric solution has no time for relaxation which would lead to a loss of aspect ratio and a bigger basement. In this way, instead, it is obtained a shrinkage of the base of cone with an improvement of microneedle's aspect-ratio.

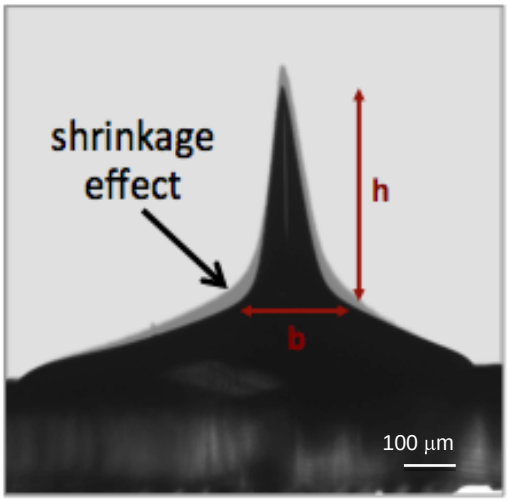


**Fig. 3.1:** Shrinkage obtained with fast evaporation solvent .

The process described above shows for the first time, to the best of our knowledge, the usage of EHT force for drawing a drop of polymer solution directly into a microneedle shape. A preliminary investigation was performed on the formation of a single microneedle from PLGA solution in order to characterize the main conditions that regulate the microneedle formation. Typically, the base drop was deposited onto a PDMS strip and had a volume ≤ 0.1 μl. The distance between the reservoir and the crystal was crucial and depended on both the volume and the contact angle of the base drop. The driving plate was heated locally in correspondence of the base drop, while approaching the base reservoir. Since the EHD force depends on the viscosity of the fluid, the control of this parameter was crucial for the successful formation of microneedles with the necessary shape. A proper range of polymer concentrations was chosen, from 20 to 30% w/v, to guarantee suitable viscosities. From experimental tests, it was concluded that the best operation condition is defined by 25% w/v of polymer solution. Viscosity was measured by Ubbelohde viscometer (figure 3.2), which uses a capillary based method. The solution was introduced into the reservoir (3) until filling between levels B and C, and then was sucked through the capillary (2). By looking at the liquid travelling back through the measuring bulb it was then taken the time to move from level B and A which allowed to measure the viscosity. In general, the pressure head in this kind of instrument only depends on a fixed height and no

longer on the total volume of liquid, thanks to a third arm extending from the end of the capillary and open to the atmosphere.

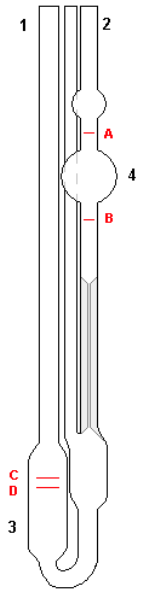


**Fig. 3.2:** Scheme of Ubbelhode viscometer, showing capillary of injection (1), reservoir (3), capillary to suck solution until complete filling of measure bulb (4)

Viscosity range, calculated from measuring the different times, and suitable for this fabrication method was around 80 to 240 $mm^2/s$. In particular, the solution at 25% w/w of PLGA, used to fabricate microneedles for this work, showed a viscosity of 125.75 $mm^2/s$ (figure 3.3).

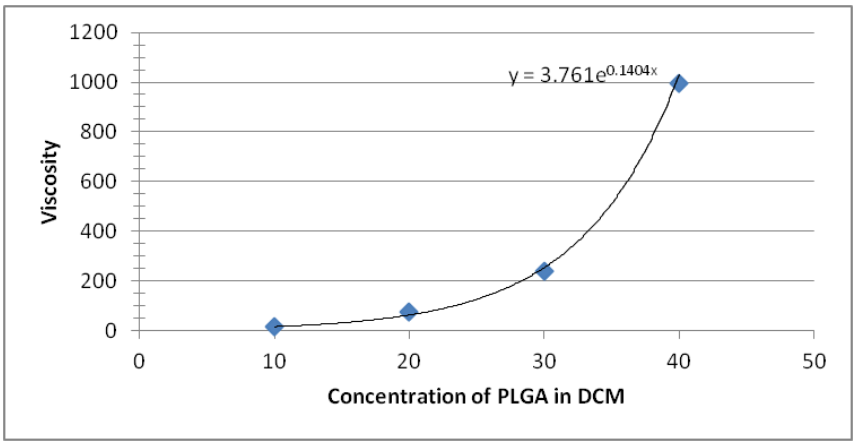


| PLGA (%) | Time (s) | Viscosity ($mm^2/s$) |
|---|---|---|
| 10 | 1.53 | 13.53591 |
| 20 | 8.7 | 76.9689 |
| 30 | 27.14 | 240.10758 |
| 40 | 112.69 | 996.96843 |

**Fig. 3.3:** Plot of viscosities for solutions at different concentration (up) and relation between times, measured with Ubbelhode, and viscosity (down).

Electro-drawing method provides remarkable degrees of freedom in moulding the shape of the microneedles. The polymer microneedle was formed in a single step by controlling the distance d between the base (contact angle θ) and the DP. In particular starting from the volume V of the drop reservoir we defined a critical distance $D_c$ so that the process takes place for values of distance shorter than the critical one:

–

In this condition controlling the volume of the drop reservoir and the critical distance it is possible to control the height of the needle produced.

## 3.2 Microneedles on pillars

As regulation of volume is a fundamental factor for the determination of the final microneedle's height, PDMS micropillars were used as base to deposit drops with hogh control on the volume uniformity. Micropillars were shaped from wells worked in PMMA by using the micro-milling technique (figure 3.4). Wells were drilled with the diameter in the range from 500 to 900 μm, to verify correlation between deposited volume and resulting microneedle.

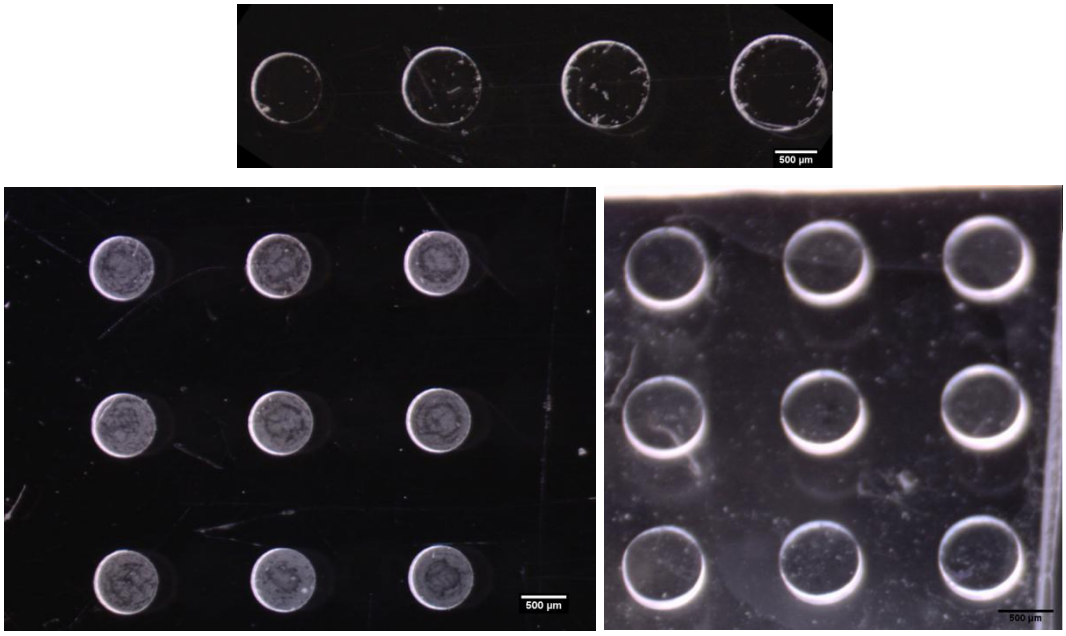


**Fig. 3.4:** Micro-wells drilled in PMMA, with increasing diameter, from 600 to 900 μm (up), and an array with 700 μm diameter (down, left). PDMS pillars replaced from wells-stamp (down, right).

Micro-drops were deposited by contacting the drop ejecting by the capillary connected to syringe pump, with the surface of pillars (figure 3.5). In this way by varying pillar's diameter it was possible to control the amount of solution that can be deposited forming reservoir for needle fabrication.

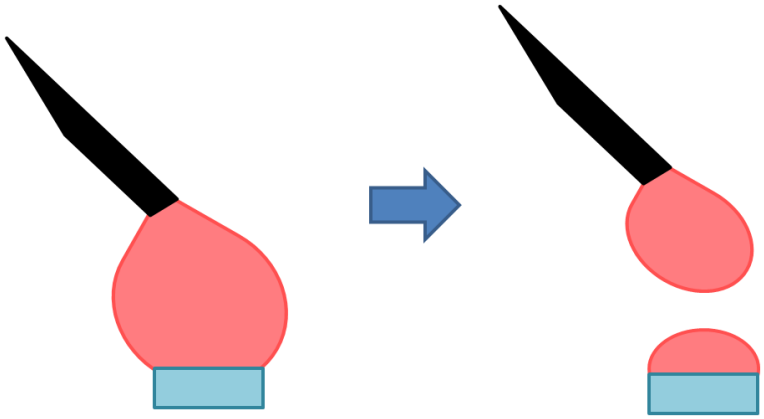

**Fig. 3.5:** Schematic representation of deposition on pillar by contact

Referring to the needle height, h, it was measured considering only the cone without the pedestal. For base drops of 0.05µl < V < 0.1 µl, the typical height of a microneedles was 300 µm < h < 500 µm, which falls within the range used for indentation applications. The method also allows controlling needle's height and aspect ratio as a function of droplets. As shown in figure 3.6, needle height increases with the volume of the drop and aspect ratio h/b can be modulated accordingly.

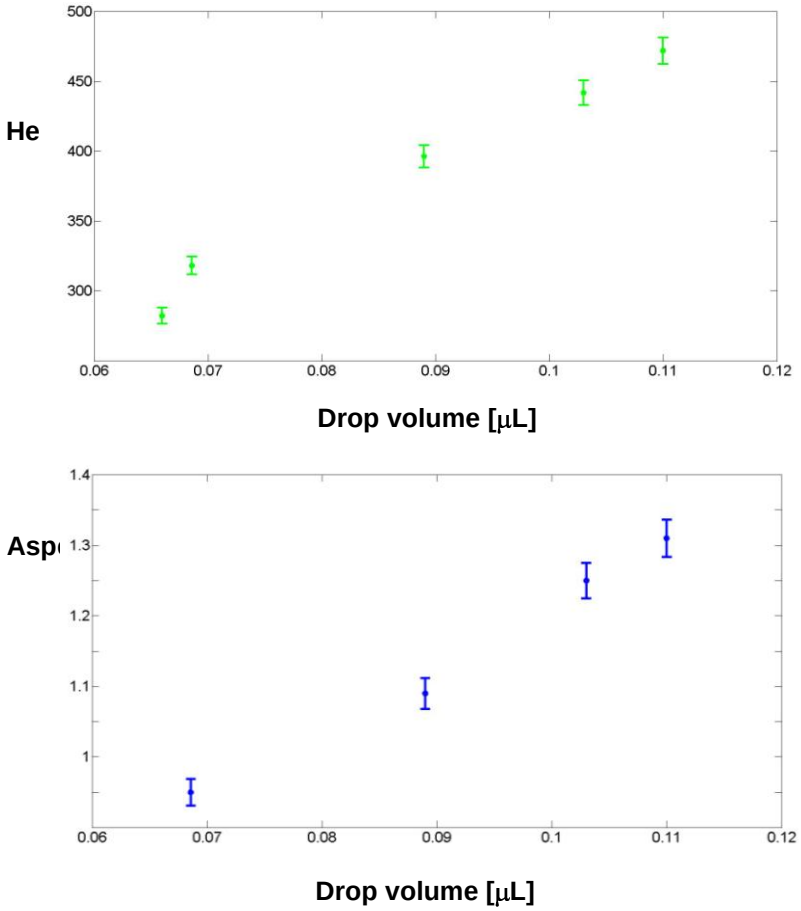


**Fig. 3.6:** Measures performed on images obtained by digital CMOS camera (1280(H) x 1024(V) spatial resolution) showing correlation between final microneedle's height (up) and aspect/ratio (down )and initial drop's volume.

For instance, aspect ratios of 1.3 were obtained starting from a 0.1 μl drop reservoir. The increase of the aspect ratio with the droplet volume is most probably due to the fast consolidation of the walls with respect to the inner core that feeds the increase of the height under the persistent electric field.

In figure 3.7 it is showed as increasing pillar's diameter, it is possible to deposit a larger drop that entails formation of taller microneedles.

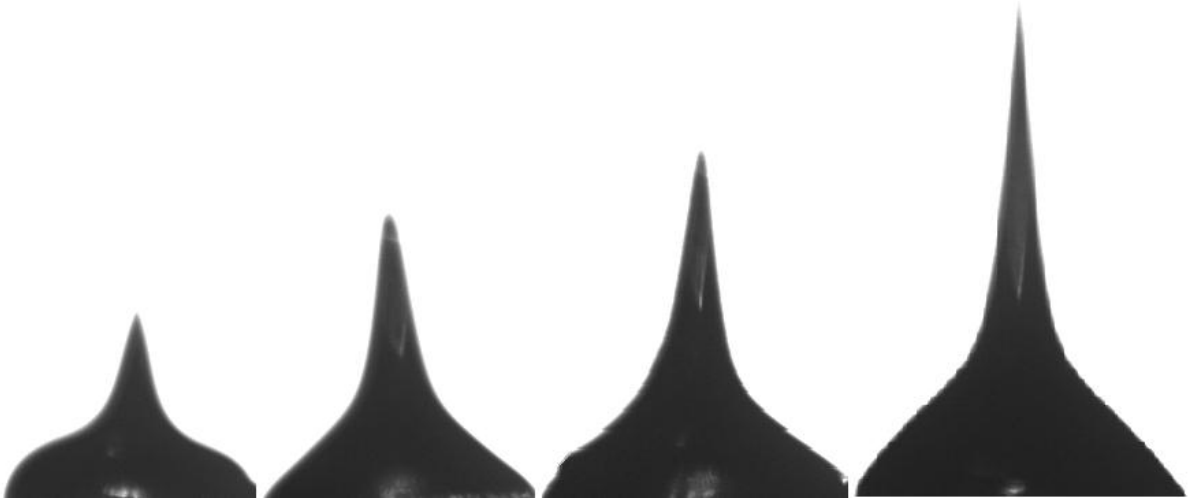

**Fig. 3.7:** Microneedles obtained by drops with increasing diameter, from 800 μm (left) to 1.1 mm (right).

Thanks to the use of PDMS pillars, the density of microneedles per area can be dictated by the distance between pillars therefore it can be easily controlled.

## 3.3 Hydrophobic and hydrophilic drugs loading

Initially a direct dissolution in the polymeric solution was proved both using Nile Red, hydrophobic chromophore, and Rhodamine 6G, hydrophilic one, at several concentrations. As summarized in table 3.1, it was possible to dissolve only a very little amount of Rhodamine in DMC, while Nile Red was completely solubilised also at higher concentrations.

| Conc. w/w to PLGA | Nile Red | Rhodamine 6G |
|---|---|---|
| **0.1%** | Solubilized | Solubilized |
| **0.2%** | Solubilized | Few small residues present in solution |
| **0.4%** | Solubilized | Residues present in solution |

**Table 3.1:** Solutions proved for electro-drawing process.

Solutions with two chromophores had a different behaviour during drawing. Rhodamine seemed to hinder cone formation, indeed we were able to form microneedles only at lower concentrations. Instead, microneedles loaded with Nile Red were obtained at all the tested concentrations. This difference is probably due to a different interaction between electric field and two chromophores, polar and apolar.

In fact, by confocal analysis on microneedle's slices it was evident that the two chromophores were distributed in different areas of microneedle. In the case of Nile Red the longitudinal measurement clearly showed that a significant increase in the fluorescence signal (around 12%) is revealed within a depth of about 150 μm from the tip of the microneedle. Additional measurements were performed along three transversal scan directions at different depths from the tip (100 μm; 200 μm; 300 μm), that showed a constant profile (figure 3.8).

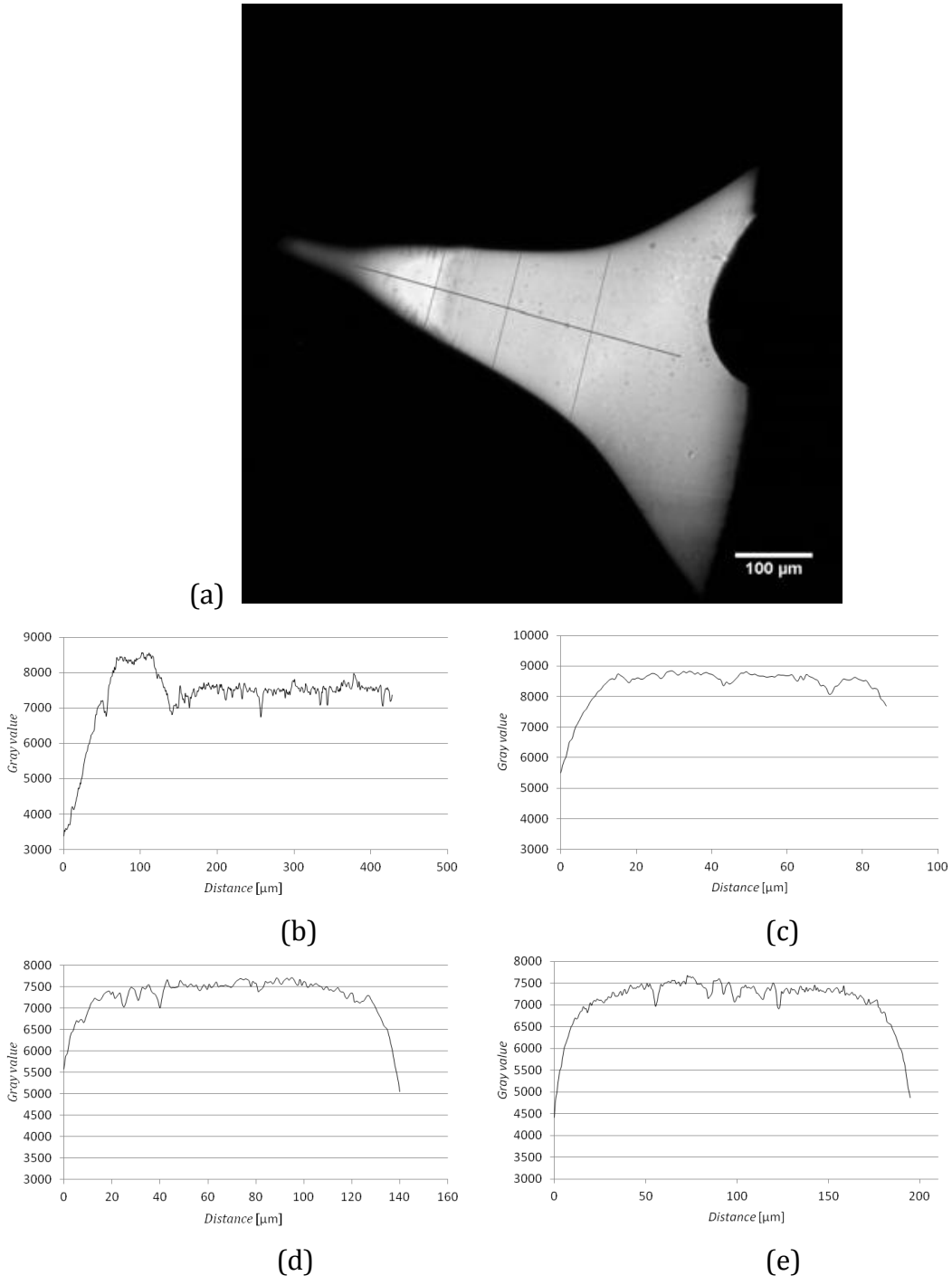


**Fig. 3.8:** Cross-sectional view of the scan directions used for confocal measure (a); emission measured on a thin sheet of the cut microneedle, in longitudinal (b) and transversal direction, at 100 (c), 200 (d) and 300µm of distance from the tip (e).

On the contrary, confocal image on slices of microneedles loaded with Rhodamine showed a feeble fluorescent signal toward tip and a higher intensity at needle's base (figure 3.9).

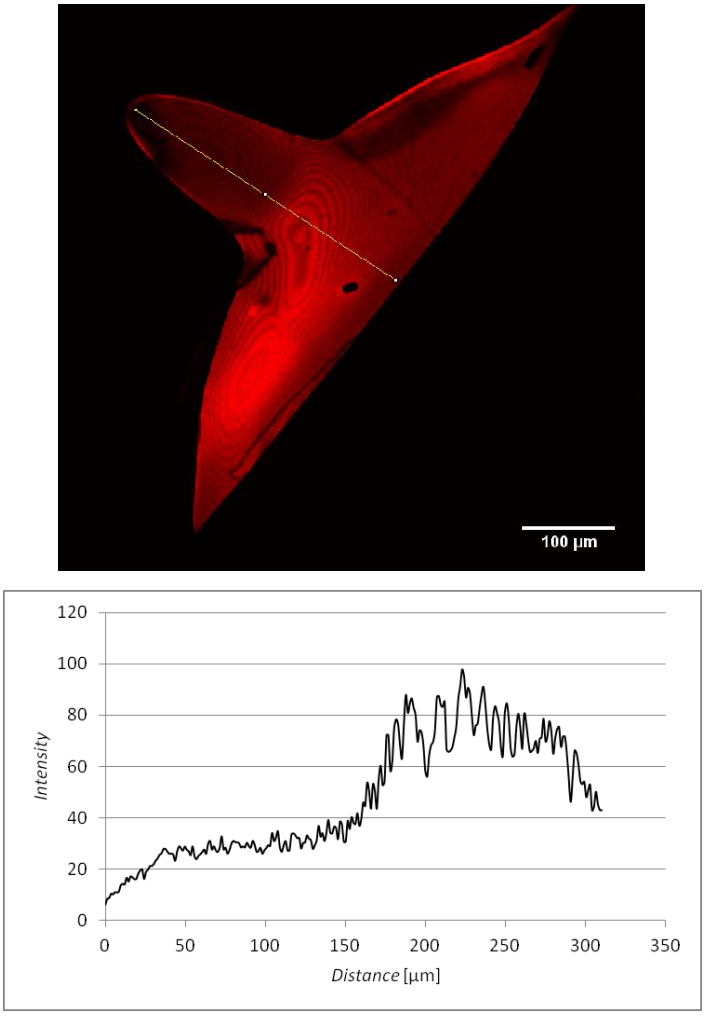


**Fig. 3.9:** Cross-sectional view of the scan directions used for confocal measure on a microneedle loaded with Rhodamine 6G (up); emission measured in longitudinal direction (down).

This distribution is not efficient for delivery, since most of the model drug was amassed outside cone.

### 3.3.1 Porous microneedles

Since most of the therapeutics of interest are hydrophilic, it was attempted to load a considerable amount of hydrophilic model drugs by dispersing water phase in microneedle's matrix.

In particular, TRITC-albumin was used as active compound. To make its dispersion possible it was prepared an emulsion of water in oil where the water phase was loaded with TRITC-albumin and the oil phase was the usual PLGA solution (figure 3.10). The opacity of solution resulting from emulsion depends on the formation of thousand micro-droplets of water which refract light rays. This means that ice jacket around sample was able to avoid evaporation of water, despite high intensity of energy dispensed to solution. Indeed, without a system to control the temperature, the water would have evaporated completely, leaving a clear solution.

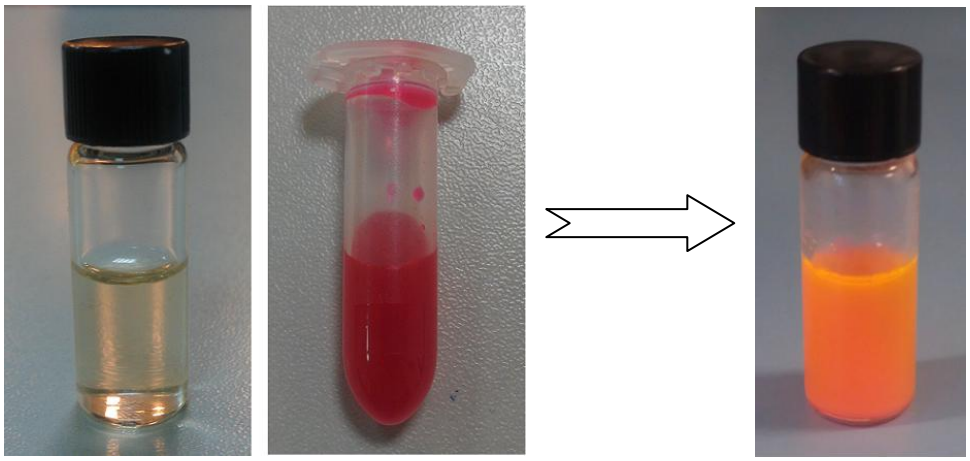

**Fig. 3.10:** PLGA dissolved in DMC at 25% and water solution loaded with Rhodamine before emulsification (left); solution resulting after sonication (right).

Even starting from an emulsion based droplet, it was possible to effectively form PLGA microneedle. The electro-drawing was not affected by the presence of the water, as reported in figure 3.11a, whereas a microneedle onto a 700 μm diameter pillar was seen by optical microscope. The uniform distribution of the hydrophilic

micro-compartments is clear by the SEM micrograph taken onto a slice of the same microneedle, figure 3.11b.

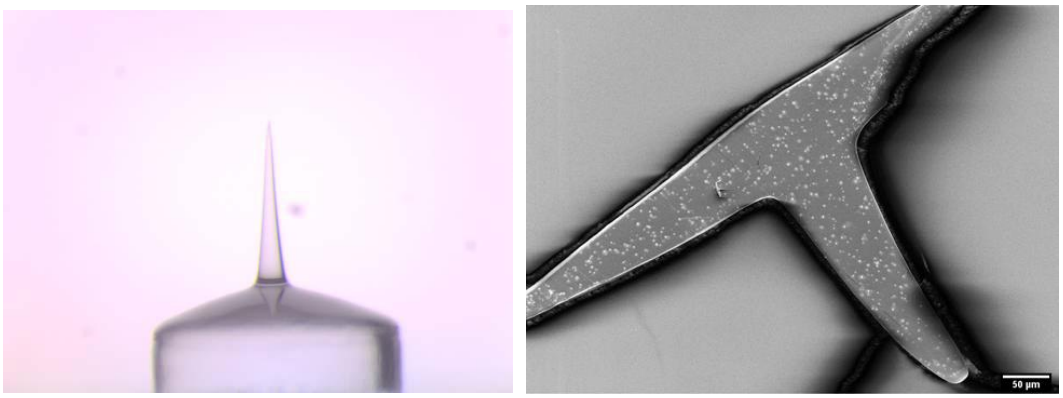


**a)** **b)**

**Fig. 3.11:** Optical image of a microneedle electro-drawn by water-in-oil emulsion (a); SEM micrograph on a slice of the microneedle on the left (b).

This is a very new and interesting result since it proves the capability to load hydrophilic compounds in PLGA microneedles. Moreover, the presence of these micro-cavities accelerate hydratation of microneedle and consequently the release of drug loaded inside. Moreover, as pores are closer and closer, thanks to the effect of degradation of PLGA matrix, it becomes even faster the formation of microchannels between pores, allowing even faster diffusion of model drug throughout microneedle.

However, the microneedle described so far present not optimal distribution of bioactive agent. Indeed, drug is uniformly distribuited throughout the cone and the pedestal region with obvious lost the drug encapsulated in the pedestal region.

### 3.3.2 Double drop deposition

To improve drug distribution within the needles regions, we also tried to load only the cone of the microneedle by using a two-stage dispensing procedure. A small drug-containing water-in-oil emulsion drop, corresponding to the volume of microneedle's cone, was dispensed on the top of a drop of drug-free PLGA solution. Thanks to the viscosity of the two solutions, even if two drops are perfectly unified, micro-drops of water instead of spread out in all drop's volume, tend to stay in apical region. The resulting composite drop was successfully electro-drawn to obtain microneedles with drug –encapsulated porous cone and a compact drug free pedestal. Microneedles structure and dye distribution are clearly shown by the optical stereo microscope analysis (figure 3.12).

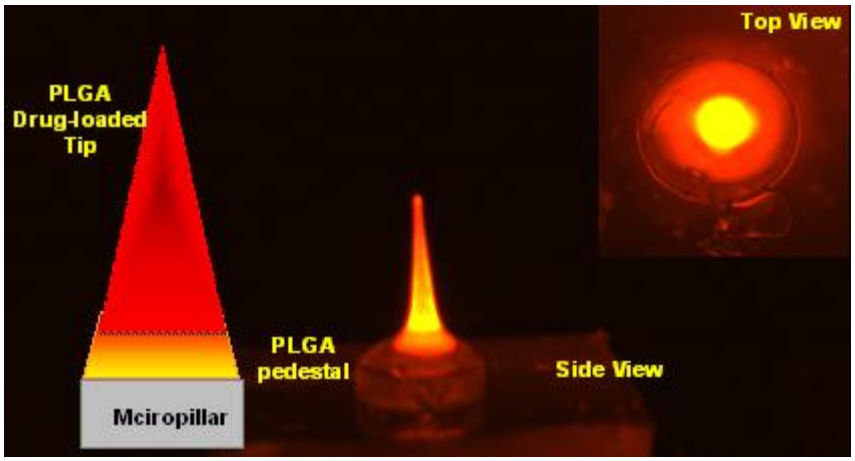


**Fig. 3.12:** Schematic representation of microneedle's structure resulting from double deposition (left); side and top view of an electro-drawn microneedle, whose cone is loaded with BSA-TRITC.

The separation of the two regions, cone and pedestal, is even more evident by the confocal optical analysis reported in figure 3.13.

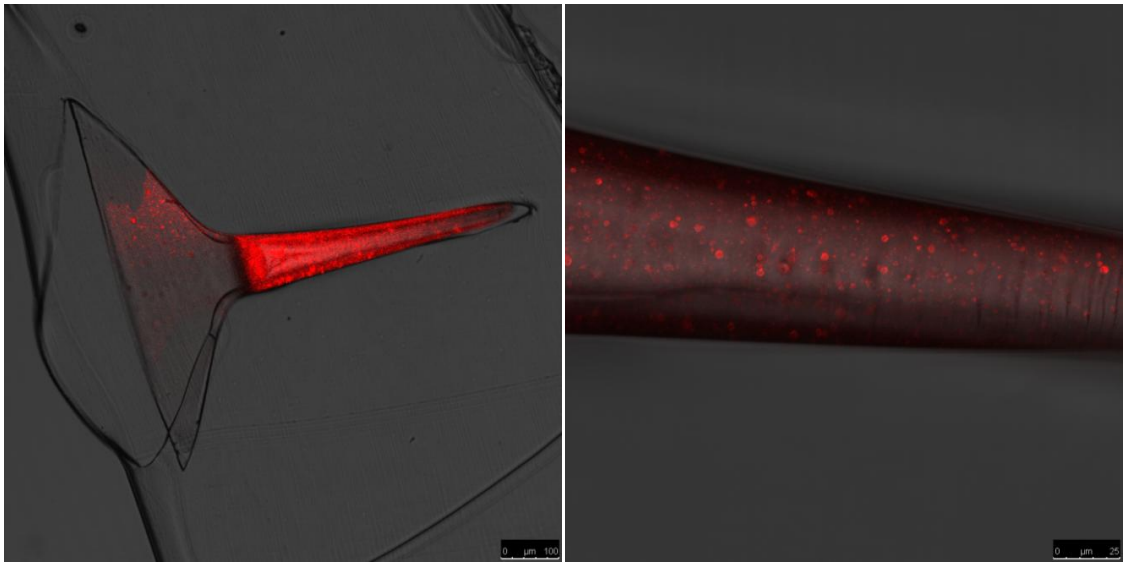

**Fig. 3.13:** Confocal images on microneedle sliced.

### 3.3.3 Porous microneedles by stamp

To study the relationship existing between microneedle's porosity and release kinetics a great number of microneedles was needed. So it was considered more convenient to fabricate microneedles by replica molding instead of electro-drawing, using same composition of starting emulsion, from which depends final porosity. Microneedles were shaped using master, whose structures have a square base of 100 x 100 µm, 250 µm height and spaced 400 µm (figure 3.14).

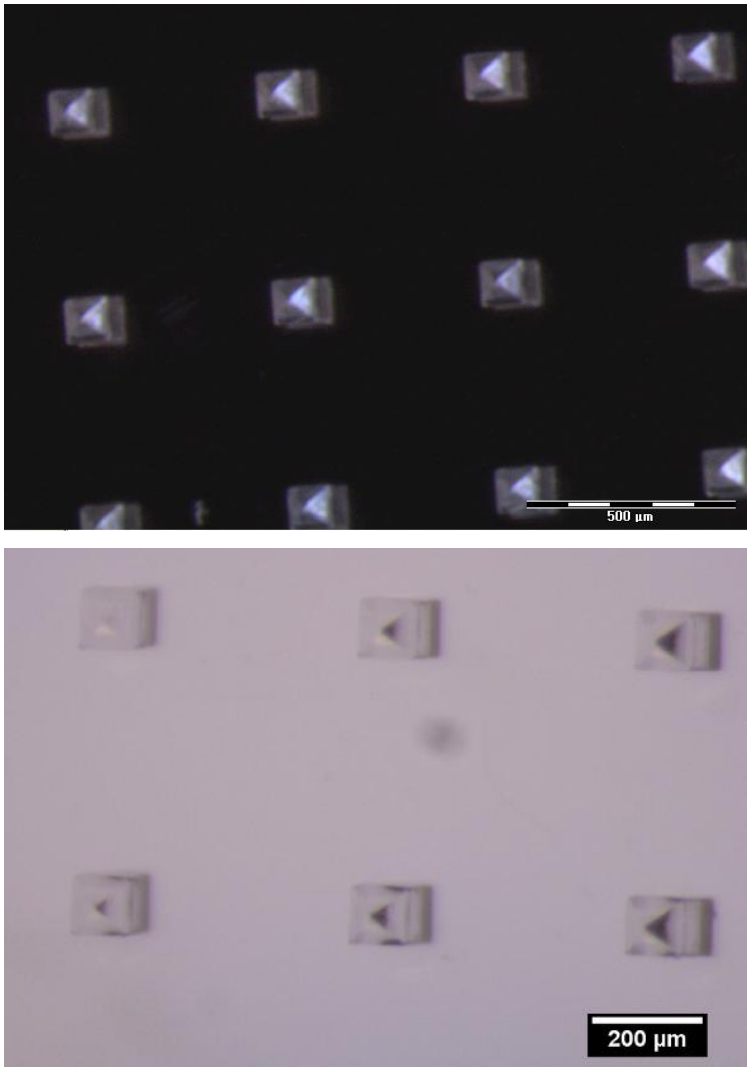


**Fig. 3.14:** Stereoscopical image of master structure in COP (up); microneedles replicated from PDMS stamp.

Few seconds under vacuum was enough to fill the PDMS stamp. By simply drying PLGA solution, perfectly shaped microneedles were obtained: there was no need to centrifuge sample to compact polymer inside holes.

As preliminary check, a comparison was made between the porosity obtained from the two fabrication techniques. Images of figure 3.15 show the porosity obtained using a solution of PLGA emulsified with 30% water phase, containing 20 mg/ml lecithin, respect to polymer mass. In both electro-drawn microneedle and microneedle fabricated by mold there was a similar number of pores of 3-4 µm in diameter.

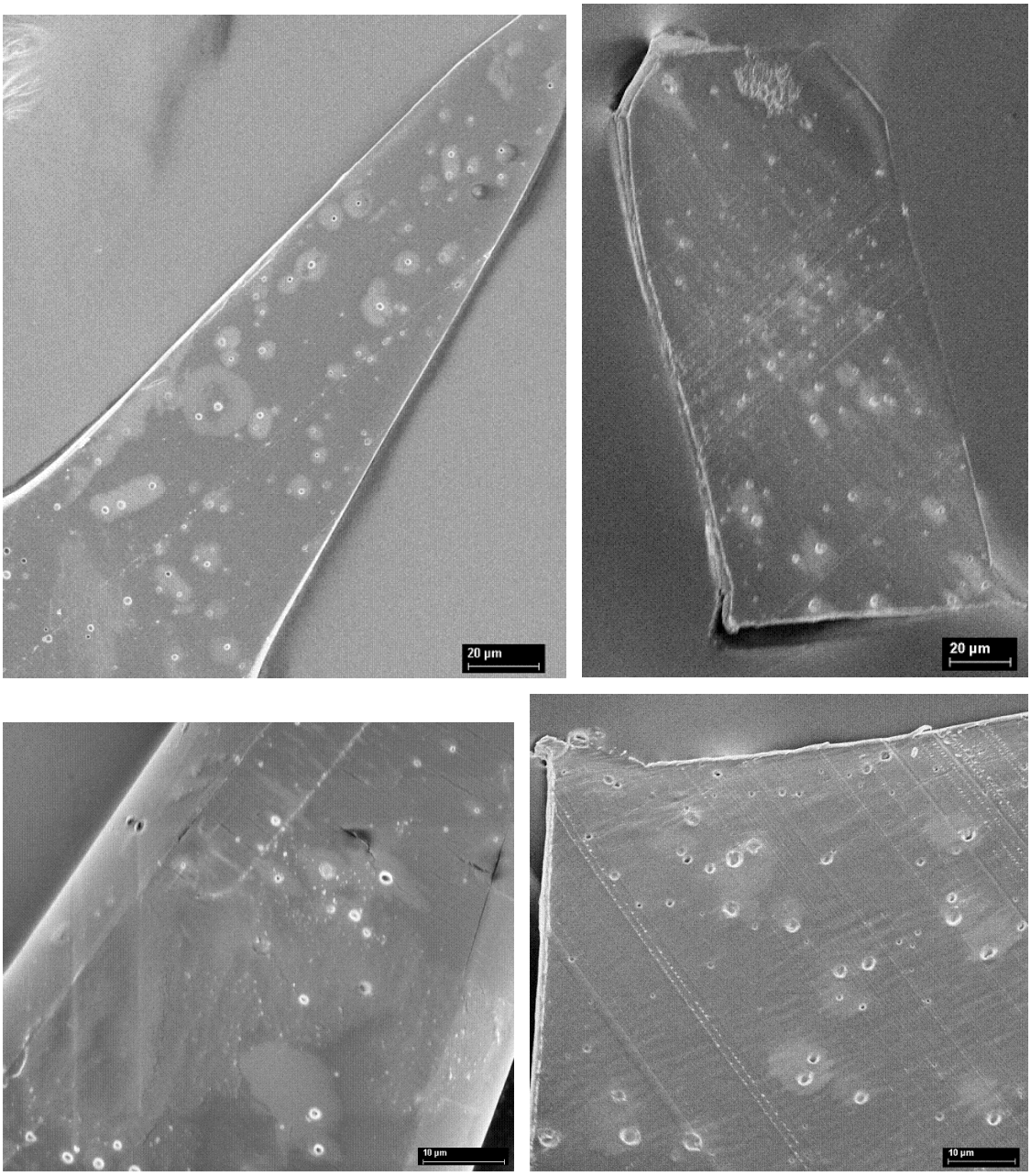


**Fig. 3.15:** SEM images on slices of microneedles included in PDMS and fabricated by electro-drawing (left) and by mold (right).

From the last evidence, it was supposed that release kinetics resulting from pyramidal microneedles was comparable to the one obtained by using electro-drawn structures.

Then, porosity degree was correlated to the amount of water emulsified inside PLGA solution. From morphological studies on slices of microneedles it was noticed a change in porosity by increasing water phase from 30% to 80% w/w

respect to PLGA. As showed in figure 3.16 microneedles containing 60% of water have a greater level of porosity, even if pore size is unchanged respect to microneedles resulting from an emulsion with lower water content. This is explainable since during the preparation of the samples, the concentration of lecithin in water was kept constant, so increasing water content also lecithin included in emulsion was increased. A greater amount of surfactant was therefore able to stabilize larger surface, preserving pore size. Instead, at higher percentages of water, as it is possible to see, some pores much wider than others were obtained. This is probably due to aggregation of water drops at a later stage of the emulsion formation.

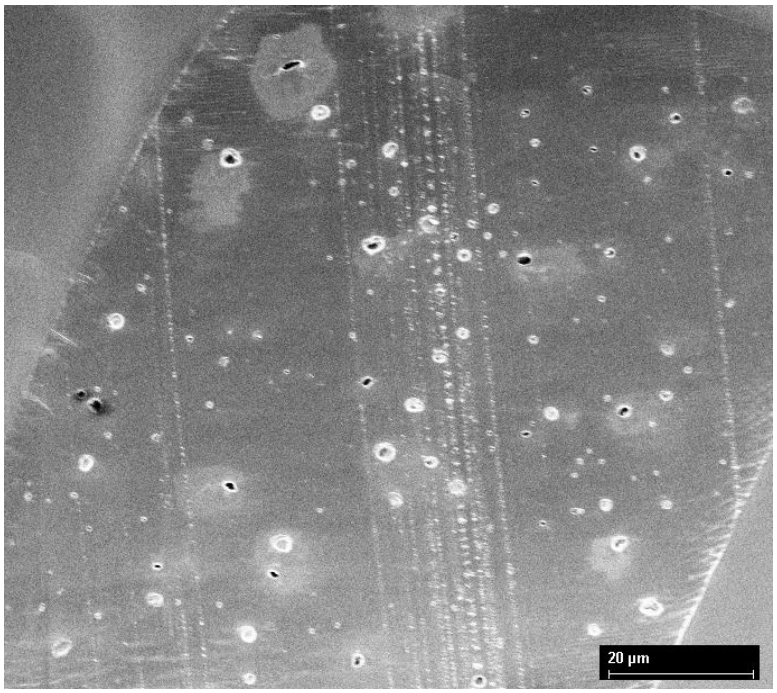

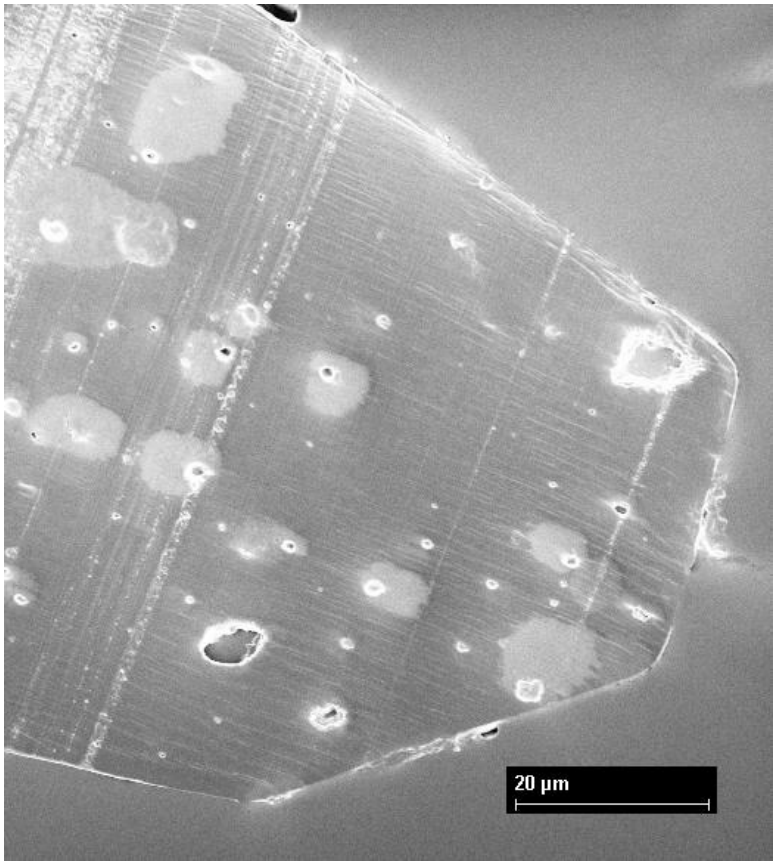


**Fig. 3.16:** SEM images of microneedles fabricated by mold containing 60% (previous page) and 80% (up) of water w/w respect to PLGA.

## 3.4 Quantification of model drug loaded

Usually a complete device includes about 100-200 microneedles, as to not exceed about 2-3 cm in size; indeed a patch too wide would be annoying for patient and come off more easily. Calculation of drugs effectively loaded in microneedles gives the possibility to understand the maximum dose administrable to a patient with one device.

For each sample, fabricated starting from different emulsion formulations, two pieces (2-3 mg weight each) were cut, dissolved in DCM and then dispersed in water. Resulting solutions were analyzed by spectrofluorometer in triplicate, acquiring fluorescence 3 times, with one minute between lectures, and finally

averaging the values. Comparing the fluorescence signal with the calibration line represented in chapter 2 (figure 2.17), it was possible to calculate for each sample, based on an array of PLGA microneedles, the BSA-TRITC concentration in the solutions where microneedles were dissolved. Knowing water volume added, it was possible to calculate the amount of BSA-TRITC included in the cut array. This value, obviously, depends on the dimension of the dissolved sample, so it was normalized respect to the mass of PLGA (figure 3.17).

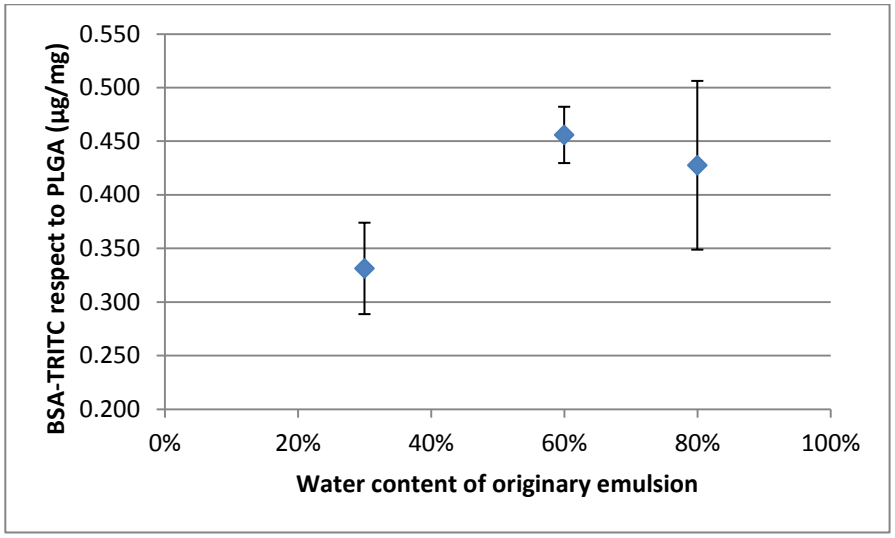


**Fig. 3.17:** Spectrofluorometric analysis for quantification of model drug.

For samples fabricated starting from solutions emulsified with different amount of water phase, the amount of BSA-TRITC was in the range of 0.33-0.45 µg per milligram of PLGA. From the difference in weight of the PLGA substrate, before and after deprivation of all microneedles, it was calculated that the weight of each of them was about 2.5 µg. This means that in an array of one hundred microneedles, it would be possible to have about 0.1 µg of model drug, loaded only in microneedles volume.

In some cases for release in vivo it is necessary to deliver some micrograms of active drugs to have a pharmacological effect. However, increasing size of microneedles and concentration of drug loaded in water phase, it could be attempted to load a useful drug's amount.

## 3.5 Drug release kinetics

Release kinetics was quantified by including microneedles in a gelatine matrix. Microneedles were cut by hand and separated from the back layer, to consider only the contribution of elements that should penetrate inside skin. The analysis by confocal microscope allows analyzing samples in a non-destructive or invasive way. During test it was analyzed the average of fluorescence on the entire volume of microneedles and the decrease of signal was attributed to diffusion in gelatine over time.

For the preparation of samples, it was chosen Norland optical adhesive as sealant. Indeed, in preliminary tests where different sealants had been used, to verify the maintaining of hydration of gelatine, it was identified as the best sealing, with a weight loss of the sample of just 8 mg after 3 days at 37 °C respect to about 200 mg. After including the microneedles in the gelatine matrix and closing them in the Petri's well with coverglass and sealant, one millilitre of water was added before locking the cover with parafilm (figure 3.18). Water was necessary to create an environment saturated with water vapour to inhibit water-loss from gelatine.

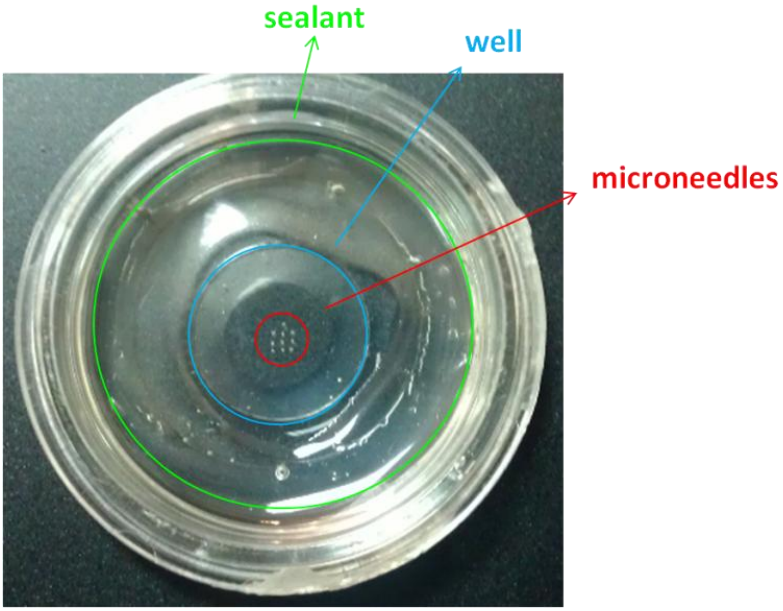


**Fig. 3.18:** Sample prepared to study drug's delivery kinetics.

This optimized system preserved hydration of gelatine even after three weeks from the beginning of the test. No any air bubble was formed inside the sample during monitoring period, differently from what occurred with other sealing systems and without water.

Since transdermal delivery with microneedles has a special attractiveness for those drugs, with protein nature, too much wide to cross intact skin and too easily degradable for gastro-intestinal ambient, it was used BSA-TRITC as model drug, a molecule with 66 kDa molecular weight. This model drug is commonly used to mimic diffusive behaviour of large size drugs. In figure 3.19 it is showed the release profile from microneedles containing 30% and 80% of water respect to PLGA in the first three days which are really important in most of the applications.

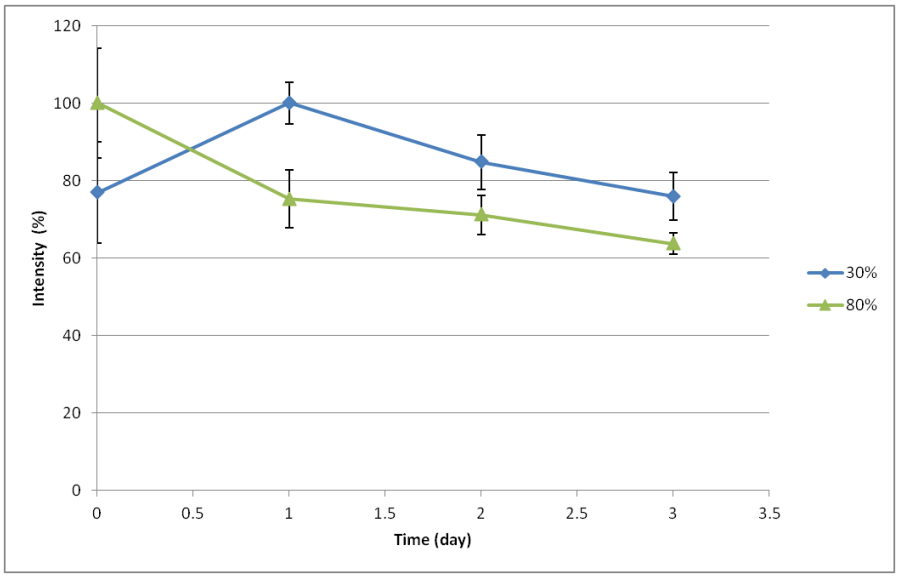


**Fig. 3.19:** Fluorescent signal over time collected during release period in gelatine at 37 °C. Are plotted fluorescence trend of microneedles fabricated from emulsion containing 30% (blue) and 80% (green) of water respect to PLGA. Each point is the average calculated on ten microneedles.

Typically, due to the very low degradation degree of the PLGA this time scale is not enough to have significant drug release especially in the case of embedded and large molecules. We saw that in both cases, even if slow, it was observed some release of the BSA-TRITC. In particular, the release of the sample with higher porosity was significantly higher than the other one even though corresponding to

few tens of % respect to the total amount of embedded drug. Working on the degree of porosity we expect to further improve the release of the PLGA microneedles. Moreover, inspecting lower molecular weight molecules it is possible to expect much higher release kinetics.

The increase in fluorescence visible after 24h in the first kind of samples is probably an optical effect that depends on needles hydration. This evidence was not found in the other sample, where maybe this increase is balanced by faster diffusion.

Following the release until 14 days it was observed about 70% of model drug released from microneedles with lower porosity degree, and about 85% of release was reached from the ones with higher degree of porosity. This is a useful information especially in the case of microneedles which are released after insertion and that can continue the release of their cargo over time without being annoying for the patient. In this case the release would be almost complete after around two weeks.

After 14 days in gelatine matrix, it was visible a leakage of material from some microneedles at 80% water content (figure 3.20). This was due to strong degradation of PLGA: from the breakage of ester linkage smaller chain lengths are formed and they can diffuse through microneedle matrix.

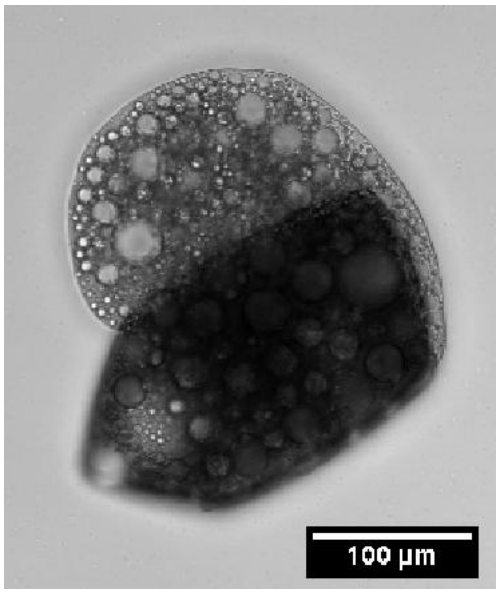


**Fig. 3.20:** Microscopy image in transmission mode showing small PLGA chain diffusing outside microneedle.

At 21st days from the beginning of release test the polymeric matrix appeared even more degraded, with some regions completely dissolved by hydrolysis (figure 3.21). Degradation stage was more advanced in microneedles with higher porosity, this is most probably due to a fast hydration that accelerate degradation.

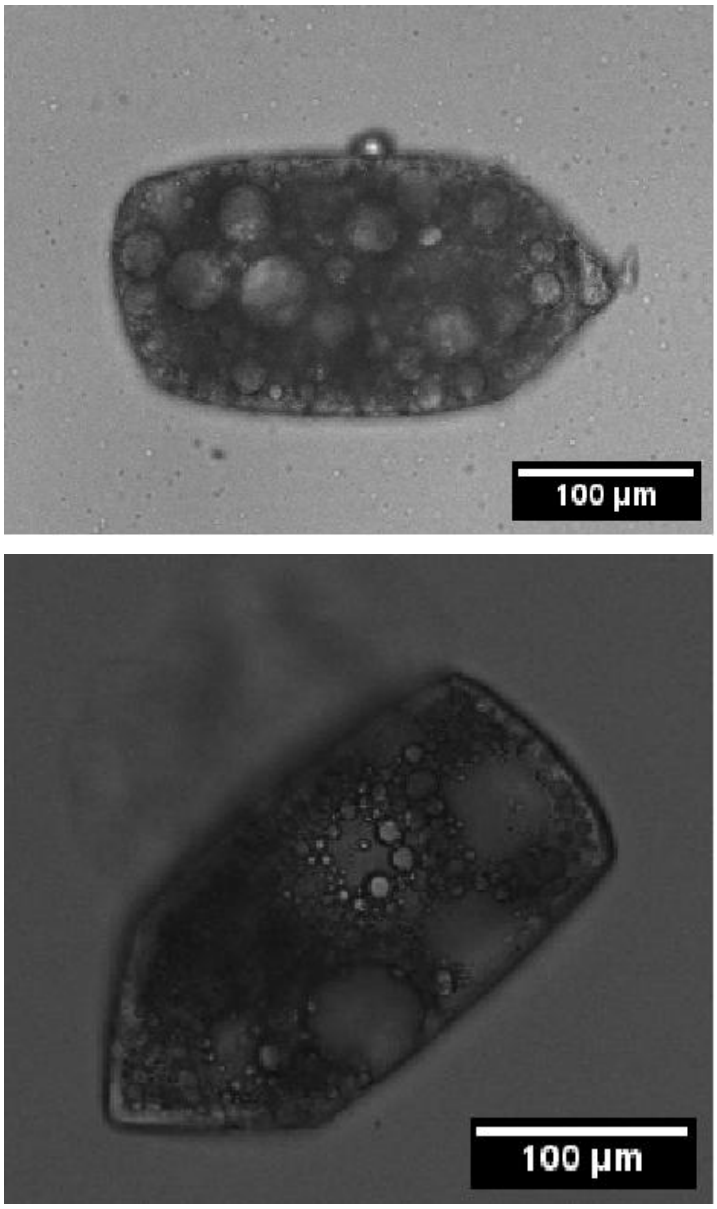


**Fig. 3.21:** Microneedle after 21 days in gelatine, with 30% (up) and 80% (down) of water content.

## 3.6 Indentations

### 3.6.1 Preliminar tests

To serve as substitute for a hypodermic needle, a microneedle should penetrate the 10 ÷ 20 μm thick stratum corneum without breakage. Preliminary indentation experiments were performed into model materials, such as wax and agarose gel, that allows an easy visualization in real time, in order to test the hardness of the microneedles. Figures 3.22 shows the microneedles while penetrating the agarose and just after ejection. No any breakage or bending was observed either in this case or for other lengths and aspect ratios of the microneedles during the insertion tests.

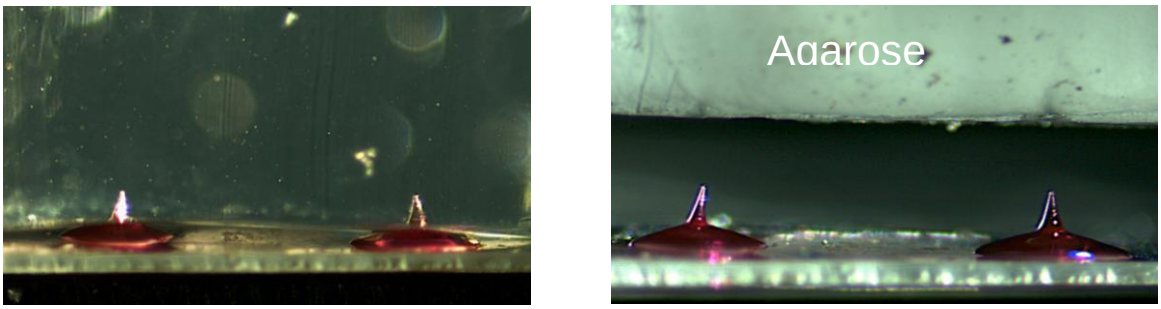


**Fig. 3.22:** PLGA microneedles loaded with NR inserted in agarose (left) and after ejection (right).

Instead, a porous microneedle, containing a 30% of water, fabricated on a PDMS pillar of 700 μm in diameter, was tested in paraffin. In figure 3.23 successivephases of indentation are showed. Microneedle was forced in paraffin wax until the pillar that respond elastically to compression, appeared deformed. Despite the applied force, microneedle was ejected without bending or tip deformations.

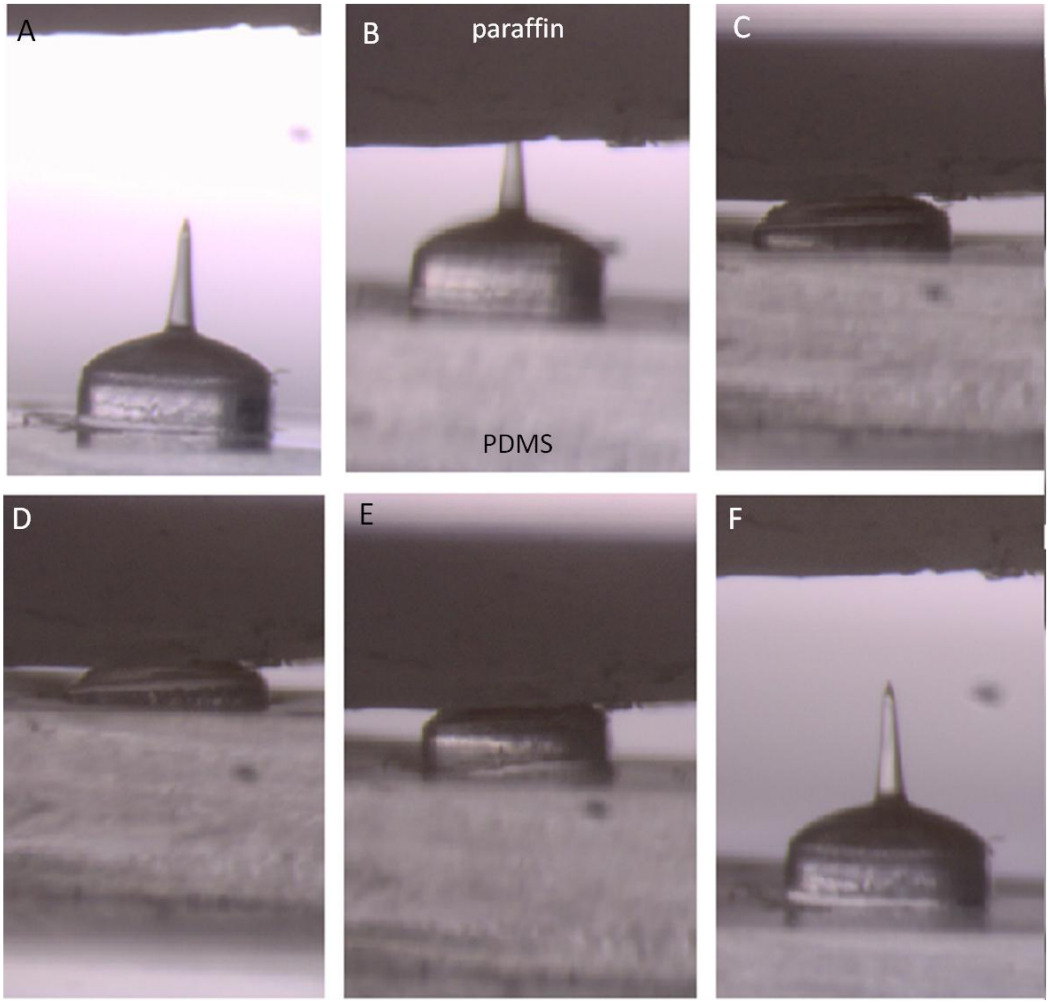


**Fig. 3.23:** Photograms showing indentation in a paraffin layer carried out with a porous microneedle containing 30% water phase.

### 3.6.2 Indentation in skin

Finally, indentation experiments were performed into real skin by inserting the Nile Red loaded microneedles obtained with post-thermal treatment. This analysis was carried out with the system showed in figure 3.24, that mimics the application of a patch through a bracelet. Pig cadaver skin was kept on absorbing paper, around tube that simulate the arm, to avoid shifts. A pressure sensor was fixed to the plastic plate of bracelet, exactly with sensitive area under microneedles in order to measure the force exerted on them. By tightening elastic cuff, microneedles were inserted into pig cadaver skin and removed after 15 min.

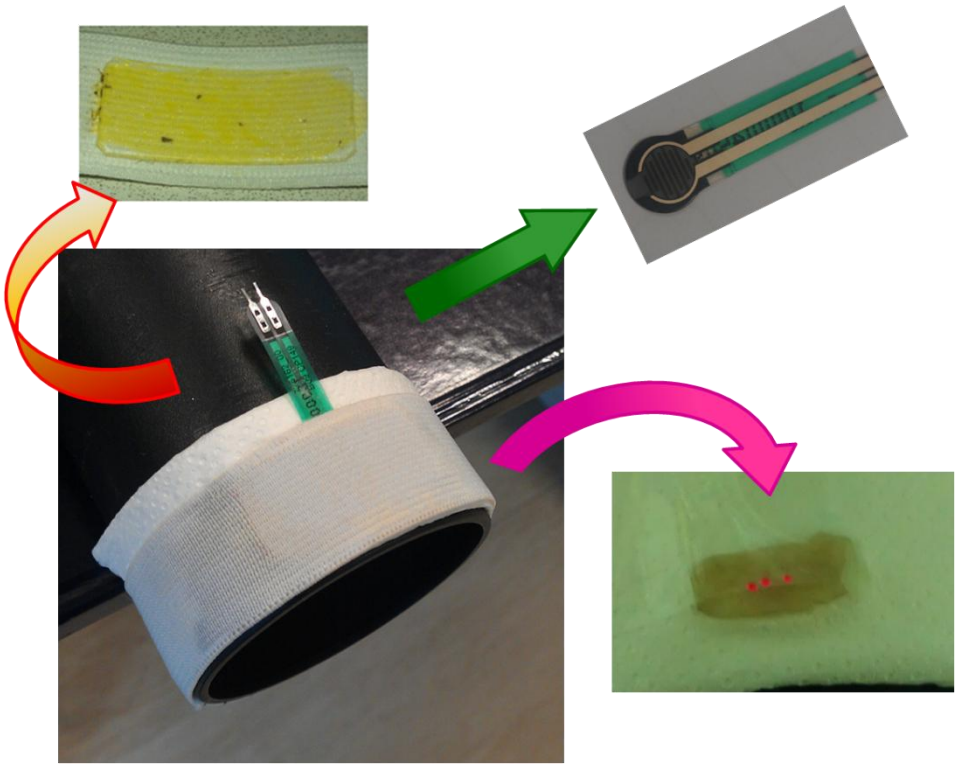

**Fig. 3.24:** Set up for indentation in pig skin, showing plastic plate fixed to the elastic cuff, the pressure sensor used to measure pressure and pig skin kept on absorbing paper.

During indentation it was measured a force about 1N, that acting on all microneedles in series, would correspond to 0.33N/microneedle. Specifically, the necessary force to produce the indentation was of around 0.01 N per microneedle

which is much lower than forces (> 1 order of magnitude) typically known to produce PLGA microneedle breakage. The effectiveness of the indentation is confirmed by the cross sectional image of the stained skin at the site of microneedle penetration (figure 3.25).

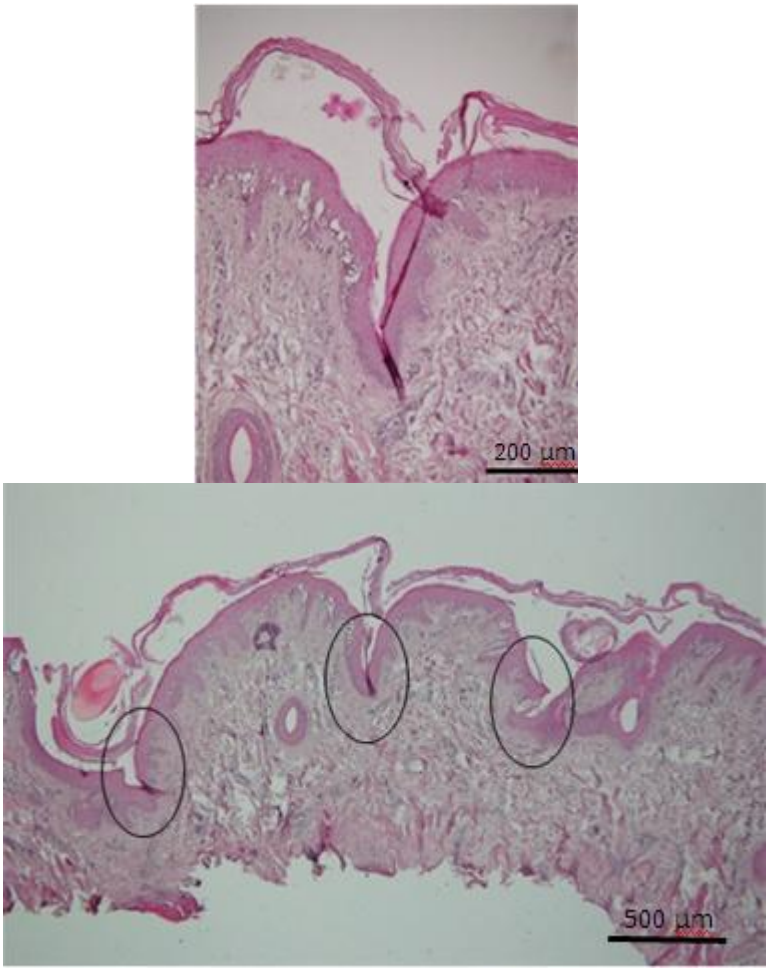


**Fig. 3.25:** Cross-sectional image of the skin after microneedle removal and skin fixing in formaline at 10%, magnification of one indentation (left) and complete image (right).

The dermis was clearly reached by the microneedle, thus confirming the potential use for drug delivery. The insertion depth was in agreement with the dimensions of the microneedles used for test having respectively around 400, 500, 450 µm length (figure 3.26).

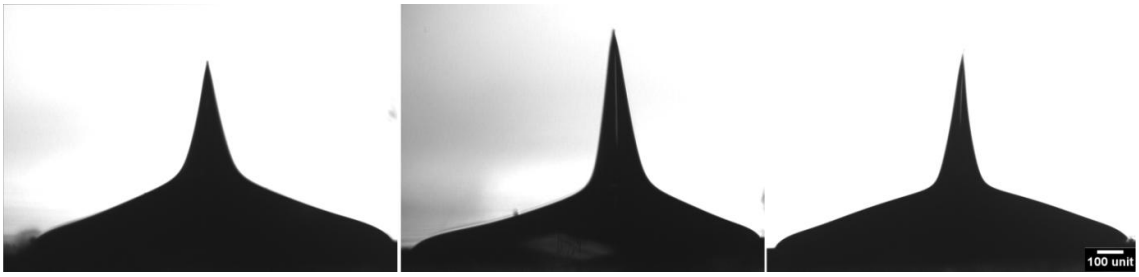


**Fig. 3.26:** Optical image of microneedles used for indentation with heights of (left) 400 μm, (middle) 500 μm, (right) 450 μm.

In particular, they were able to penetrate all the layers of the epithelium and part of the papillary dermis. These results confirmed the effectiveness of these microneedles which combined with the technological simplicity of the technique could provide a significant breakthrough in the clinical development of the biodegradable microneedles.

### 3.6.3 Nanoindentation

The mechanical resistance of the polymeric matrix used to fabricate microneedles, is an essential factor to be considered in order to ensure the success of indentation. A microneedle must withstand the force required to pierce stratum corneum without reaching breaking load. The elastic modulus of polymeric matrix was evaluated by indenting samples with a standard berkovich tip (figure 3.27).

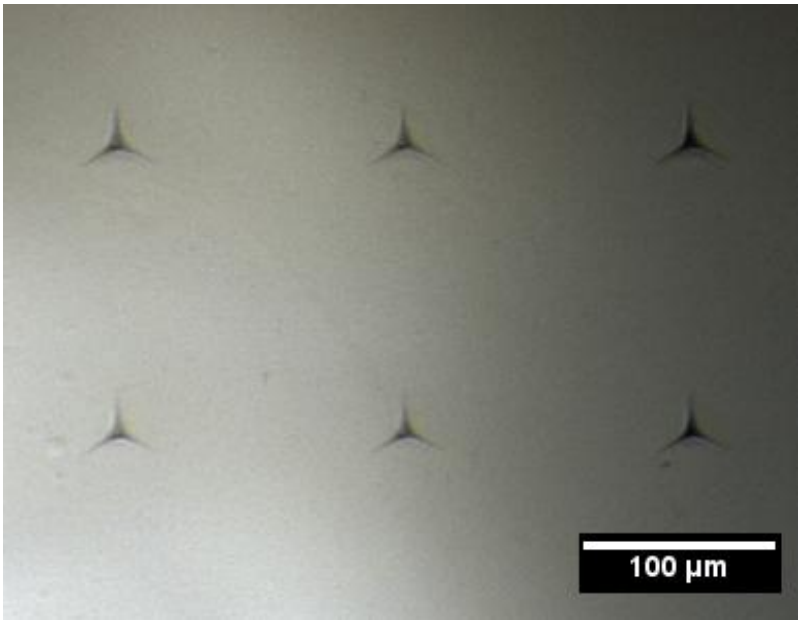


**Fig. 3.27:** Substrate tested with berkovich tip of nanoindenter.

Mechanical tests were accomplished on samples worked by different methods. As it is showed in plot (figure 3.28), PLGA dried after dissolution in DMC has an elastic modulus lower that the one obtained in case of sample fabricated by direct melting. This is probably explainable with a different compression state of polymeric chains, dissolution of polymer in a solvent, even after lyophilisation, might have caused formation of a network with larger mesh. Despite this significant loss of resistance electro-drawn microneedles, fabricated by a PLGA solution, were able to indent.

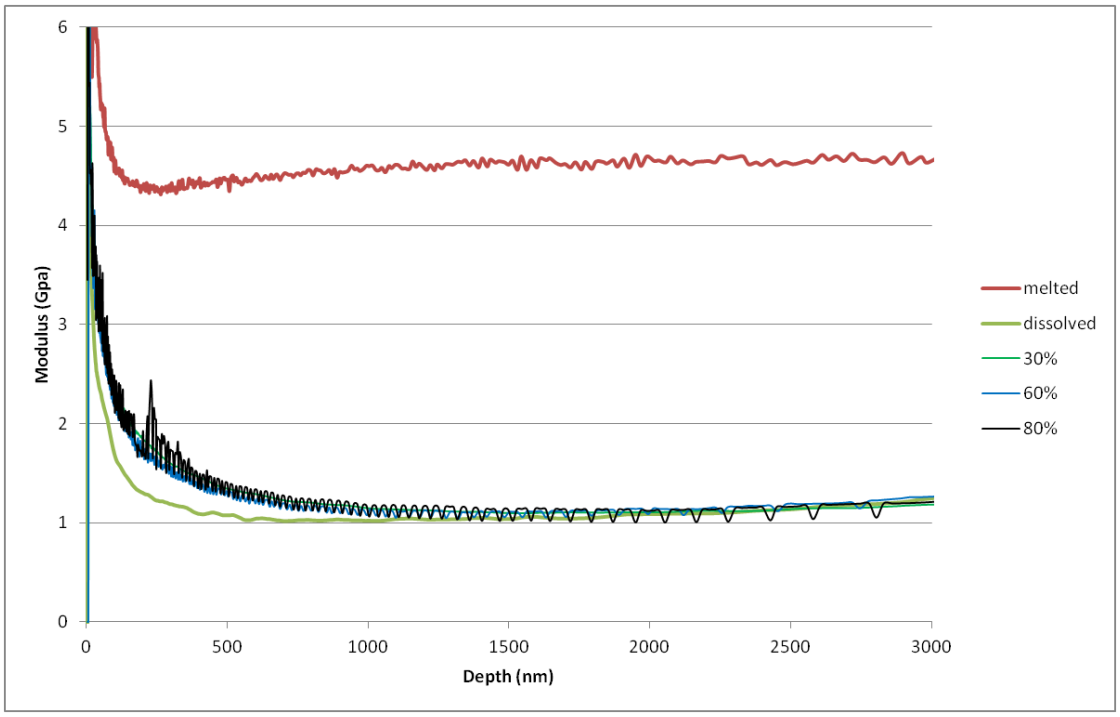


**Fig. 3.28:** Comparison between elastic modulus, calculated through nanoindentation, of PLGA worked by melting and dissolving, and different formulation of emulsion.

In addition, mechanical tests, performed by nanoindentation of samples obtained by solution emulsified with different amounts of water, proved that there was no significant difference between the different samples. Probably, this is due to the kind of distribution of the pores which are small and not interconnected, therefore, they do not affect the elastic modulus of the polymeric matrix. It is, therefore, reasonable to suppose that also porous microneedles should be able to drill skin.

## 3.7 Conclusion

Biodegradable microneedles are considered as a great alternative to hypodermic injection and current system for drug delivery. Indeed, it is established that with this new approach it is possible to obtain an efficient release of vaccines and other drugs. Microneedles solve in a simple way the problems related to permeability of stratum corneum, also for molecules with large sizes, therefore are suitable for many applications. An attractive point for a future use in human patients is the sharpness loss of microneedles after the first use. Both in the case of good indentation with following hydration and drug release, and failed indentation, in which microneedle's tip is damaged, the disposable is not able to pierce again. This limits the risk of disease transmission from one person to others.

This thesis project was focused on the development of a new fabrication method that allows overcoming some limitations of common procedures. Some of these limits originate from the fact that the drug is included in the polymer matrix, so if process conditions are such to degrade it, then it is required a very large amount of drug to obtain a pharmacological effect. This drug's overload can make production uneconomical.

In this work it is showed for the first time a fabrication method based on electro-drawing. Electrical field is generated from a heated pyroelectric crystal. This is the only element brought to high temperature, while the temperature of the polymeric solution, in which is included the drug, never overcomes 40 °C. So this process results very interesting especially for thermolabile drugs, such as proteins. To shape microneedles it is not used any stamp: in the whole process the polymeric solution comes into contact only with the flexible substrate, that is the support of the microneedles array. So it is avoided any cross-contamination between devices produced in series.

It has also been demonstrated the ability to form porous microneedles, by the drawing of a drop of emulsion. This gives the possibility to load, also contemporary, an hydrophilic and lipophilic drug in the same microneedle. In addition, with double drop deposition, the active compound has been localized into

the cone, or in other words in the only region that will be completely inserted in skin. This is important since drug localization maximizes the efficiency of release.

# Appendix Instruments

## A.I.1 Confocal Microscope

Illuminating and observing a sample, two physical processes significantly limit the sharpness of the observed image:

1) by illuminating the entire sample, the light spreads in it disturbing the image of the focus plane: to solve this problem it is needed to illuminate only small areas of the sample.
2) while it is possible to observe a focus plane of the sample, also the light reflected from the plans not in focus comes to the eyes, making a confusing picture: the revolutionary idea compared to conventional microscopy is to block as much as possible the information derived from the above and below planes to the desired through a small opening.

Confocal microscopy allows overcoming the limits of conventional optical microscopy. Indeed, it is an optical imaging technique used to increase optical resolution and contrast of a micrograph by using point illumination and a spatial pinhole, in input and in output, to eliminate out-of-focus light in specimens that are thicker than the focal plane. The image therefore is not disturbed by unwanted reflections or fluorescences by the plans not in focus and the points of focus plane that are not observed. It enables the reconstruction of three-dimensional structures from the obtained images.

As it is possible to see from the figure A.I.1, the beam excitation passes through the illuminating pinhole, irradiating only a small region of the sample.

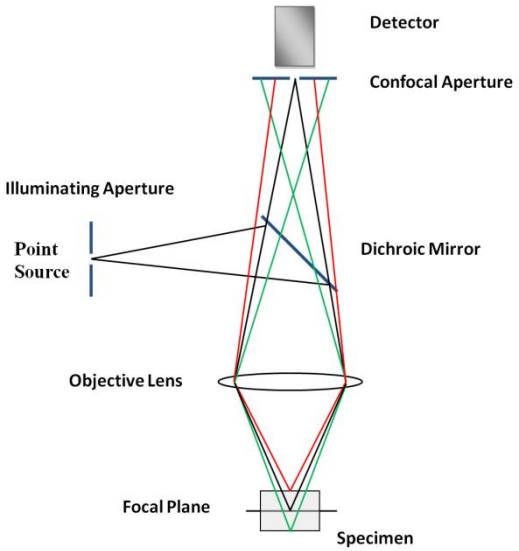


**Figure A.I.1:** Simplified optics of a Laser Scanning Confocal Microscope (LSCM).

Before detection a second confocal aperture, a detector pinhole, reduces the contributions of the above and below planes to the focus. By scanning techniques, it is possible to study the entire sample surface. The fundamental principle of any scanning microscope is to illuminate a point of the sample at a time; the signal resulting from the interaction between the incident radiation and the sample is recorded and processed to form a reproduction of the sample to visualize. Compared to a conventional microscope that immediately provides the full image, with the confocal microscope the sample is probed point by point.

In confocal microscopy, as excitation source it is often used a laser beam. This provides a high intensity and monocromatic light source. It is first filtered and attenuated so to use a correct intensity and proper excitation spectrum to produce fluorescence that is the emission of a secondary photon upon absorption of a photon of higher wavelength (figure A.I.2). Most molecules at normal temperatures are at the lowest energy state, the so-called 'ground state'. Occasionally, a molecule may absorb a photon and increase its energy to the excited state. From here it can very quickly transfer some of that energy to other molecules through collisions (red) and spontaneously emits the remaining energy by emitting a photon (green) with a lower wavelength to return to the ground state.

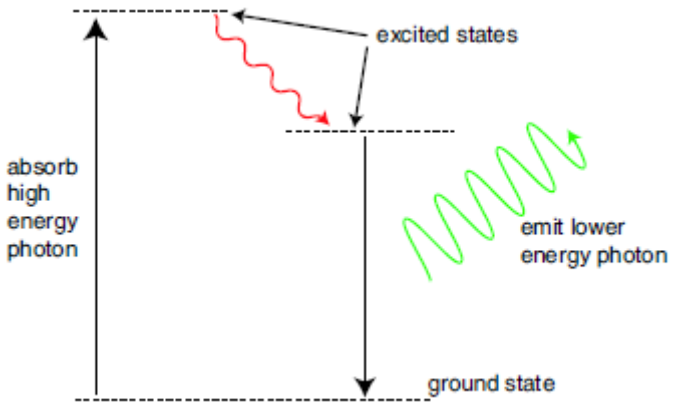


**Figure A.I.2:** Scheme of the fluorescence mechanism.

In fluorescence microscopy, fluorescent molecules, in order to increase the signal, are designed to be attached to specific parts of a sample, thus identifying them when imaged. Multiple fluorophores can be used to simultaneously identify different parts of a sample. There are two options when using multiple fluorophores:

- fluorophores can be chosen that respond to different wavelengths of a multi-line laser;
- fluorophores can be chosen that respond to the same excitation wavelength but emit at different wavelengths.

While the intensity of incident radiation can be increased, fluorophores may become saturated if the intensity is too high. Moreover, they can present photobleaching that is an irreversible fade when they are exposed to excitation light for a long time being able to emit only a limited number of photons. This may be due to reaction of the molecules' excited state with oxygen or oxygen radicals. Photobleaching can be limited by reducing the oxygen available or by using free-radical scavengers. Some fluorophores are more robust than others, so choice of fluorophore is very important.

## A.I.2 Multiphoton fluorescence microscopy

The multiphoton fluorescence microscope (MPM) uses pulsed long-wavelength light to excite fluorophores within the specimen being observed. The fluorophore absorbs the energy from two long-wavelength photons which must arrive simultaneously in order to excite an electron into a higher energy state, from which it can decay, emitting a fluorescence signal (figure A.I.3). It differs from traditional fluorescence microscopy in which the excitation wavelength is shorter than the emission wavelength, as the summed energies of two long-wavelength exciting photons will produce an emission wavelength shorter than the excitation wavelength.

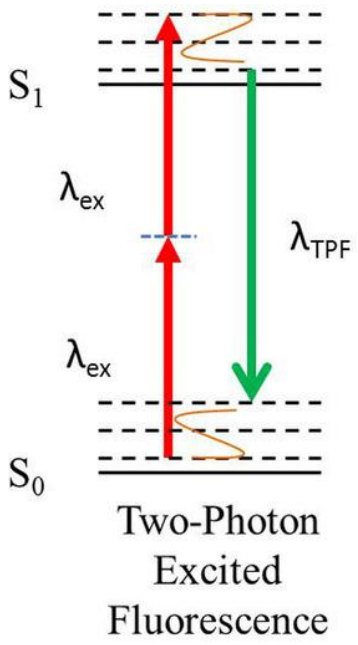


**Fig. A.I.3:** Diagram indicating the absorption of two NIR photons to excite the fluorescent molecule to an excited state and the visible fluorescence emitted during relaxation.

Multiphoton fluorescence microscopy has similarities to confocal laser scanning microscopy. Both use focused laser beams that scan the sample to generate images, and both have an optical sectioning effect. Unlike confocal microscopes, multiphoton microscopes do not contain pinhole apertures, which give confocal

microscopes their optical sectioning quality. The optical sectioning produced by multiphoton microscopes is a result of the point spread function of all elements included in optical path, namely depends on how the system blurs the image of a bright spot formed where the pulsed laser beams coincide.

Compared to similar optical imaging techniques, MPM holds inherent advantages for imaging living tissues by improving depth penetration and reducing photodamage. This is a direct result of employing near infrared (NIR) femtosecond lasers to generate observable nonlinear signals in the visible range. The NIR excitation enhances the ability to image deeper into a sample through a reduction light scattering proportional to the fourth power of the excitation wavelength.

## A.I.3 Immersion sonicator

One of the equipments used in the preparation of the water-PLGA emulsion for porous microneedles fabrication, is the immersion sonicator. In figure A.I.4 it is reported the one used in the thesis which was the Ultrasonic Processor VCX500 Sonic and Materials.

**Fig. A.I.4:** Picture of the Ultrasonic Processor VCX500 Sonic and Materials.

The ultrasonic power supply converts 50/60 Hz line voltage to high frequency electrical energy transmitted to the piezoelectric transducer within the converter, where it is changed to mechanical vibrations. The vibrations from the converter are intensified by the probe, creating pressure waves in the liquid. This rapid changes in pressure causes the formation of cavities during phase of low pressure, and their implosion during high pressure, that generate intense shock waves. The sum of energy released by each individual implosion is minimal, but the cumulative effect causes extremely high levels of energy to be released into the liquid. Temperature is monitored therefore if a pre-fixed threshold is overcome, sonication will stop. To avoid this condition it is possible to alternate pulse off and/or more effectively create an ice jacket to improve heat dissipation and keep temperature below the threshold. The Ultrasonic Processor is designed to deliver constant amplitude. As the resistance to the movement of the probe increases, additional power will be delivered by the power supply to ensure that the excursion at the probe tip remains constant. Furthermore, the amplitude control allows the ultrasonic vibrations at the probe tip to be set to any desired level.

Probes consist of two sections each having different cross-sectional areas. Brought to resonant frequency, the probe expands and contracts longitudinally about its center. Amplification factor increases with the mass ratio between the upper section and the lower section. Probes with smaller tip (figure A.I.5.A) diameters produce greater intensity of cavitation, but the energy released is restricted to a narrower, more concentrated field. Conversely, probes with larger tip (figure A.I.5.B) diameters produce less intensity, but the energy is released over a greater area.

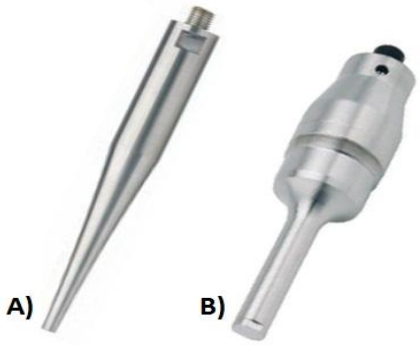


**Fig. A.I.5:** Small (A) and large (B) types of probes.

High gain probes produce higher intensity than standard probes of the same diameter, and are usually recommended for processing larger volumes. Probes are fabricated from high grade titanium alloy Ti-6Al-4V because of its high tensile strength, good acoustical properties at ultrasonic frequencies, high resistance to corrosion, low toxicity, and excellent resistance to cavitation erosion. They are autoclavable and available with threaded ends to accept replaceable tips, microtips and extenders.

## A.I.3 Fluorescence Spectroscopy

In this work, fluorescence spectroscopy was used to quantify the amount of BSA-TRITC loaded in microneedles, through the intensity of fluorescence signal. In following figure A.I. 6 is reported the EnSpire Multimode Plate Reader 2300-0000, Perkin Elmer used in this work.

**Figure A.I.6:** Picture of the spectrofluorimeter EnSpire Multimode Plate Reader 2300-0000, Perkin Elmer.

Fluorescence occurs when a substance that has absorbed light or other electromagnetic radiation, emits light with different wavelength. When a substance absorbs energy, the electronic state of the molecules changes from the ground electronic state (low energy state) to a one of the vibrational states of the excited electronic state. Excited molecule can collide with other molecules causing as a result lose of energy until the molecule reaches the lowest vibrational state of the excited electronic state, and finally, as consequence of collisions, the molecule drops again into one of the various vibrational levels of the ground electronic state, emitting a photon in the process. Because the molecules can drop in any of the different vibrational levels of the ground state, the emitted photons will have different energies and in consequence, different frequencies.

## A.I.4 Nano Indenter

To characterize PLGA matrix employed to fabricate microneedles, a Nano Indenter G200 Agilent Technologies was used (figure A.I. 7). This instrument is able to apply loads and to sense displacements in the micro and down to nano scale.


**Fig. A.I. 7:** Picture of Nano Indenter G200, Agilent Technologies.

Indentation testing is a method that consists essentially of touching the material of interest, whose mechanical properties such as elastic modulus are unknown, with another material whose properties are known. The difference from others conventional indentation hardness tests is the indirect measurement of contact area. In nanoindentation tests, the size of the residual impression is of the order of microns and too small to be conveniently measured directly. Thus, it is customary to determine the area of contact by measuring the depth of penetration of the indenter into the specimen surface. This, together with the known geometry of the indenter's tip, provides an indirect measurement of contact area. For this reason, nanoindentation testing is referred to as depth-sensing indentation (DSI) [61].
Depending on the test that one wants to perform and on the type of sample, different tip indenters can be used, some of which are showed in figure A.I. 8.

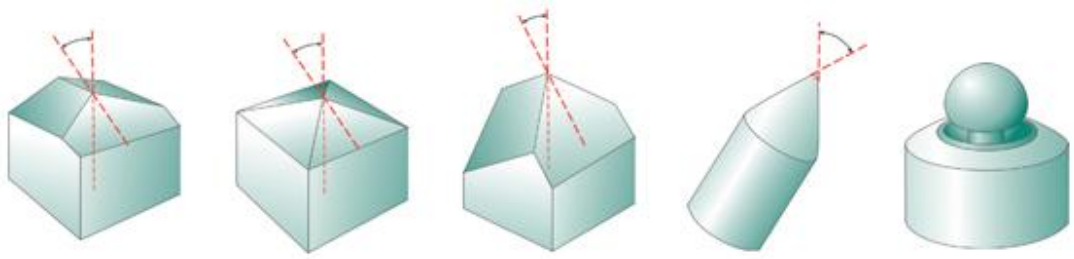

**Fig. A.I. 8:** Rapresentation of geometries most used for indentation: Berkovich, Vickers, Cube-Corner, Cone and Sphere (from left).

A schematic representation of indenter's elements is showed in figure A.I. 9. During an indentation, corresponding values of load and displacement of the diamond tip (indentation depth) are recorded, and from the resulting curve the hardness and the E-modulus are calculated. The load is applied by running a current through the load application coil. Magnetic field so generated interact with permanent magnet mounted onto indenter shaft, thus pushing diamond tip. The indenter displacement is measured by the capacitive displacement sensor.

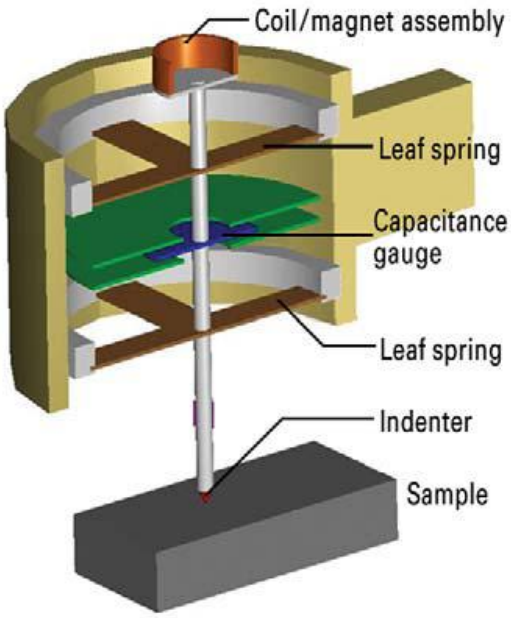


**Fig. A.I. 9:** Diagram of the nanoindenter system used. The force imposed on the indenter is generated through a coil that sits within a circular magnet. The displacement sensing system consists of a three-plate (circular disks) capacitor.

Load transducers must be capable of measuring forces in the micro-newton range and displacement sensors are very frequently capable of sub-nanometer resolution. Environmental isolation is crucial to the operation of the instrument. Vibrations transmitted to the device, fluctuations in atmospheric temperature and pressure, and thermal fluctuations of the components during the course of an experiment can cause significant errors.

## A.I.5 Cryo UltraMicrotome

An ultramicrotome is a tool used to cut extremely thin slices of material; it can cut until few tens of nanometers thickness. Importantly in science, microtome is used in microscopy, allowing for the preparation of samples for observation under transmitted light or electron radiation. Microtomes use steel, glass, or diamond blades depending upon the specimen being sliced and the desired thickness of the sections being cut. In this work was used a Leica EM UC7 Ultramicrotome, with Cryo chamber EM FC7 for sectioning in environment cooled with liquid nitrogen, showed in figure A.I. 10.

**Fig. A.I. 10:** Picture of Ultramicrotome Leica EM UC7 (left) and Cryo chamber EM FC7 (right).

The reduced temperature allows for the hardness of the sample to be increased, such as by undergoing a glass transition, which allows for the preparation of thin samples.

The instrument used belongs to the class of rotary microtome. This device operates with a staged rotary action such that the actual cutting is part of the rotary motion. In a rotary microtome, the knife is typically fixed in a horizontal position. Through the motion of the sample holder, the sample is cut by the knife position 1 to position 2), at which point the fresh section remains on the knife. At the highest point of the rotary motion, the sample holder is advanced by the same thickness as the section that is to be made, allowing for the next section to be made (figure A.I. 11).

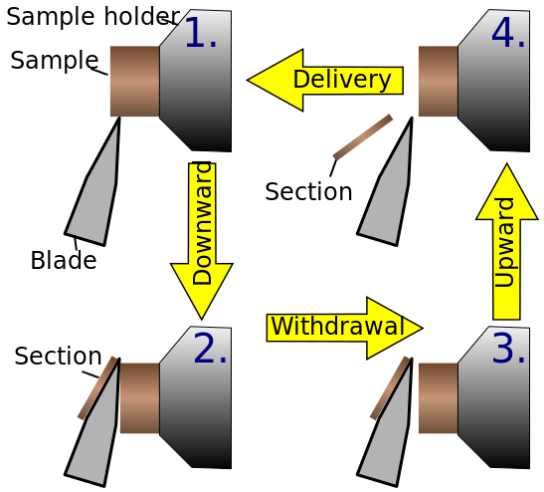


**Fig. A.I. 11:** Principle of sample movement for making a cut on a rotary microtome.

## A.I.6 Scanning Electron Microscope

For morphological analysis of microneedles sectioned a field emission SEM (Ultra plus Zeiss) was used. A scanning electron microscope (SEM) is a type of electron microscope that produces images of a sample by scanning it with a focused beam of electrons. The electrons interact with atoms in the sample, producing signals that can be detected and that contain information about the sample's surface topography and composition. In a typical SEM, an electron beam is thermoionically emitted from an electron gun fitted with a tungsten filament cathode. The electron beam, which typically has an energy ranging from 0.2 keV to 40 keV, is focused by one or two condenser

lenses to a spot about 0.4 nm to 5 nm in diameter. The beam passes through pairs of scanning coils or pairs of deflector plates in the electron column, typically in the final lens, which deflect the beam in the x and y axes so that it scans in a raster fashion over a rectangular area of the sample surface (figure A.I.12).

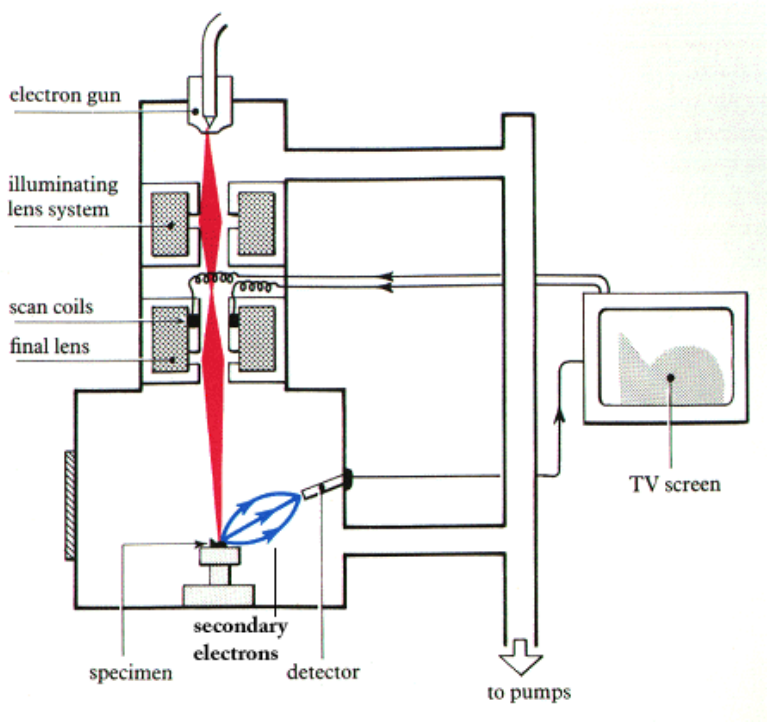


**Fig. A.I.12:** Functioning scheme of a scanning electron microscope.

When the primary electron beam interacts with the sample, the electrons lose energy by repeated random scattering and absorption within a region of sample's volume, whose extension depends on the electron's landing energy, the atomic number of the specimen and the specimen's density. The interaction between electron beam and surface sample produce a great number of particles, like secondary electrons (SE), back-scattered electrons (BSE), characteristic X-rays and transmitted electrons. In the standard detection mode, secondary electron imaging or SEI, the SEM can produce very high-resolution images of a sample surface. Instead, back-scattered electrons (BSE) are beam electrons that are reflected from the sample by elastic scattering. BSE are often used in analytical SEM along with the spectra made from the characteristic X-rays, because the intensity of the BSE signal is strongly related to the atomic number (Z) of the specimen.

# References

[1] Vilar,G., Tulla-Puche, J., and Albericio,F., Polymers and Drug Delivery Systems. *Current Drug Delivery*, **2012** (9), 1-28.

[2] Moeller, E.H., Jorgensen, L., Alternative routes of administration for systemic delivery of protein pharmaceuticals. *Drug discovery today: technologies,* **2008** (5), e89-94.

[3] Langer, R. Drug delivery and targeting. *Nature,* **1998**, 392-395.

[4] Uhrich, E.K., Cannizzaro, S.M., Lager, R.S., Shakesheff, K.M., Polymeric systems for controlled drug release. *Chemical Reviews,* **1999** (99), 3181-3198

[5] Suman, Chauhan, M., Asymmetric Membrane Capsule: New Prospects in Osmotic Delivery. *International Journal of Drug Delivery,* **2011** (3), 185-193.

[6] Deacon, B., Abramowiz, J., Fear of needles and vasovagal reactions among phlebotomy patients. *Anxiety Disorders,* **2006** (20), 946–960.

[7] Gill, H.S., Prausnitz, M.R., Coated microneedles for transdermal delivery. *Journal of Controlled Release*, **2007** (117), 227–237

[8] Baria, S.H., Gohel, M.C., Mehta, T.A., and Sharma, O.P., Microneedles: an emerging transdermal drug delivery system. *Journal and Pharmacy Pharmacology*, **2012** (64), 11-29.

[9] Kirschner, N., Houdek, P., Fromm, M., Moll, I., Brandner, J.M., Tight junctions form a barrier in human epidermis. *European Journal of Cell Biology*, **2010** (89), 839–842.

[10] Hadgraft, J., and Lane, M.E., Skin: the ultimate interface. *Physical Chemistry Chemical Physics*. **2011** (13), 5215–5222.

[11] Nemes, Z., and Steinert, P.M., Bricks and mortar of the epidermal barrier. *Experimental and Molecular Medicine*, **1999** (31), 5-19.

[12] Trommer, H., Neubert, R.H.H., Overcoming the Stratum Corneum: The Modulation of Skin Penetration. *Skin Pharmacology and Physiology*, **2006** (19), 106–121.

[13] Prausnitz, M.R., Langer, R., Transdermal drug delivery. *Nature Biotechnology*, **2008** (26), 1261-1268.

[14] Fang, J-Y., Hong, C-T., Chiu, W-T., Wang, Y-Y., Effect of liposomes and niosomes on skin permeation of enoxacin. *International Journal of Pharmaceutics,* **2001** (219), 61–72.

[15] Andrews, S.N., Jeong, E., Prausnitz, M.R., Transdermal Delivery of Molecules is Limited by Full Epidermis, Not Just Stratum Corneum. *Pharmaceutical Research,* **2013** (30),1099–1109.

[16] Karande, P., Mitragotri, S., Enhancement of transdermal drug delivery via synergistic action of chemicals. *Biochimica et Biophysica Acta,* **2009** (1788), 2362–2373.

[17] Mitragotri, S., Current status and future prospects of needle-free liquid jet injectors. *Nature reviews*, **2006** (5), 543-548.

[18] Gupta, J., Prausnitz, M.R., Recovery of Skin Barrier Properties after Sonication in Human Subjects. *Ultrasound in Medicine and Biology*, **2009** (35), 1405–1408.

[19] Gupta, J., Microneedles for transdermal drug delivery in human subject. Degree Doctor of Philosophy in the School of Chemical & Biomolecular Engineering, **2009**.

[20] McAllister, D.V., Allen, M.G., and Prausnitz, M.R., Microfabricated microneedles for gene and drug delivery. *Annual Review of Biomedical Engineering*, **2000** (02), 289–313.

[21] Donnelly, R.F., Singh, T.R.R., Tunney, M.M., Morrow, D.I.J., McCarron, P.A., O'Mahony, C., and Woolfson, A.D., Microneedle Arrays Allow Lower Microbial Penetration Than Hypodermic Needles In Vitro. *Pharmaceutical Research,* **2009** (26), 2513–2522.

[22] Al-Qallaf, B., and Das, D.B., Optimizing Microneedle Arrays to Increase Skin Permeability for Transdermal Drug Delivery. *Annals of the New York Academy of Sciences*, **2009**, 83-94.

[23] Park,J-H., Prausnitz, M.R., Analysis of the Mechanical Failure of Polymer Microneedles by Axial Force. *Journal of the Korean Physical Society*, **2010** (56), 1223-1227.

[24] Davis, S.P., Landis, B.J., Adams, Z.H., Allen, M.G., Prausnitz, M.R., Insertion of microneedles into skin: measurement and prediction of insertion force and needle fracture force. *Journal of Biomechanics,* **2004** (37), 1155–1163.

[25] Crichton, M.L., Ansaldo, A., Chen, X., Prow, T.W., Fernando, G.J.P., Kendall, M.A.F., The effect of strain rate on the precision of penetration of short densely-packed microprojection array patches coated with vaccine. *Biomaterials,* **2010** (31) 4562-4572.

[26] Donnelly, R.F., Singh, T.R.R., and Woolfson, A.D., Microneedle-based drug delivery systems: Microfabrication, drug delivery, and safety. *Drug Delivery*, **2010** (17), 187–207.

[27] van der Maaden, K., Jiskoot, W., Bouwstra, J., Microneedle technologies for (trans)dermal drug and vaccine delivery. *Journal of Controlled Release,* **2012** (161), 645–655.

[28] Henry, S., McAllister, D.V., Allen, M.G., and Prausnitz, M.R., Micromachined needles for the transdermal delivery of drugs. *Micro Electro Mechanical Systems*, **1998**, 494-498.

[29] Badrana, M.M., Kuntschea, J., Fahra, A., Skin penetration enhancement by a microneedle device (Dermaroller®) in vitro: Dependency on needle size and applied formulation. *European Journal of Pharmaceutical Sciences,* **2009** (36), 511–523.

[30] McGrath, M.G., Vrdoljak, A., O'Mahony, C., Oliveira, J.C., Moore, A.C., Creana, A.M., Determination of parameters for successful spray coating of silicon microneedle arrays. *International Journal of Pharmaceutics*, **2011** (415), 140– 149.

[31] Kim, Y-C., Quan, F-S., Compans, R.W., Kang, S-M., Prausnitz, M.R., Formulation and coating of microneedles with inactivated influenza virus to improve vaccine stability and immunogenicity. *Journal of Controlled Release*, **2010** (142), 187–195.

[32] Kim, Y-C., Quan, F-S., Compans, R.W., Kang, S-M., and Prausnitz, M.R., Formulation of Microneedles Coated with Influenza Virus-like Particle Vaccine. *AAPS PharmSciTech*, **2010** (11), 1193-1201.

[33] Crichton, M.L., Ansaldo, A., Chen, X., Prow, T.W., Fernando, G.J.P., Kendall, M.A.F., The effect of strain rate on the precision of penetration of short densely-

packed microprojection array patches coated with vaccine. *Biomaterials*, **2010** (31), 4562-4572.

[34] Gill, H.S., Prausnitz, M.R., Pocketed microneedles for drug delivery to the skin. *Journal of Physics and Chemistry of Solids,* **2008** (69), 1537–1541.

[35] Gupta, J., Park, S.S., Bondy, B., Felner, E.I., Prausnitz, M.R., Infusion pressure and pain during microneedle injection into skin of human subjects. Biomaterials, **2011** (32), 6823-6831.

[36] Park, J-H., Allen, M.G., Prausnitz, M.R., Biodegradable polymer microneedles: Fabrication, mechanics and transdermal drug delivery. *Journal of Controlled Release*, **2005** (104), 51–66.

[37] Lee, J.W., Park, J-H., Prausnitz, M.R., Dissolving microneedles for transdermal drug delivery. *Biomaterials*, **2008** (29), 2113-2124.

[38] Sullivan, S.P., Murthy, N., and Prausnitz, M.R., Minimally Invasive Protein Delivery with Rapidly Dissolving Polymer Microneedles. *Advanced Material*, **2008** (20), 933–938.

[39] del Campo, A., and Greiner, C., SU-8: a photoresist for high-aspect-ratio and 3D submicron lithography. *Journal of Micromechanics and Microengineering*, **2007** (17), R81–R95.

[40] Chu, L.Y., Choi, S-O., Prausnitz, M.R., Fabrication of Dissolving Polymer Microneedles for Controlled Drug Encapsulation and Delivery: Bubble and Pedestal Microneedle Designs. *Journal of pharmaceutical science*, **2010** (99), 4228-4238.

[41] De Muth, P.C., Garcia-Beltran, W.F., Ai-Ling , M.L., Hammond, P.T., and Irvine, D.J., Composite Dissolving Microneedles for Coordinated Control of Antigen and

Adjuvant Delivery Kinetics in Transcutaneous Vaccination. *Advanced Functional Material*, **2013** (23), 161–172.

[42] Chu, L.Y., Prausnitz, M.R., Separable arrowhead microneedles. *Journal of Controlled Release*, **2011** (149), 242–249.

[43] Park, J-H., Choi, S-O. Kamath, R., Yoon, Y-K., Allen, M.G., Prausnitz, M.R., Polymer particle-based micromolding to fabricate novel microstructures. *Biomedical Microdevices*, **2007** (9),223–234.

[44] Kim, M.Y., Jung, B., Park, J-H., Hydrogel swelling as a trigger to release biodegradable polymer microneedles in skin. *Biomaterials*, **2012** (33), 668-78.

[45] Lee, K., Lee, C.Y., Jung, H., Dissolving microneedles for transdermal drug administration prepared by stepwise controlled drawing of maltose. *Biomaterials*, **2011** (32), 3134-3140.

[46] Lee, K., Kim, J.D., Lee, C.Y., Her, S., Jung, H., A high-capacity, hybrid electro-microneedle for in-situ cutaneous gene transfer. *Biomaterials*, **2011** (32), 7705-7710.

[47] Kochhar, J.S., Goh, W.J., Chan, S.Y., and Kang, L., A simple method of microneedle array fabrication for transdermal drug delivery. *Drug Development and Industrial Pharmacy*, **2012**, 1-11.

[48] Kim, Y-C., Quan, F-S., Compans, R.W., Kang, S.M., Prausnitz, M.R., Stability Kinetics of Influenza Vaccine Coated onto Microneedles During Drying and Storage. *Pharmaceutical Research*, **2011** (28),135–144.

[49] Hirschberg, H.J.H.B., van de Wijdeven, G.G.P., Kraan, H., Amorij, J-P., Kersten, G.F.A., Bioneedles as alternative delivery system for hepatitis B vaccine. *Journal of Controlled Release*, **2010** (147), 211–217.

[50] Kim, Y-C., Quan, F-S., Yoo, D-G., Compans, R.W., Kang, S-M., Prausnitz, M.R., Improved influenza vaccination in the skin using vaccine coated microneedles. *Vaccine*, **2009** (27), 6932–6938.

[51] Quan, F-S., Kim, Y-C., Compans, R.W., Prausnitz, M.R., Kang, S-M., Dose sparing enabled by skin immunization with influenza virus-like particle vaccine using microneedles. *Journal of Controlled Release*, **2010** (147), 326–332.

[52] Daddona, P.E., Matriano, J.A., Mandema, J., Maa, Y-F., Parathyroid Hormone (1-34)-Coated Microneedle Patch System: Clinical Pharmacokinetics and Pharmacodynamics for Treatment of Osteoporosis. *Pharmaceutical Research*, **2011** (28), 159–165.

[53] Jiang, J., Gill, H.S., Ghate, D., McCarey, B.E., Patel, S.R., Edelhauser, H.F., and Prausnitz, M.R., Coated Microneedles for Drug Delivery to the Eye. *Investigative Ophthalmology & Visual Science*, **2007** (48), 4038-4043.

[54] Preetha, J.P., Karthika, K., Cosmeceuticals-an evolutionInternational. *Journal of ChemTech Research*, **2009** (1), 1217-1223.

[55] Mukerjee, E.V., Collins, S.D., Isseroff, R.R., Smith, R.L., Microneedle array for transdermal biological fluid extraction and in situ analysis. *Sensors and Actuators,* **2004** (A114), 267–275.

[56] Chakraborty, S., Liao, I-C., Adler, A., Leong, K.W., Electrohydrodynamics: A facile technique to fabricate drug delivery systems. *Advanced Drug Delivery Reviews*, **2009** (61), 1043–1054.

[57] Coppola, S., Vespini, V., Grilli, S., Ferraro, P., Self-assembling of multi-jets by pyro-electrohydrodynamic effect for high throughput liquid nanodrops transfer. *Lab on a Chip*, **2011**, 11, 3294-3298.

[58] Grilli, S., Miccio, L., Vespini, V., Finizio, A., De Nicola, S., Ferraro, P., Liquid micro-lens array activated by selective electrowetting on lithium niobate substrates. *Optics Express*, 2008 (16), 8084-8093.

[59] Klose, D., Siepmann, F., Willart, J.F., Descamps, M., Siepmann, J., Drug release from PLGA-based microparticles: Effects of the "microparticle:bulk fluid" ratio. *International Journal of Pharmaceutics*, **2010** (383), 123–131.

[60] Versypt, A.N.F., Pack, D.W., Braatz, R.D., Mathematical Modeling of Drug Delivery from Autocatalytically Degradable PLGA Microspheres—A Review. *Journal of Control Release*, **2013** (165), 29–37.

[61] Fischer-Cripps, A.C., Nanoindentation. Springer 2002.

[62] Lu, L., Peter, S.J., Lyman, M.D., Lai, H-L., Leite, S.M., Tamada, J.A., Uyama, S., Vacanti, J.P., Langer, R., Mikos, A.G., In vitro and in vivo degradation of porous poly(DL-lactic-co-glycolic acid) foams. *Biomaterials*, **2000** (21), 1837-1845.

# Acknowledgements

My PhD journey was magnificent as well as demanding and stressful, and I would not be able to finish it without the help of many people. Here is a small tribute to all them.

I would like to thank my tutor prof. Paolo Antonio Netti, for introducing me in microneedle's world. I am very proud to have had the opportunity to work in his group. I am very grateful to my supervisor Ing. Raffaele Vecchione, for his patience, motivation and enthusiasm. His guidance helped me all the time duting research and writing of this thesis.

Moreover, I would like Pietro Ferraro and Sara Coppola, working at CNR-INO, for having made available the instrumentation for microneedle's electro-drawing. I would also like to thank prof. Peter Dubreil from Ghent University and dr. Antonelli Carmela of ASL Napoli 2 Nord to have readily supplied the materials needed for my work.

Then, I would like to thank Fabio Formiggini, which helped me to solve all my problems with microscopy analyses, and all my lab-mates that have made unique this period.

At last but not least I would like to thank very much my family and my love, for their encouragement and support, and for putting up with me even in the hardest times.

Thanks to all!